ICLLT-2024

16 – 18 MAY
ANKARA-TÜRKİYE

4th INTERNATIONAL CONFERENCE ON LIGHT AND LIGHT-BASED TECHNOLOGIES

Abstract and Proceeding Book

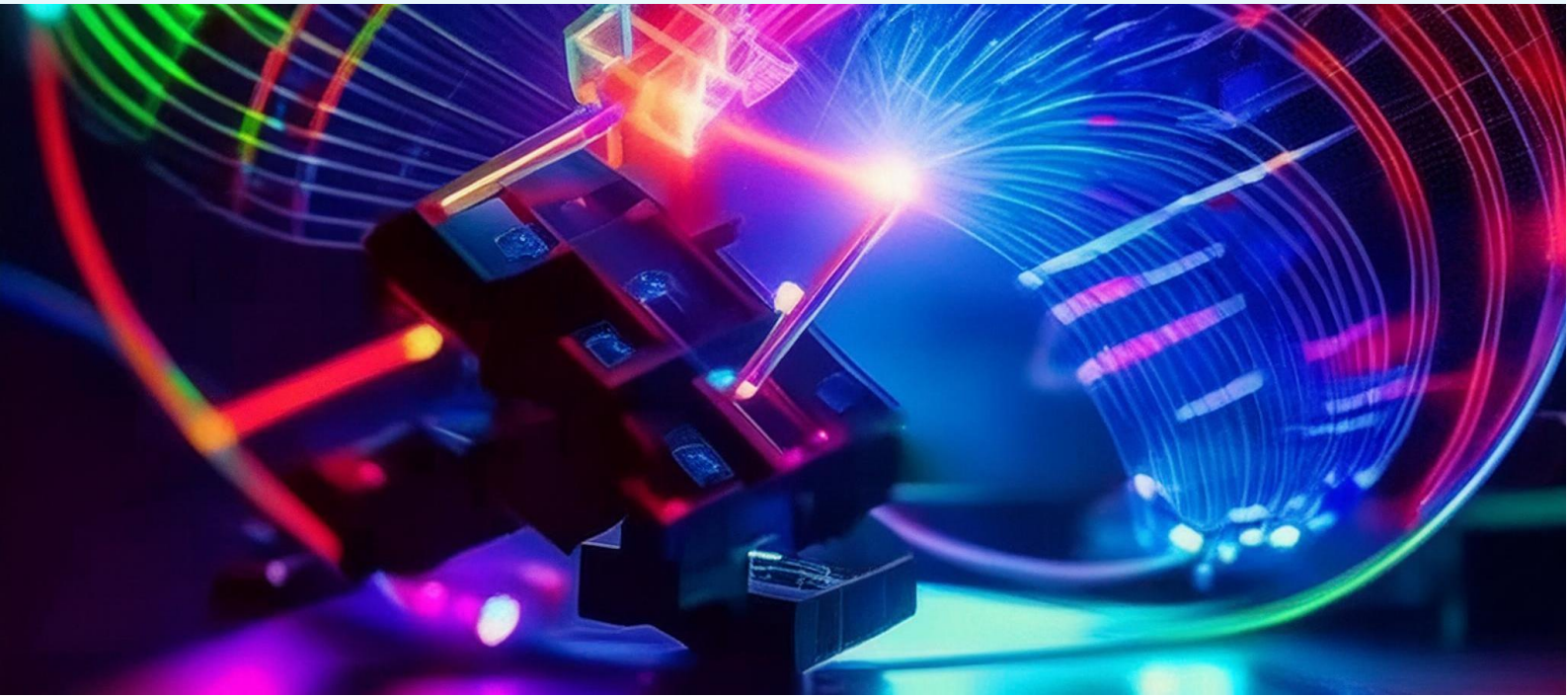

ABSTRACT AND PROCEEDING BOOK

4th International Conference on Light and Light-Based Technologies (4th ICLLT 2024)

16th-18th May 2021, Gazi University, Ankara, Türkiye

Edited by

Prof. Dr. Süleyman ÖZÇELİK

First Published, Nov 6, 2024

This book is available on the ICLLT website: *https://icllt-4.gazi.edu.tr/*

ORGANISERS

- Photonics Application & Research Center (Gazi Photonics), Gazi University
- Photonics Department of Applied Science Faculty, Gazi University

Welcome to the 4th ICLLT-2024

Dear Distinguished Participants and Colleagues

"International Day of Light" has been declared on 16 May at UNESCO 39th General Conference held in Paris between 30 October and 14 November 2017. UNESCO aims with this precious day to raise awareness of people in all United Nations countries in light and light-based technologies. The goal of sharing knowledge and increasing cooperation from R&D studies on photonics, nanotechnology, microtechnology and semiconductor technology of Gazi University Photonics Application and Research Center is in line with UNESCO's goal of creating Light Science awareness. With this aim, "4th International Conference on Light and Light-based Technologies (4th ICLLT-2024)" was held at the Gazi University (Ankara, Turkey), from 16 to 18 May 2024.

The 4th ICLLT-2024 conference targets guests from various branches and disciplines related to Optics and Photonics Technologies**.** Its interdisciplinary approach is the key to maximizing the potential and development of light-based technologies and tools for various applications. The purpose of the conference is to explore new ideas, effective solutions and collaborative partnerships for business growth by catalyzing the creation of a beneficial synergy between researchers, engineers, manufacturers, suppliers, and end-users of all sectors and making full use of this potential. At this event, the world's leading scientists in Optical and Photonic technologies discussed the latest developments in related technologies. 57 oral presentations, including 4 keynote speakers and 20 invited speakers, and 33 poster presentations were made by researchers from 9 different countries. While 50 of the presented papers (37 oral presentations and 13 posters) were presented by researchers from abroad, 40 papers (20 oral presenations and 20 posters) were presented by researchers from Türkiye. The event was held with 290 registered participants.

On behalf of the organizing committee, we would like to thank all participated academics, research institutions and organizations and especially young students from around the world for exchange of ideas and experiences at ICLLT-2024.

We are honored to invite you to the 5th ICLLT conference will be held in May 2025!

Prof. Dr. Süleyman ÖZÇELİK
Conference Chair

COMMITTEES

International Organizing Committee

Prof. Süleyman Özçelik *Gazi Univ.,* Türkiye
Prof. Yashar Azizian-Kalandaragh *Gazi Univ.,* Türkiye
Prof. Andrew Forbes *Witsatersrand Univ., South Africa*

Local Organizing Committee

Prof. Musa Yıldız *Gazi Univ.,* Türkiye
Prof. Süleyman Özçelik, *Gazi Univ.,* Türkiye
Prof. Yashar Azizian Kalandaragh, *Gazi Univ.,* Türkiye
Prof. Barış Kınacı, *Gazi Univ.,* Türkiye
Assoc. Prof. Nihan Akın Sönmez, *Gazi Univ.,* Türkiye
Assist. Prof. Tuğçe Ataşer, *Gazi Univ.,* Türkiye
Assist. Prof. Meltem Dönmez Kaya, *Gazi Univ.,* Türkiye
Assist. Prof. İsa Hatipoğlu, *Gazi Univ.,* Türkiye
Eng. Süha Gül Kara, *Gazi Univ.,* Türkiye
Eng. Berk Serbest, *Gazi Univ.,* Türkiye

Scientific Committee

Prof. Andrew Forbes, Witwatersrand Univ, South Africa
Prof. Luis. L. Sanchez-Soto, Univ. Complutense de Madrid, Spain
Prof, Mustafa Bayram Muradov, Baku State University, Azerbaijan
Prof. Abdollah Borhanifar, UMA, Iran
Assoc. Prof. Yunus Özen, Gazi Univ. Türkiye
Prof. Alina Manshina, St. Petersburg State University, Russia
Prof. Manijeh Razeghi, Northwestern University, USA
Dr. Barbara Sartori, Elettra, Italy
Prof. Şemsettin Altındal, Gazi Univ., Türkiye
Prof. Benedetta Marmiroli, Graz University of Technology, Austria
Prof. Alpan Bek, METU, Türkiye
Prof. Barış Kınacı, Gazi Univ., Türkiye
Prof. Mehmet Çakmak, Gazi Univ., Türkiye
Prof. Süleyman Özçelik (Chair), Gazi Univ., Türkiye
Prof. Oliver Martin, EPFL, Lausanne, Switzerland
Prof. Nahida Musayeva, Azerbaijan National Academy of Sciences, Azerbaijan
Prof. Ekmel Özbay, Bilkent Univ., Türkiye
Prof. Tarık Asar, Gazi Univ., Türkiye
Prof. Mustafa Kemal Öztürk, Gazi Univ., Türkiye
Prof. Samie Şebnem Aydın, Gazi Univ., Türkiye
Prof. Raşit Turan, Middle East Technical Univ., Türkiye

Dr. Halil İbrahim Efkere, Gazi Univ. Türkiye
Prof. Canan Varlıklı, İzmir Institute of Technology, Türkiye
Prof. Martin Booth, University of Oxford, UK
Prof. Gerd Leuchs, Max Planck Institute for the Science of Light in Erlangen, Germany
Prof. Hamidreza Khalesifard, IASBS, Iran
Assoc. Prof. Nihan Akın Sönmez, Gazi Univ. Türkiye
Dr. Meltem Dönmez Kaya, Gazi Univ., Türkiye
Dr. Isa Hatıpoğlu, Gazi Univ., Türkiye
Dr. Tuğce Ataşer, Gazi Univ., Türkiye
Dr. Ehsan Ahadi-Akhlaghi, IASBS, Iran
Prof. Yashar Azizian-Kalandaragh, Gazi Univ. Türkiye

PARTNERS & SPONSORS

The Best Presentation Awards for the top three presenter were supported by ASENTEK Company.

PROGRAM

Thursday 16th May (Address: Mimar Kemalettin Hall, Rectorate Building of Gazi University)

09:00 – 09:30	**Opening Ceremony** Prof. Süleyman Özçelik *Conference Chair* *Director of Photonics Application and Research Center, Gazi University, Ankara, Türkiye* Prof. M. Öcal Oğuz *President of Turkish National Commission for UNESCO* Prof. Musa Yıldız *Rector of Gazi University, Ankara, Türkiye*
Session I	**Chair:** Prof. Yashar Azizian-Kalandaragh *Department of Photonics, Faculty of Applied Sciences, Gazi University, Ankara, Türkiye*
09:30 – 10:20	Plenary Speaker / Prof. Luis L. Sánchez-Soto *Faculty of Physics, Complutense University of Madrid, Spain* **Quantum Superresolution in Time and Frequency**
10:20 – 10:40	**Coffee Break**
10:40 – 11:10	Invited Speaker / Prof. Ihor Pavlov *Middle East Technical University, Ankara, Türkiye* **High-Power Fiber Lasers: Advancements and Applications in Material Processing**
11:40 – 12:10	Invited Speaker / Dr. Daryoush Abdollahpour *Department of Physics, Institute for Advanced Studies in Basic Sciences (IASBS), Zanjan, Iran* **Light-sheet Fluorescence Microscopy: The Need for Speed and Quality**
12:10 – 13:30	**Lunch Break**
Session II	**Chair:** Prof. Mehmet Çakmak *Department of Photonics, Faculty of Applied Sciences, Gazi University, Ankara, Türkiye*
13:30 – 14:20	Plenary Speaker / Prof. Hamidreza Khalesifard *Department of Physics, Institute for Advanced Studies in Basic Sciences (IASBS), Zanjan, Iran* **Optical remote sensing of aerosols that may raise from the dried lake beds**
14:20 – 14:50	Invited Speaker / Dr. Muhammet Zeki Güngördü *Electrical and Electronic Engineering, Igdir University, Türkiye* **Deep Learning Assisted Design of Metamaterial-Based Terahertz Polarizer**
15:10 – 15:40	Invited Speaker / Dr. Devrim Anıl *ASELSAN Microelectronic Guidance and Electro Optic Sector, Türkiye* **Future of the Optical Design and Electro Optics at ASELSAN**
15:40 – 16:00	**Coffee Break**
Session III	**Chair:** Dr. İsa Hatipoğlu *Department of Photonics, Faculty of Applied Sciences, Gazi University, Ankara, Türkiye*
16:00 – 16:40	Invited Speaker / Prof. Alexey Andrianov *Quantum Confined Intense Light Laboratory, Institute of Applied Physics of the Russian Academy of Sciences* **Multicore optical fibers with coupled cores for high-peak-power amplification, nonlinear pulse compression, and wavelength conversion**
16:40 – 17:10	Invited Speaker / Prof. Arash Sabatyan *Quantum Confined Intense Light Laboratory, Institute of Applied Physics of the Russian Academy of Sciences* **Capability of Zone-Based Diffractive Elements in Shaping and Structuring Optical Beams**

17:10 – 17:40	Invited Speaker / Dr. Özgür Selimoğlu *Department of Engineering, Ankara University and Poloptech Company, Ankara, Türkiye* **Optical Production Technics and Considerations for Manufacturable Design**

Friday 17th May (75. Yıl Conference Hall, Faculty of Science, Gazi University)

Session I	**Chair:** Prof. Alpan Bek *Middle East Technical University, Türkiye*
09:00 – 09:50	Plenary Speaker / Prof. Tayfun AKIN *Middle East Technical University, Türkiye* **Evaluation of Infrared Detector and ROIC Development Activities in Türkiye**
09:50 – 10:00	**Short Break**
Session I	**HALL I** **Chair:** Prof. Alpan Bek *Middle East Technical University, Türkiye*
10:00 – 10:30	Invited Speaker / Prof. Benedetta Marmiroli *Graz University of Technology, Graz, Austria* **Deep X-ray Lithography for Optics and Photonics**
10:30 – 11:00	Invited Speaker / Prof. Alina Manshina *Institute of Chemistry, St. Petersburg state university, Russia* **How to make optical and electrochemical sensors with laser**
11:00 – 11:20	**Coffee Break**
11:20 – 11:40	Speaker / Barbara Sartori *Graz University of Technology, Institute of Inorganic Chemistry* **Synchrotron Radiation for Structural Biology**
11:40 – 12:00	Speaker / Erkut Emin AKBAŞ *Gazi University, Ankara, Türkiye* **Design Of All-Fiber Er-Doped ASE Source For Fiber Optic Sensors**
12:00 – 12:20	Speaker / Uğur Özçelik *Gazi University, Ankara, Türkiye* **The investigation of frequency dependent electrical parameters and density distribution of interface-traps (D_{it}) of the Au/(ZnO:CeO_2:PVP)/n-Si (MPS) Schottky diodes (SDs) by utilizing impedance spectroscopy model in the frequency range of 2kHz-1MHz**
12:20 – 13:30	**Lunch Break**
Session I	**HALL II** **Chair:** Dr. Daryoush Abdollahpour *Department of Physics, Institute for Advanced Studies in Basic Sciences (IASBS), Zanjan, Iran*
10:00 – 10:30	Invited Speaker / Prof. Abdollah Borhanifar *University of Mohaghegh Ardabili (UMA), Iran* **Interaction and efficiency of three optical pulses in optical fiber**
10:30 – 11:00	Invited Speaker / Dr. Berna Morova *Istanbul Technical University* **Tailored Light Beams: An Innovative Approach in Micromachining**
11:00 – 11:20	**Coffee Break**
11:20 – 11:40	Speaker / Sabreen A. Hameed *Department of Physics, College of Science, University of Diyala, Diyala, Iraq* **Intersection behavior in the forward bias I-V curves and current transport mechanisms (CTMs) in the Al/Al_2O_3/Ge/p-Si heterostructures in temperature range of 90-420 K**
11:40 – 12:00	Speaker / Mina Mollaei *Department of Physics, Institute for Advanced Studies in Basic Science (IASBS), Zanjan, Iran* **Optimization of photolithography exposure by Lenslets**
12:00 – 12:20	Speaker / Mohammad Khanjani *Department of Physics, Institute for Advanced Studies in Basic Science (IASBS), Zanjan, Iran* **Improving Illumination and Enhancing the Accuracy of White Light Interferometry Using Array Lenses**

12:20 – 13:30	**Lunch Break**
Session I	**HALL III** **Chair:** Prof. Arash Sabatyan *Urmia University, Iran*
10:00 – 10:30	Invited Speaker / Dr. Zeynep Demircioğlu *Tübitak, SAGE* **Production and characterization of amorphous Silicon thin film solar cells on flexible substrates**
10:30 – 11:00	Invited Speaker / Alihan KUMTEPE *Kalyon PV, Türkiye* **Technological roadmap of KalyonPV R&D Center**
11:00 – 11:20	**Coffee Break**
11:20 – 11:40	Speaker / Buğra Yalçın *Nanotechnology Research Center, Bilkent University* **Raman OTDR Based Distributed Temperature Sensing for Environmental and Structural Monitoring**
11:40 – 12:00	Speaker / Behnaz Javidi *Physics Department, Urmia University,Urmia,Iran* **Impact of Astigmatism on diffractive features of spiral checkerboard zone plate**
12:00 – 12:20	Speaker / Maryam Fatehi *University of Urmia - Faculty of Science - Optics & Laser Group* **Innovative Optical Beam Shaping with One-Dimensional Fresnel-Zone Plates: Novel Complex Structures**
12:20 – 13:30	**Lunch Break**
Session II	**Chair:** Prof. Luis L. Sánchez-Soto *Faculty of Physics, Complutense University of Madrid, Spain*
13:30 – 14:20	Plenary Speaker / Prof. Gerd Leuchs *Max Planck Institute, Germany* **International scientific exchange and collaboration**
14:20 – 14:30	**Short Break**
Session II	**HALL I** **Chair:** Prof. Luis L. Sánchez-Soto *Faculty of Physics, Complutense University of Madrid, Spain*
14:30 – 15:00	Invited Speaker / Prof. Saifollah Rasouli *Department of Physics, Institute for Advanced Studies in Basic Sciences (IASBS), Zanjan, Iran* **Diffraction from periodic structures, Talbot effect, and beam shaping**
15:00 – 15:20	Speaker / Mozhgan Hashemi *Department of Physics, Institute for Advanced Studies in Basic Science (IASBS), Zanjan, Iran* **Polarimetric Analysis of Whitefly Larvae on Pomegranate Leaves via Mueller Matrix Imaging**
15:20 – 15:40	Speaker / Mahkame Abolfathi *Department of Physics, Institute for Advanced Studies in Basic Science (IASBS), Zanjan, Iran* **Using the highly sensitive surface plasmon resonance sensors to accurately determine organic dyes and some inorganic minerals in water**
15:40 – 16:00	Speaker / Sinan Genç *Middle East Technical University* **Using optical interference and machine learning to categorize microbeads in water**
16:00 – 17:00	**Coffee Break and Poster Presentations**
Session II	**HALL II** **Chair:** Dr. Sumea Klokic *Ceric-Eric, Trieste, Italy*

14:30 – 15:00	Invited Speaker / Dr. Ehsan Ahadi-Akhlaghi *Department of Physics, Institute for Advanced Studies in Basic Sciences (IASBS), Zanjan, Iran* **Optical Metrology: 3D Imaging**
15:00 – 15:20	Speaker / Sina Zeynali *Department of Physics, Institute for Advanced Studies in Basic Science (IASBS), Zanjan, Iran* **SPR simulation of exosome with different drugs**
15:40 – 16:00	Speaker / Zahra Akbarpour *Institute for Advanced Studies in Basic Sciences (IASBS)* **Investigating the Mechanical Properties of Biological Cells using Dual-beam Optical Tweezers**
16:00 – 17:00	**Coffee Break and Poster Presentations**
Session II	**HALL II** **Chair:** Dr. İsa Hatipoğlu *Department of Photonics, Faculty of Applied Sciences, Gazi University, Ankara, Türkiye*
14:30 – 15:00	Invited Speaker / Prof. Şemsettin Altındal *Gazi University, Ankara, Türkiye* **The investigation of basic physical parameters, energy dependent profiles of interface traps (N_{ss}) and their lifetimes (τ) of the Au/n-Si structurers with (PVA-Fe_3O_4) interlayer**
15:00 – 15:20	Speaker / Parisa Pashaei *Gazi University, Ankara, Türkiye* **Flexible Interdigital Ag Electrode Fabrication for UV-photodetectors: A Comparative Study of Aerosol Jet Printing and Thermal Evaporation Methods**
15:20 – 15:40	Speaker / Mohammad Reza Ataii *Department of Physics, Institute for Advanced Studies in Basic Science (IASBS), Zanjan, Iran* **Periodic SPR Nano-Sensors in Form of a 6-Point Shuriken**
15:40 – 16:00	Speaker / Abdulkadir Yentur *TOBB University of Economics and Technology* **SOA-based broadband light source relative intensity noise suppression**
16:00 – 17:00	**Coffee Break and Poster Presentations**
Session III	**HALL I** **Chair:** Prof. Hamidreza Khalesifard *Department of Physics, Institute for Advanced Studies in Basic Sciences (IASBS), Zanjan, Iran*
17:00 – 17:30	Invited Speaker / Prof. Alpan Bek *Middle East Technical University, Türkiye* **Environmental Photonics: From ultrafast IR laser material processing to trace molecule detection**
17:30 – 17:50	Speaker / Ferhat Hanife *Gazi University, Photonics Application and Research Center* **Utilizing Interference Microscopy to Determine Micro-Sized Objects**
18:10 – 18:30	Speaker / Ömer Faruk Dinç *Nanotechnology Research Center, Bilkent University* **Pulse Distortion Optimization Caused by EDFA Transient Effect**
18:30 – 18:50	Speaker / Yiğit Levent Çeçen *Department of Photonics, Gazi University Graduate School of Natural and Applied Sciences* **Investigation of Quantum Confinement Effects in Cadmium Sulfide Polymer Nanocomposites and Their Role in Optoelectronic Device Applications**
Session III	**HALL II** **Chair:** Dr. İsa Hatipoğlu *Department of Photonics, Faculty of Applied Sciences, Gazi University, Ankara, Türkiye*
17:00 – 17:30	Invited Speaker / Dr. Sumea Klokic *Ceric-Eric, Trieste, Italy* **Structural dynamics in photo-responsive crystalline film systems: a multi-technique approach**

17:30 – 17:50	Speaker / Narges Rezaei *Department of Physics, Institute for Advanced Studies in Basic Science (IASBS), Zanjan, Iran* **Fabrication and Calibration a Spectral-Domain Optical Coherence Tomography in Infrared Range**
17:50 – 18:10	Speaker / Sara Aminian *Department of Physics, Institute for Advanced Studies in Basic Science (IASBS), Zanjan, Iran* **Refractometry based on reflection phase step spectroscopy**
18:10 – 18:30	Speaker / Sharareh Jalali *Urmia University* **Exploring Novel Techniques for Optical Vortex Beam Generation and Detection Using Mach-Zehnder Interferometer and Spiral Zone Plate**
18:30 – 18:50	Speaker / Sima Hosseini *Department of Physics, Institute for Advanced Studies in Basic Science (IASBS), Zanjan, Iran* **Surface Topography Measurement through Fringe Visibility Analysis**
Session III	**HALL III** **Chair:** Dr. Barbara Sartori *Graz University of Technology, Institute of Inorganic Chemistry*
17:00 – 17:30	Invited Speaker / Dr. Sevilay Sevinçli *Department of Photonics, İzmir Institute of Technology, Türkiye* **Ultra-cold Rydberg Atoms and Quantum Technologies**
17:30 – 17:50	Speaker / Utku TOPCU *Gazi University, Photonics Application and Research Center* **Fabrication of Different Patterns of Diffraction Grating with Aerosol Jet Printing System**
17:50 – 18:10	Speaker / Mahammad Baghir Baghirov *Baku State University* **Study of optical properties of asymmetric AgNWs/PVA/Ag_2S nanocomposites by vapor phase sulfidation process**
18:10 – 18:30	Speaker / Fateme Gheibi *Department of Physics, Institute for Advanced Studies in Basic Science (IASBS), Zanjan, Iran* **White light spectroscopy of structured surface plasmon resonance biosensors**

Saturday 18th May

09:00 – 09:50	Photonics Application and Research Center of Gazi University Tour
11:00 – 17:30	Cultural Program - Ankara
18:00 – 20:00	**Closing Ceremony and Best Presentation Awards** (Address: Gazi Concert Hall)

TABLE OF CONTENTS

PLENARY SPEAKERS

PS1

International scientific exchange and collaboration

Gerd Leuchs[1,2,3]

[1]*Friedrich-Alexander-Universität Erlangen-Nürnberg, Germany*
[2]*Max Planck Institute or the Science of Light, Erlangen, Germany*
[3]*Department of Physics, University of Ottawa, Canada*

Abstract: Over the centuries, scientific progress has been the result of the research work by people from societies, cultures, and countries all around the world. To mind come Greece, Egypt, China, the Mayas, India, the Arabs and Persians with the whole Middle East and many more. Modern style research took off in Europe 500 years ago triggered by the 'Renaissance'. Europe refers to many different countries between Lisbon and St. Petersburg. In fact, some of our knowledge about what the Greeks have done would have been lost had it not been for the Arabs who preserved it so that the work is available for us to see today. During my scientific career, which started in the mid 1970's, I enjoyed and benefitted greatly from discussions and exchange with scientists from many different countries including the United States and the Soviet Union (!). My mentor and supervisor, Professor Herbert Walther, was well connected and we had many visitors come by. In a way, these were lucky circumstances for me because I soon got to know many of the leading scientists in my field. This helped me in my own career. After getting used to and befitting from fairly free exchange between scientists worldwide in the field of fundamental physics, I now notice increasing restrictions because of political tensions building up and societies changing in our world [see 1, 2]. Science is part of human culture and reflects our curiosity to learn about who we are and what we can learn about the universe we are living in. This is best done by free exchange and discussions among scientists world-wide, including collaborations whenever appropriate. This is a perfect frame embracing all scientists. I sincerely hope that we can continue with this mode of operation in the years to come. At the moment, some scientists are having difficulties to obtain visas to go to conferences to which they are invited. Fortunately, there are countries such as Turkey or former Soviet Republics (such as Kazakhstan and Armenia) for which visas are currently not required (for a majority of countries) and where scientists can meet without these restrictions. Also, in that sense, the International Conference on Light and Light-based Technologies (ICLLT) provided a perfect platform for scientists in the field.

1. https://opnmedia.blob.core.windows.net/$web/opn/media/images/pdf/2024/0724/004-005_opn_07_24.pdf?ext=.pdf
2. https://www.optica-opn.org/home/articles/volume_35/september_2024/departments/president_s_message/

PS2

Quantum Superresolution in Time and Frequency

Luis L. Sánchez-Soto[1, 2]

[1]*Faculty of Physics, Complutense University of Madrid, 28040 Madrid, Spain*
[2]*Max Planck Institute for the Science of Light, 91058 Erlangen, Germany*

Abstract: Accurate time is at the core of many modern technologies. I will present new schemes that allow one to achieve the ultimate quantum precision for the estimation of the time (or frequency) offset of an incoherent mixture of ultrashort pulses at the single-photon level. Amazingly, these techniques are able to resolve temporal separations 10 times smaller than the pulse duration, as well as imbalanced intensities differing by a factor of 10^2. This represents an improvement of more than an order of magnitude over the best standard methods based on intensity detection and pave the way for new technologies in this field.

PS3

Optical remote sensing of aerosols raising from the dried lake beds

Hamid R. Khalesifard[1,2], Salar Alizadeh[1], Ruhollah Moradhaseli[3]

[1]Department of Physics and [2]Research Center for Climate Change and Global Warming, Institute for Advanced Studies in Basic Sciences, Zanjan, Iran.
[3]Department of Physics, Azad University-Zanjan Branch

Abstract: As the evaporation and drainage rate of a lake increase with respect to its water income, the lake will start its drying scenario. Dried lake beds are potential sources of mineral aerosols. As a lake gets dry, its water salinity increases, and lots of salt cover its dry parts. Therefore, intense winds blowing over the lakes surface may take considerable amounts of dust, salt-dust, and wet salt particles into the atmosphere. Aral Lake in Uzbekistan, Sambhar Lake in India, Urmia Lake in Iran, and Great Salt Lake in the US are samples of such lakes. Salt particles are harmful to human health, agriculture, wildlife, etc. It is important to investigate the number of salt particles fed into the atmosphere and the spatial-temporal range that may be transported by wind and atmospheric systems. Such atmospheric particles can be studied by optical remote sensing techniques from ground, air, or space. We used the recordings of a horizontally-aligned scanning-polarization-lidar, to characterize salt-dust plumes over the Urmia Lake in northwest Iran.

The lidar was installed just at the southwest coast of the lake and horizontally scanned the atmosphere at altitudes less than 100 m above the lakebed. The campaign was carried out in September 2022. We employed Klett and modified POLIPHON methods to classify the atmospheric aerosols into dust, salt-dust, and wet-salt particles. In these investigations, we also used satellite data like aerosol optical depth (AOD) from the Moderate Resolution Imaging Spectroradiometer (MODIS) onboard Aqua and Terra satellites, the NOA Hysplit Lagrangian trajectory model and the Meteosat recordings. Different cases are studied based on their depolarization- and lidar-ratio (δp and S) profiles. Results indicate the dominance of salt-dust and wet-salt particles inside the plumes that are rising from the lakebed. The profiles of δp and S are used to distinguish different particle types, revealing δp varies from ~0.05 to ~0.30, and S from ~25 to ~40 sr for these cases. These results depict the recorded aerosol plumes over the lake, containing 36% dust, 29% salt-dust, and 35% wet salt particles.

INVITED SPEAKERS

IS1

Ultrafast Spin Dynamics

Halime Gül Yağlıoğlu

[1]*Engineering Physics Department of Ankara University, 06100 Besevler/Ankara, Türkiye*
[2]*Turkish Accelerator and Radiation Laboratory, Bahçelievler Mh. 306 Sk. No: 11/N 06830 Gölbaşı/Ankara, Türkiye*
email: gyaglioglu@tarla-fel.org, yoglu@eng.ankara.edu.tr

Abstract: Due to the need for faster and more energy-efficient data processing, basic research to develop new technologies becomes important more than ever. Ultrafast control of spin dynamics brings spintronic applications areas to femtosecond time scales. Ultrafast Magnetization Group (UMAG) has been conducting research on the ultrafast controlling of spin dynamics in Ankara University Engineering Physics Department and TARLA (Turkish Acceleration and Radiation Laboratory).

Spin crossover (SCO) molecular complexes of transition metal ions, whose properties can be photo-switched on ultrashort time scales, have attracted much attention in recent years due to possible applications such as sensors, optical memory devices, magnetic data storage, molecular electronics, spintronic devices etc. The role of ligand field (LF) states in photo-physics of the reverse light-induced excited spin state trapping (reverse-LIESST) effect of an Iron (II) spin crossover (SCO) complex has been demonstrated experimentally in solution at room temperature by using ultrafast transient absorption spectroscopy technique. We showed that selective photo-switching between high spin (HS) and low spin (LS) states, i.e. HS→HS or HS→LS transitions, is possible by photoexcitation from the HS ground state to the HS metal-ligand charge transfer (MLCT) states (at 400 nm pumping) or to the low spin (LS) ligand-field (LF) state (at 435 nm pumping), respectively. This is an effective direct observation of the reverse-LIESST effect through LF state pumping in solution at room temperature. We have proposed different relaxation pathways along with the ultrafast relaxation time components that account for HS→HS and HS→LS transitions [1].

Laser-induced switching of ferromagnetism, driven by a disorder–order transition on FeAl thin films, has been experimentally demonstrated in the literature. The switching of ferromagnetic ordering by ultrafast laser pulses in FeAl thin films may open new possible applications of this material such as magnetic data storage and manipulation. Since the speed of the magnetic switching of magnetic states in thin films is one of the critical parameters for these applications, here we used time resolved magneto-optical Kerr measurements to investigate the demagnetization dynamics of $Fe_{60}Al_{40}$ thin films at room temperature. We have for the first time observed a clear transition from one-step dynamics (type I) to two-step (type II) dynamics in the same material by increasing pump laser fluence. This experimental observation may give a strong confirmation that the ultrafast demagnetization process can be treated as a thermal process and is driven by the difference between temperatures of the electron and spin systems [2].

References

1. Damla Beşe, Kübra Gürpinar, E. Uzay Karakaya , F. Gülşah Akça, Hasan Nazir , Baris Emre, Orhan Atakol, Eyüp Duman, Halime Gul Yaglioglu, to be published.
2. M. Arslan, C. Bese, Z. Tabak, T. Bozdag,1 E. Duman, and H. G. Yaglioglu, J. Appl. Phys. 131, 093904 (2022); doi: 10.1063/5.0073069

IS2

High-Power Fiber Lasers: Advancements and Applications in Material Processing

Pavlov I.*[1], Bek A.[1], Goodarzi A., Akhtaryarazar D.

[1]*Physics Department, Middle East Technical University, 06800 Ankara, Türkiye*
email: ipavlov@metu.edu.tr

Abstract: Since the advent of high-power fiber lasers, they have become indispensable tools in various fields due to their ability to control parameters such as pulse duration, wavelength, and power with high precision. This study focuses on development and tailoring the properties of Erbium (Er)- and Ytterbium (Yb)-doped fiber lasers, for different applications in the field of laser-material interactions.
Er-doped fiber lasers, which perform excellently in the 1.5 µm wavelength range, are ideal for applications requiring eye-safe operation. However, managing Amplified Spontaneous Emission (ASE) is critical, especially in high-power Er nanosecond (ns) fiber lasers. By carefully adjusting all the parameters of each stage of the laser and optimizing the pulse duration, we successfully controlled ASE, ensuring stable operation at high powers [1]. The laser with this parameters was successfully applied to laser material processing allowing us for the first time to the best of our knowledge 3D subsurface Si modification and sculpturing [2].

Yb-doped fiber lasers, operating primarily around the 1 µm wavelength, are favored for their higher efficiency and broader gain bandwidth, allowing construction of short pulse femtosecond laser operation. Nonlinearity management is a key challenge in high pulse energy Yb femtosecond (fs) fiber lasers, where precise control over dispersion and pulse shaping is required to avoid detrimental nonlinear effects [3]. This laser, with the specified parameters, proved effective in material processing applications. Notably, it was employed in Nonlinear Laser Lithography, where it successfully produced Laser-Induced Periodic Surface Structures (LIPSS), illustrating its precision in pattern creation on surfaces [4]. Furthermore, research into laser-material interactions revealed the fiber lasers' capability in liquid crystal alignment and surface texturing for solar cells.

Acknowledgement: This work was partially supported by Scientific and Technological Research Council of Türkiye (TÜBİTAK) Project Number: 113M930, 114F256, 118F375

References

1. Pavlov, et al., Optics Letters, 39(9), p. 2695, (2014).
2. O. Tokel, et al., Nature Photonics, 11, 639-645, (2017).
3. I. Pavlov, et al., CLEO Europe, CJ_6_5, (2013).
4. B. Öktem, I. Pavlov, et al., Nature Photonics, 11, 639-645, (2013).

IS3

Light-sheet Fluorescence Microscopy: The Need for Speed and Quality

Daryoush Abdollahpour[1]

[1]*Department of Physics, Institute for Advanced Studies in Basic Sciences (IASBS), Zanjan, Iran*

Abstract: The advent of 3D tomographic optical microscopy has revolutionized our ability to visualize and analyze biological specimens with unprecedented clarity and depth. Among these, light-sheet fluorescence microscopy (LSFM) stands out due to its unique ability to illuminate a thin plane within a sample, thereby minimizing phototoxicity and maximizing imaging efficiency. However, despite its advantages, LSFM is often challenged by issues related to imaging artifacts and the need for rapid acquisition of high-quality data.

This talk will explore the foundational principles of LSFM and introduce a novel approach that significantly enhances the quality of images produced by this technique. By utilizing scanning non-diffracting beams, our method effectively suppresses imaging artifacts, offering clearer and more accurate visualization of biological structures. This innovation addresses one of the key limitations of traditional LSFM, pushing the boundaries of what can be achieved in biological imaging.

In addition to improving image quality, the talk will delve into the critical aspect of imaging speed—a parameter of paramount importance in dynamic biological processes. The presentation will demonstrate how increasing the depth of field (DOF) in LSFM can directly contribute to faster imaging speeds. This enhancement is achieved by imprinting a cubic phase on the detection microscope within the LSFM setup, thereby significantly extending the DOF. It will also be discussed that post-processing of the captured 3D images is critically important in LSFM, especially with extended DOF imaging.

Finally, the implications of these advancements for functional brain imaging will be discussed. The talk will highlight how, with the appropriate camera setup, the only limitation on imaging speed becomes the frame rate and dark current level of the image sensor. This paves the way for using LSFM in high-speed, high-resolution imaging of neural activity in model organisms, opening new avenues for research in neurobiology and beyond.

In summary, this presentation will not only showcase the latest technological advancements in LSFM but also underline the critical balance between speed and quality in biological imaging, ultimately contributing to a deeper understanding of complex biological systems.

IS4

Optical Production Technics and Considerations for Manufacturable Design

Özgür Selimoğlu*1

Department of Engineering, Ankara University and Poloptech Company, Ankara, Türkiye
email: Ozgur.Selimoglu@ankara.edu.tr

Optical systems that are produced in high volumes should be considered starting from the initial optical design phase. Optics should be designed for low cost and high yield if there is an aim of mass manufacturing intention. Optics are manufactured by passing through many steps. Optical manufacturing starts with obtaining the raw material. Raw materials for the prototypes can be obtained from large blocks and necessary dimensions are obtained by cutting the small rectangular blocks from it. This rough process followed by edging to reach a cylindrical blank material that is suitable for grinding process. This process generally wastes at least 2-3 times more material than the finished product, therefore only suitable for small amount production such as prototyping or low volume special small projects. For the mass manufacturing, glass is pressed to the final shape with tolerances less than a millimeter. After suitable blank or pressed material is obtained, then the grinding processes starts. At this step, the surfaces are grinded to the final shape with a tolerance of less than 5-micron PV. Surfaces at this stage is rough and behaves like a diffuser as the surface roughness is higher or comparable with the visible light wavelength. The grinding process keeps 20–50-micron excess material at the surfaces for the polishing process. Polishing performance within the clear aperture will be better if the diameter of the lens at the polishing is larger than 3mm. As the edges experience higher forces during polishing, the surface accuracy at the edges are tends to be lower. These edges can be removed at the centering operation and a higher quality lens is achieved.

To be able use larger lens at the polishing stage, design of the lens should be suitable. To reach this aim, at the design phase, chip zones and edge thickness constraints should be added. Using 1.5 mm chip zone with the edge thickness constraint that keeps the edge larger than 0.8 mm is a good design choose. Moreover, the thickness of the lens should be high enough to prevent the bending of the lens by the applied polishing pressure. Center thickness larger than 1.5 mm for the mid-size lenses (15mm-50mm) is generally recommended. After the polishing, coating operation is needed. While holding with a fixture, edges will not be coated because of the shadow of the fixture. Clear aperture of the lens should be at least 1 mm smaller than the final mechanical size of the lens for classical lens fixtures at coating process.

Spherical lens production using cup tools for grinding. This tool and spherical glass interaction is a line and grinding speed is high. For the aspherical lenses, cutting tool can only touch the surface at a single point and it is a slower process. Additionally, spherical lens polishing process uses tools that touch to surface at a large area and polishing all the surface at the same time. While aspherical polishing only touches to the surface at a single point. Spherical polishing is much quicker than the aspherical

polishing and using only spherical surfaces makes the design more manufacturable and cost effective. Therefore, spherical lenses should be the first choice for the lens designers.

IS5

Future of the Optical Design and Electro Optics at ASELSAN

Devrim Anıl[1]

[1]*ASELSAN Microelectronic Guidance and Electro Optic Sector, Türkiye*

Abstract: In this presentation, how optical design is started and which steps are applied are summarized. For this purpose, very simple double gauss and Cooke triplet sample optical designs are presented. Some optical design forms and layouts are presented for the designers that can be chosen as a starting point. Finally optical design with optomechanics is shown for illustration for the Double Gauss design. This was just a simple optical design and afterwards some more complex optic and optomechanical designs of ASELSAN is presenter. These are the ASELFLIR 500 Electro optical Payload and AVCI Head Up Display. As a final remark how the optical designs of ASELSAN are became complex and evolved during past 20 years are shown with some more optical design layouts.

IS6

Multicore optical fibers with coupled cores for high-peak-power amplification, nonlinear pulse compression and wavelength conversion

Andrianov A.V.*[1], Anashkina E.A.[1], Balakin A.A.[1], Skobelev S.A.[1], Salnikov N.I.[1,2], Litvak A.G.[1]

[1]*A.V. Gaponov-Grekhov Institute of Applied Physics of the Russian Academy of Sciences, 46 Ulyanov Street, Nizhny Novgorod 603950, Russia*
[2]*Advanced School of General and Applied Physics, Lobachevsky State University of Nizhny Novgorod, 23 Gagarin Ave., Nizhny Novgorod 603022, Russia*
email: andrian@ipfran.ru

Abstract: Fiber laser systems with high peak and average power are in great demand for many applications. However, the peak power of fiber systems is severely limited by nonlinear effects. The prospects for significant increase in power are associated with the use of multi-core optical fibers (MCFs). In MCFs with interacting cores radiation can propagate in the form of collective modes of all cores (supermodes), while coherence between the cores can be maintained. Special designs of multicore fibers with coupled cores, such as a square lattice of cores and a ring of even number of cores, support coherent propagation of out-of-phase supermodes (in which phases alternate between 0 and π in neighbouring cores) that are stable in presence of disturbances at high power levels. We experimentally demonstrated selective excitation and amplification of chirped pulses at 1 μm in Yb-doped 6-core ring fiber up to 1 μJ energy and peak power of 18 kW. In numerical simulations we showed that peak powers up to 55 MW in 1.1 ns chirped pulses at 1 μm can be achieved in Yb-doped tapered MCF with 11x11 cores array. Coherent combining of the out-of-phase mode into a single beam can be achieved with >90% efficiency.

MCFs with coupled cores are promising for nonlinear light control. We demonstrated numerically and experimentally that dispersion properties of the out-of-phase mode can differ significantly from single-mode dispersion of a waveguide made of the same material, for example, anomalous dispersion can be achieved near 1 μm. Dispersion control using MCFs is utilized to harness nonlinear processes of soliton compression below 20 fs duration and soliton Raman self-frequency shift. This may be especially important in mid-infrared region, where fibers made of soft glasses such as tellurite and chalcogenide glasses are widely used. We developed a design of tellurite MCF with 10 core ring structure and numerically simulated 1.5 nJ soliton wavelength shift from 2.3 μm to 4 μm. Even longer wavelength of 6.2 μm can be achieved using in 7x7 MCF made of chalcogenide glass, as was shown in our numerical modeling.

We look forward to further development of advanced ultrashort pulse lasers that combine several multicore fiber technologies, e.g., stable amplification in the out-of-phase supermode and saturable absorption due to discrete diffraction suppression.

This work was supported by the Russian Science Foundation, grant no. 23-12-00248.

IS7

Capability of Zone-Based Diffractive Elements in Shaping and Structuring Optical Beams

Arash Sabatyan*[1]

[1]*Department of Physics, Urmia University, Urmia, Iran*
email: a.sabatyan@urmia.ac.ir

Abstract: With the increasing significance of diffractive components across various fields such as science, technology, and industry, we are uncovering a crucial aspect concerning the manipulation of optical beams. Optical beam shaping involves controlling the intensity, phase, and polarization of light beams through profile adjustments, creating patterns or structures within the beam, changing its direction and focal point, producing arrays of beams in different geometries, and generating multi-focusing elements. In the realm of diffractive elements, particular attention is given to Fresnel zone plates (FZPs).

The focal point is initially on the well-known Fresnel zone plate, which comprises concentric bright and dark zones acting as a spherical lens to focus incoming plane beams. The radial phase-shifted element, a variant of the FZP created by shifting the zones radially inward or outward, results in the production of an annular beam at the focal plane, with the focus positioned farther from or closer to the element depending on the direction of the phase shift. Combining inward and outward radial phase shifts leads to the formation of a new bifocal element, generating two foci with a bottle beam between them.

Exploring further, the discussion shifts to a petal-shaped zone plate achieved by introducing an azimuthal-dependent radial phase shift. This element functions as a bifocal lens capable of creating a bottle beam between two focal points and has been found to shape light beams into star-like or petal-like patterns. Integrating a grating-like component into a Fresnel zone plate structure results in the creation of a 2D array spot generator.

Adjusting the phase of a zone plate using a helical pattern leads to the production of a spiral zone plate (SZP), featuring helical Fresnel zones designed to generate optical vortices characterized by a screw-dislocation singularity where phase transitions from zero to 2π in a cycle. A composite SZP can be formed by combining two separate SZPs to control optical vortices and create a variety of shapes and structures. Additionally, modifying the azimuthal phase shift of a SZP can generate spiral and light-arm beams carrying different topological charges.

Modifying the phase of a linear zone plate (LZP) results in the generation of diverse 1D optical beams. Further, overlapping two orthogonal LZPs forms an orthogonal zone plate useful for focusing, imaging, and miniaturization in optical systems, utilizing a rectangular focusing element. The diffractive efficiency can be increased by manipulating the phase structure to transform it into a checkerboard zone plate.

Continued research reveals that introducing a helical phase into orthogonal zone plates or checkerboard zone plates causes them to generate optical vortices hosting monopole and dipole vortices that interact while propagating—a fascinating phenomenon previously unexplored in the context of vortices.

References

1. Arash Sabatyan, and Bahar Meshginqalam, 2014, Generation of annular beam by a novel class of Fresnel zone plate, *Applied Optics*, 53, 5995-6000 .
2. Fatemeh Seifi, Arash Sabatyan, 2021, Coherence combination to create a long depth bifocal diffractive lens capable of generating tailorable biannular and bottle beam, *Optics and Quantum Electronics*, 53, 1-10.
3. Arash Sabatyan, Marjan Golbandı 2018, Petal-lıke zone plate long depth bıfocal dıffractıve lens and star-lıke beam generator J. Optıcal Socıety Amerıca A 35 1243-1253.
4. Arash Sabatyan and Babak Fathi, 2018, High-efficiency arrays of any desired optical beams using modified grating-based elements, *Optical and Quantum Electronics*, 50:238.
5. N. R. Heckenberg, R. McDuff, C. P. Smith, and A. G. White, “Generation of optical phase singularities by computer-gener ated holograms,” Opt. Lett. 17, 221–223 (1992).
6. Arash Sabatyan, 2019, Comprehensive focusing analysis of bi-segment spiral zone plate in producing a variety of structured light beams,*journal of the Optical Society America B*, 36.
7. Jila Rafighdoost, and Arash Sabatyan, 2017, Spirally phase-shifted zone plate for generating and manipulating multiple spiral beams, *Journal of the Optical Society of America B*, 608-612, 34.
8. Arash Sabatyan and Jila Rafighdoost, 2018, Considerable diversity in generation light-arm beams using multi-twisted phase structure zone plate ,*Optics and Laser Technology*.
9. Arash Sabatyan and Shima Gharbi, 2017, Appearance of fractional vortex dipoles by using spiral linear zone plate, *Optical and Quantum Electronics*, 49., 226.
10. Arash Sabatyan and Maryam Fatehi, 2018, Azimuthal-segmented linear zone plate: 1D beam structuring and topological charge detecting, *Journal of Optical Society America B*.
11. Arash Sabatyan, and Jila Rafighdoost,, 2015, Focusing specification of cross-like Fresnel zone plate, *OPTIK*, 126, 2015, Pages 4796–4799.
12. Jila Rafighdoost, and Arash Sabatyan, Remarkable ability of spiral orthogonal zone plate in generating various focused optical vortices, *Optics and Laser in Engineering 86*, 275–280 (2016).
13. Behnaz Roozbeh, Arash Sabatyan, Diffractive analysis of spiral checkerboard zone plate, Optics & Laser Technology 158, 108927 (2023).

IS8

Deep Learning Assisted Design of Metamaterial-Based Terahertz Polarizer

M. Zeki Güngördü[*1,2], Abby Sanders[2], Reefaz Rahman[2], Patrick Kung[2], Seongsin Margaret Kim[2]

[1]Electrical and Electronic Engineering, Igdir University, Igdir, TURKIYE 76000
[2]Electrical and Computer Engineering, University of Alabama, Tuscaloosa, AL, USA 35487
email: mzekigungordu@gmail.com

Abstract: Polarization conversion devices enable electromagnetic waves to be manipulated according to their polarization status in photonics. Artificial intelligence (AI)-based data-driven approaches are revolutionizing nanophotonics by allowing efficient inverse design methods. The development of Terahertz (THz) devices in areas such as communication, imaging, and remote sensing has contributed to the development of technology. We propose using the power of AI for rapid and high-efficiency inverse design of THz stereo-metamaterial polarizers and accelerate the analysis of the desired device.

We applied a stereo-metamaterial (SMM) structure to new-generation THz polarizers, which convert linearly polarized waves to circularly and elliptically polarized waves in reflection mode at the THz frequency range. A technique for the inverse design of SMM is presented, which utilizes an artificial intelligent technique that has been trained with various parameters, including polarization status and ellipticity angle, to determine the most efficient device performance. By training and testing the deep neural network with the created datasets through simulation, design parameters were obtained by employing an artificial EM response or an ellipticity angle spectrum or vice versa more efficiently and rapidly. Utilizing THz polarimetry spectroscopy to detect polarization statuses, the device fabricated based on an ANN-powered design was demonstrated to detect different polarization statuses effectively.

IS9

Deep X-ray Lithography for Optics and Photonics

Marmiroli B.*[1], Turchet A.[2]

[1]*Institute of Inorganic Chemistry, Graz University of Technology, 8010 Graz, Austria*
[2]*Elettra-Sincrotrone Trieste, 34149 Trieste, Italy*
email: benedetta.marmiroli@tugraz.at

Abstract: The creation of novel micro/nano optic and photonic components presenting functional materials in desired areas of the device, requires both the development of tailored materials and the selection of a suitable fabrication process. Deep X-ray Lithography (DXRL) is a lithographic technique based on controlled irradiation of samples using high energy X-rays (1-30 keV). The process allows obtaining high resolution and penetration depth, high aspect ratio (ratio between height and minimum lateral dimension of the structure), vertical sidewalls, and surfaces of optical quality. Many components in the field of micromechanics, microoptics, microfluidics, microelectronics can be fabricated. More recently, DXRL has been employed to irradiate novel materials, changing their structural and functional properties in a selective way [1]. In this communication, we present the latest outcomes of the application of DXRL to tune optical properties of materials (among which Metal Organic Frameworks [2,3]), showing the possibility to fabricate a new generation of microdevices for sensing applications. The research was performed at the DXRL beamline at Elettra-Sincrotrone Trieste (Italy). A short description of the future projects will also be given together with the information on how to get access to the DXRL beamline.

References

1. A. Bharti, A. Turchet, B. Marmiroli, X-Ray Lithography for Nanofabrication: Is There a Future, Frontiers in Nanotechnology. 4. 835701. (2022) https://doi.org/10.3389/fnano.2022.835701
2. M. Tu et al., Direct X-ray and electron-beam lithography of halogenated zeolitic imidazolate frameworks Nat. Mater. 20, 93-99. (2021) https://doi.org/10.1038/s41563-020-00827-x.
3. M. deJ Velásquez-Hernández, M. Linares-Moreau et al., Fabrication of 3D Oriented MOF Micropatterns with Anisotropic Fluorescent Properties, Advanced Materials. 35, 2211478 (2023), https://doi.org/10.1002/adma.202211478

IS10

Interaction and efficiency of three optical pulses in optical fiber

Abdollah Borhanifar*[1]

[1]University of Mohaghegh Ardabili (UMA), Iran
email: aborhanifar@yahoo.com

Abstract: In recent years, femtosecond light pulses are widely used in various fields of science and technology, and the scope of their application is expanding. However, there is only a limited number of wavelengths on which laser data pulses are now generated. The most real way of obtaining light femtosecond pulses on another wavelength is frequency conversion. The goal of the work was to construct conservative difference schemes for the problem of propagation of three femtosecond pulses in an optical fiber described by a system of nonlinear combined Schrödinger equations. Optical fiber uses light pulses instead of electrical pulses to transmit information, thus delivers hundreds of times higher bandwidth than traditional electrical systems.

Light pulse propagation in optical fiber is described by the following wave equation

$$\frac{\partial^2 E(x,t)}{\partial x^2} - \frac{1}{c^2}\frac{\partial^2 E(x,t)}{\partial t^2} = \frac{4\pi}{c^2}\frac{\partial^2 P(x,t)}{\partial t^2},\ 0 < t < L_t,\ 0 < x < L_x$$

With corresponding initial and boundary conditions. Here E(x, t) is an electric field strength, x−coordinate along which the light pulse is propagated, t−time, and are the time interval and medium length correspondingly on which the propagation of waves is investigated, c-light velocity, P describes medium polarization. For the medium with quadratic nonlinear response its polarization can be written as:

$$P(\omega) = \chi(\omega)E + \chi^{(2)}(\omega,\omega)E^2$$

To write the equation for slowly varying amplitude we'll represent electric field strength in the following way

$$E(x,t) = \frac{1}{2}[A_1 e^{i(\omega_1 t - k_1 x)} + A_2 e^{i(\omega_2 t - k_2 x)} + A_3 e^{i(\omega_3 t - k_3 x)}] + c.c.$$

References

1. S. A. Akhmanov, V. A. Vysloukh, and A. S. Chirkin, Optics of Femtosecond Laser Pulses [in Russian], Nauka, Moscow (1988).
2. G. Agrawal, Nonlinear Fiber Optics [Russian translation], Mir, Moscow (1996).
3. A. P. Sukhorukov, Nonlinear Wave Interactions in Optics and Radio Physics [in Russian], Nauka, Moscow (1988).
4. V. A. Trofimov, A. G. Volkov, and S. A. Varentsova, "Influence of dispersion of nonlinear response on self-focusing or femtosecond pulse propagation in optical fiber," in: V. L. Derbov et al. (eds.), Laser Physics and Photonics, Spectroscopy and Modeling II, Proc SPIE, Vol. 4706 (2002), pp. 88–97.

5. S. A. Varentsova and V. A. Trofimov, “Invariants of nonlinear interaction of femtosecond laser pulses with third-order dispersion,” Zh. Vychisl. Matem. Mat. Fiziki, 42, No. 5, 709–717 (2002).
6. V. A. Trofimov, “A new approach to modeling nonlinear propagation of supershort laser pulses,” Zh. Vychisl. Matem. i Mat. Fiziki, 38, No. 5, 835–839 (1998).
7. A. A. Samarskii, Theory of Difference Schemes [in Russian], Nauka, Moscow (1977).
8. A. Borhanifar and V. A. Trofimov, “Comparing the efficiency of various approaches to computer simulation of nonlinear interaction of three femtosecond pulses in an optical fiber,” Vestnik MGU, ser. Vyschisl. Matem. Kibern., No. 2 (2004).
9. V. A. Trofimov and A. Borhanifar, “Conservative difference schemes for three waves interaction of femtosecond pulses in optical fiber,” Mathematical Modeling and Analysis, Troka

IS11

Production and characterization of amorphous Silicon thin film solar cells on flexible substrates

Zeynep Demircioğlu[1]

[1]*Tübitak, SAGE, Mamak PDM Pk. 16, 06484, Ankara, Türkiye*

Abstract: Thin film photovoltaic (PV) panels are promising technologies in the PV market due to their low production costs and other advantages such as heat resistance and indirect radiation performance. Thin-film photovoltaic panels can be fabricated not only on rigid substrates but also on flexible substrates. Flexible solar cells have many advantages due to their flexibility, light weight, mobility and easy transportation. In this study, thin film growth and laser processes on flexible substrates in plasma-assisted chemical vapor deposition (PECVD) chambers were optimized. The properties of a-Si:H thin film for flexible solar cells, a novel surface process by direct laser writing to obtain surface texture on transparent conductive oxide thin film, and a monolithic series-connected flexible solar module from a single-junction solar cell are presented. The scope of the presented work is to investigate different laser wavelengths of surface texturing for flexible solar cell fabrication are investigated. Aluminum-doped zinc oxide (AZO) films were deposited on flexible substrates for photovoltaic applications and the roughening of this layer was studied by a novel method. The effects of different laser wavelengths on the roughening of the AZO layer are comparatively presented.

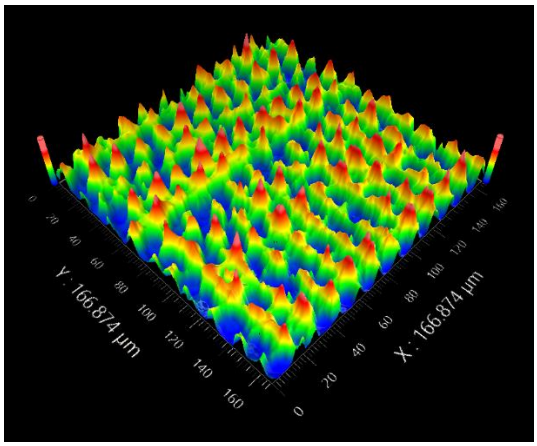

Figure 1. Laser-textured AZO thin film at 532 nm wavelength

Keywords: Flexible Solar Cell, Amorphous Silicon, PECVD, Sputtering, Laser Processing

IS12

How to make optical and electrochemical sensors with laser

Manshina A.A.*[1], Vasileva A.A.[1], Levshakova A.S.[1], Khayrullina E.M.[1], Bikbaeva G.I.[1]

[1]*Institute of chemistry, St Petersburg state university, 26 Universitetskii prospect, Petergof, St. Petersburg, Russia*
email: a.manshina@spbu.ru

Abstract: General urgent tasks of modern society are detection and identification of wide list of analytes important in healthcare, ecology, food safety, security, etc. Optical and electrochemical sensors are considered nowadays as the most promising for the listed problems. Performance of modern optical and electrochemical sensors is based on nanostructured materials having plasmonic response (for SERS optical sensors) or electrochemical response (for electrochemical sensors). Thus, the key requirements for optical and electrochemical sensors are creation of substrates controllably decorated with metal nanoparticles that are SERS or electrochemically active.

Here we present laser-induced deposition (LID) as an all-purpose approach for fabrication of optical and electrochemical sensors. LID is based on illumination of substrate/solution interface with laser irradiation followed by formation of metal nanoparticles (NPs) in the laser-affected area of the substrate. Liquid phase here is a solution of various metal precursors (metalorganic complexes or salts) thus providing diversity of the deposited metals. Metal NPs are formed because of heterogeneous laser-induced redox process occurring at the substrate surface. Variation of type of metal precursor, its concentration, solvent, laser wavelength and laser illumination time provides fine-tuning of deposits morphology and functionality. LID process allows decoration with NPs of various substrates – amorphous, crystalline, including flexible polymers, and even 3D substrates – such as Si nanowires and anodic alumina membranes. Functionality of LID-decorated substrates were demonstrated as SERS sensors for toxins and bioanalytes, and electrochemical sensors for glucose, paracetamol, dopamine, etc [1-4].

This work was supported by RSF project 23-49-10044. Authors are grateful to “Centre for Optical and Laser materials research” and ‘‘Interdisciplinary Resource Centre for Nanotechnology’’ Research Park of Saint Petersburg State University for technical support.

References

1. O. Eremina et al. Talanta, 266, 2024, 124970
2. A. Levshakova et al. Materials 16, 2023, 7225
3. A. Vasileva, et al. Nanomaterials 13 (6), 2023, 1002
4. A. Vasileva, et al. Nanomaterials 13 (1), 2023, 88

IS13

Tailored Light Beams: An Innovative Approach in Micromachining

Morova B.*[1]

[1]*Physics Engineering Department, Istanbul Technical University, 34469 Sariyer Istanbul, Türkiye*
email: bmorova@itu.edu.tr

Abstract: Ultrashort laser pulses have become essential tools across various scientific fields. These pulses offer unique temporal resolutions for studying phenomena occurring within similar time frames. Moreover, concentrating optical energies into such brief time intervals results in extraordinarily high peak powers and intensities, facilitating novel light-matter interactions. Also, recent advancements in spatial light intensity and phase modulation devices enable the creation of laser beam profiles with remarkable physical properties. By combining these advancements, optics researchers now possess the capability to manipulate light both spatially and temporally, unlocking new realms of physical interactions and greatly enhancing laser applications.

Commonly used beam classes can be summarized as non-diffracting beams like Bessel and Airy beams, optical vortices and other beam types such as regular polygon beams. Bessel and Airy beams provide long propagation distances without changing the profile in comparison to Gaussian beams due to their non-diffractive nature and they exhibit self-reconstruction property [1-2]. Differently from the Bessel beams, Airy beams propagates with acceleration even in free space [3]. These unique properties of Bessel and Airy beams make them extremely useful for a wide range of applications such as laser microfabrication [4], where precise control over the focal spot size and intensity distribution is essential. While tailored beams can be used to manufacture 3D structures in transparent materials without the need for sample scanning, thereby avoiding additional scattering losses, they also provide nano-scale fabrication by overcoming the practical obstacles such as near-diffraction-limit focusing or optical aberrations. Here, we present a scheme for generating high-quality, high-power non-diffractive beams and discuss their interaction with various materials. Our results show that there are many potentials for the use of beam shaping both for fundamental studies and for enhancing or enabling certain light-matter interactions.

Acknowledgement: This work was supported by Scientific Research Projects Department of Istanbul Technical University. Project Number: 44400.

References

1. J. Durnin, J. Opt. Soc. Am. A 4, 651-654 (1987).
2. J. Broky, G. A. Siviloglou, A. Dogariu, and D. N. Christodoulides, Opt. Express 16, 12880–12891 (2008).
3. G. A. Siviloglou, J. Broky, A. Dogariu, and D. N. Christodoulides, Phys. Rev. Lett. 99, 213901–4 (2007).
4. F. Courvoisier, P.-A. Lacourt, M. Jacquot, M. K. Bhuyan, L. Furfaro, and J. M. Dudley, Optics Letters 34, 3163–3165 (2009).

IS14

Technological Roadmap of KalyonPV R&D Center

Alihan KUMTEPE[1,2], Nesrin TÖRE ŞEN[1]

[1]Kalyon PV Research and Development Center, Kalyon Güneş Teknolojileri Üretim A.Ş., Ankara, Turkey
[2]Department of Photonics, Faculty of Applied Sciences, Gazi University, 06560 Ankara, Turkey

Kalyon Solar Technologies Factory (Kalyon PV) is a production facility for the integrated production of crystalline silicon solar modules by starting from poly-silicon. As Europe's first producer of ingots for the M10 size cell, it is a significant contribution to the advancement of solar energy technologies not only in Turkey, but also throughout Europe. For four years, it has been continuously producing modules from crystalline silicon (c-Si) ingot production with the CZ (Czochralski) method and has been continuously developing in this field. The know-how gained in this process has played an important role in the process of developing Kalyon PV's technological capabilities. Kalyon PV carries out many national and international projects as an R&D Center with the vision of carrying the knowledge gained in c-Si production to a further level.

In this study, Kalyon PV's roadmap and projects including research and development activities are presented. The R&D roadmap consists of four stages. The first phase includes domestic seed and EPE film production, loss analysis and recycling studies. In the second phase, small-scale BIPV installations and the establishment of a new generation photovoltaic cell laboratory are targeted. The third phase focuses on floating photovoltaic system installation and N-type ingot/wafer production. In the fourth phase, studies on PV/T systems and green hydrogen were targeted and a presentation was made on Kalyon PV's domestic production achievements and innovative R&D activities.

IS15

Diffraction from periodic structures, Talbot effect, and beam shaping

Saifollah Rasouli*[1,2]

[1]*Department of Physics, Institute for Advanced Studies in Basic Sciences (IASBS), Zanjan 45137-66731, Iran*
[1]*Optics Research Center, Institute for Advanced Studies in Basic Sciences (IASBS), Zanjan 45137-66731, Iran*
email: rasouli@iasbs.ac.ir

Abstract: In optics, a grating device has been known for many years and is one of the most widely used optical components. The gratings have a periodic transmission or reflection structure and can disperse a beam of various wavelengths into a spectrum of associated lines. Therefore, a grating is used as a light-dispersing part in spectroscopy. This feature of the grating is due to the diffraction pattern of the far field of the grating. Another interesting feature of diffraction from one-dimensional (1D) and two-dimensional (2D) periodic structures is related to their near-field diffraction. When light passes through a periodic structure, the distribution of the optical field immediately after the structure is reproduced at certain distances from it. This phenomenon is called the Talbot effect. Since no imaging system is used in this field distribution reconstruction, it is also called a self-imaging phenomenon. This effect is created in the near field diffraction region and from the superposition of different diffraction orders of the structure. For this reason, this diffraction pattern changes under propagation rapidly, and as long as the diffraction orders overlap, this phenomenon will be seen.

This lecture presents the Talbot effect under the diffraction of a plane wave from 1D and 2D periodic structures. Then it is shown that if 1D and 2D periodic structures are illuminated with structured light beams like Laguerre-Gaussian (LG) beams, an array of LG beams or Hermit-Gaussian modes can be produced in certain Talbot planes. In addition, a new diffractive optics component, say Almost Periodic Structures (APSs) is introduced and it is shown that these structures can be used for the generation/multiplication of structured beams in an array at the far field diffraction region. The production of an array of vortex beams at Talbot planes/far-field is used in various fields, especially in optical lithography, multiple particles/atoms trapping, and multiple particle manipulation.

Finally, the diffraction of plane wave and Gaussian beam from radial gratings with different transmission profiles will be presented and it will be shown that due to the presence of phase singularity in the center of the radial structures, their diffraction patterns lead to the generation of a large family of solutions to the wave equation that they are known as Combined half-integer Bessel-like beams, which themselves include the family of radial carpet and petal-like beams, and so on.

IS16

Optical Metrology: 3D Imaging

Ehsan Ahadi-Akhlaghi*[1]

[1]*Department of Physics, Institute for Advanced Studies in Basic Sciences (IASBS), Zanjan, Iran*
email: e.a.akhlaghi@iasbs.ac.ir

Abstract: The research group at the Institute for Advanced Studies in Basic Sciences specializes in optical metrology, focusing on advanced techniques such as fluorescence microscopy, diffractometry, and the design of optical measurement devices. Our group places special emphasis on the development and application of 3D imaging systems, including Phase Shift Interferometry, Digital Holography Microscopy (DHM), and Optical Coherence Tomography (OCT). These systems play a crucial role in research related to biological sample analysis and industrial measurements, offering precise and non-invasive imaging solutions.

Our objective is to advance optical metrology by enhancing the accuracy and accessibility of these techniques. The group explores innovative methods such as using microspheres to improve image resolution and applying digital holography for real-time imaging. Research in Phase Shift Interferometry has led to significant advances in surface profiling and thickness measurement. Meanwhile, the development of DHM and OCT has expanded the capabilities of imaging systems in medical diagnostics and materials science.

Beyond technical achievements, the group is dedicated to furthering the understanding and application of optical metrology through interdisciplinary collaboration and knowledge dissemination. They work closely with academic institutions, industrial partners, and research organizations to translate their findings into practical solutions for real-world challenges. The group's efforts have resulted in the creation of new optical devices and systems, enhancing the accuracy and efficiency of measurements and ultimately benefiting both scientific research and industrial processes.

IS17

The investigation of basic physical parameters, energy dependent profiles of interface traps (N_{ss}) and their lifetimes (τ) of the Au/n-Si structurers with (PVA-Fe_3O_4) interlayer

Şemsettin Altındal*[1]

[1]*Department of Physics, Faculty of Science, Gazi University, Ankara-Turkey*

Abstract: In this article, the capacitance/conductance-voltage-frequency (C/G-V-f) measurements of the fabricated Au/(PVA-Fe_3O_4)/n-Si Schottky diodes (SDs) were carried out in wide range of frequency (100 Hz-1 MHz) and voltage (±3 V). Some important electrical parameters of SD such as diffusion-potential (V_D), Fermi energy (E_F), barrier-height (F_B), depletion layer (W_D), maximum electric field (E_m) were extracted from the reverse bias C^{-2}-V plots for various frequency. The voltage dependent profiles of the surface states (N_{ss}) were obtained from high-low frequency capacitance (C_{hf}-C_{lf}), Hill-Coleman, and parallel conduction methods and compared each other. The voltage dependent profile of resistance (R_i-V) was also extracted from the E. H. Nicollian & J. R. Brews for each frequency. All experimental results are indicated that all these electrical parameters are strong function voltage and frequency due to the existence of N_{ss}, their lifetimes (τ), interlayer, series resistance (R_s), interface and dipole polarizations. But, while N_{ss} are effective especially in depletion and inversion regions, R_s is effective only at accumulation region at enough high frequency.

Keywords: Organic interlayer; Au/(PVA-Fe_3O_4)/n-Si Schottky diodes; Frequency/voltage dependence; Conductance method; Surface states (N_{ss})

IS18

Environmental Photonics: From Ultrafast IR Laser Materials Processing for Photovoltaics to Trace Molecule Detection

Arian GOODARZI[1], Ghazanfar Ali KHAN[2], Waqqar AHMED[2], Ihor PAVLOV[1,3], Alpan BEK[1, *3]

[1] *Center for Solar Energy Research and Applications, ODTÜ-GÜNAM, Ankara, Turkey*
[2] *Department of Physics, COMSATS University, Islamabad, Pakistan*
[3] *Department of Physics, Middle East Technical University, Ankara, Turkey*
email: bek@metu.edu.tr

Abstract: Environmental photonics is a developing field of research. Any environmental challenge taken by the light science and technology finds itself in the realm of this field. In this context, both already highly advanced field of photovoltaics research and still developing research fields of optical trace molecule detection, light-based decontamination, and mitigation of environmental pollutants can be listed under the interests of environmental photonics. And this list is only a very partial one. One fact worth to mention is that developing new photonic technologies for the already well-established and highly advanced fields of research such as photovoltaics is more challenging than for the upcoming fields of research. In this respect, two applications of what ultrafast-laser based materials processing technology may have to offer for the photovoltaics research will be presented. Both of the two examples are about ultra-fast laser based fabrication of improved light management interfaces for photovoltaic panels, first being directly applied on the very solar cell surfaces (Fig. 1a), the other applied on the solar panel glass surface (Fig. 1b).

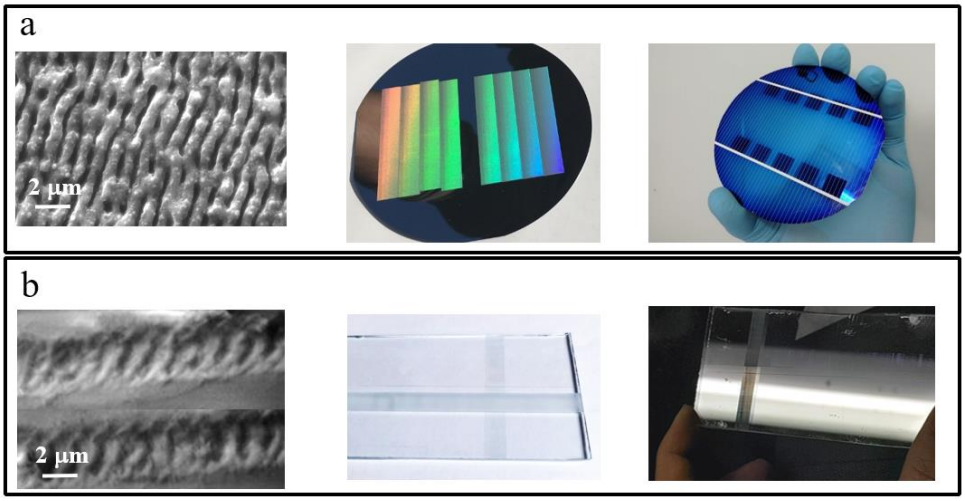

Figure 1. a) Ultra-fast laser modified surface of a Si solar cell, SEM view, wafer and finished test cells. b) Ultra-fast laser modified panel glass surface, SEM, day light and reflection images.

Additionally, several examples from the research line of surface enhanced Raman spectroscopy based trace molecule detection and decontamination will be

presented as examples of what other environmental challenges can be tackled with photonics technology [1, 2].

References

1. S. N. Erkizan, F. İdikut, Ö. Demirtaş, A. Goodarzi, A. K. Demir, M. Borra, I. Pavlov., A. Bek, Advanced Optical Materials, 10 (2022) 22.
2. G. A. Khan, Ö. Demirtaş¸ A. Bek, W. Ahmed, Materials Science and Engineering B, 297 (2023) 116737.

IS19

Structural dynamics in photo-responsive crystalline film systems: a multi-technique approach

Sumea Klokic*[1,2], Benedetta Marmiroli[2], Giovanni Birarda[3], Barbara Sartori[2], Simone Dal Zilio[4], Lisa Vaccari[3], Paolo Falcaro[5], Heinz Amenitsch[2]

[1]CERIC-ERIC, SAXS Beamline, S.S. 14, 163.5 km, Basovizza, Trieste 34149, Italy
[2]Institute of Inorganic Chemistry, Graz University of Technology, 8010 Graz, Austria,
[3]Elettra Sincrotrone Trieste, SISSI Beamline, S.S. 14, 163.5 km, Basovizza, Trieste 34149, Italy
[4]IOM-CNR, Laboratorio TASC, S.S. 14, 163.5 km, Basovizza, Trieste 34149, Italy
[5]Institute of Physical and Theoretical Chemistry, Graz University of Technology 8010 Graz, Austria
email: sumea.klokic@elettra.eu

Abstract: The design of responsive crystalline structures capable to react to external stimuli, such as light, while maintaining a controllable structural response holds significant promise for advancing applications like mechanical energy storage, drug delivery or gas sequestration.[1] One key challenge, particularly in film systems, lies in accurately characterizing both the magnitude and duration of the induced structural photo-response. These aspects are vital for tailoring structures with adjustable response kinetics that can be triggered remotely.

Using epitaxially grown metal-organic framework model film systems as a case study,[2-4] we reveal that the dynamic behaviour is intricately linked to crystallite geometry, morphology, and chemical composition. Consequently, employing a multi-technique approach becomes essential to unravel these interdependencies and infer the timescale of the initiated dynamics. In this context, we showcase the efficacy of time-resolved grazing incidence X-ray scattering and infrared spectroscopic techniques in precisely quantifying the structural response when triggered by light. Results demonstrate that such photo-responsive crystalline structures are attractive candidates for mechanical energy storage or in gas sequestration (such as CO2). Our findings pave the way for a deeper understanding of timescales and responsive behaviours in similar or more advanced soft-matter film systems, offering a new avenue for research in this field.

References

1. Klokic, S., Naumenko, D., Marmiroli B., Carraro, F., Linares Moreau, M., Dal Zilio, S., Birarda, G., Kargl, R., Falcaro, P., Amenitsch, H., Chem. Sci., 2022, 13, 11869-11877.
2. Klokic, S., Marmiroli B., Naumenko, D., Birarda, G., Dal Zilio, S., Velasquez-Hernandez, M.-J., Falcaro, P., Vaccari, L., Amenitsch, H., accepted in CrystEngComm, 2024.
3. Linares-Moreau, M.; Brandner, L.; Kamencek, T.; Klokic, S.; Carraro, F.; Okada, K.; Takahashi, M.; Zojer, E.; Doonan, C.; Falcaro, P. Adv. Mater. Interfaces 2021, 8 (21), 2101039.

4. Klokic, S., Marmiroli B., Birarda, G., Holzer, P., Sartori, B., Asbaghi-NA, B., Dal Zilio, S., Vaccari, L., Amenitsch, H., to be submitted, March 2024.

IS20

Ultra-cold Rydberg Atoms and Quantum Technologies

Sevilay Sevinçli[1]

[1]*Department of Photonics, İzmir Institute of Technology,* Gülbahçe Campus, 35430 Urla, İzmir *Türkiye*

Abstract: Rydberg atoms are atoms that are excited to very high principal quantum numbers. These atoms, which can be cooled to ultra-cold temperatures, have become the focus of interest in many theoretical and experimental studies due to their extraordinary features, such as extreme sensitivity to external fields and strong interactions among themselves. The combination of Rydberg gases and quantum coherence phenomena such as Electromagnetically Induced Transparency (EIT) enables very high nonlinear effects for applications such as slowing and storing light. These nonlinear effects, which are difficult to observe in conventional environments with low-intensity light sources, can be achieved in this system at a level that can provide effective interaction between photons even for low intensities. Therefore, Rydberg atoms provide an excellent environment for nonlinear optical effects such as the giant Kerr effect and single-photon generation.

Moreover, the ability to trap Rydberg atoms in optical lattices has opened up new opportunities for examining many-body problems. Quantum simulation, which aims to solve many-body problems in complex systems with more accessible systems, has succeeded as a new tool. With their strong correlations and manipulability, Rydberg atoms are also perfect candidates for this task.

In this talk, we will first introduce the nonlinear optical effects that can be achieved with cold Rydberg-EIT systems. Then, we will focus on our work on a three-photon excited Rydberg-EIT system and the Electromagnetically Induced Absorption (EIA) phenomenon which is a similar quantum coherence effect. We present a self-consistent many-body model to study interacting Cs and Rb atomic ensembles in a four-level ladder-type scheme with EIT and EIA effects[1]. The many-body simulation produces results that agree with recent experiments[2,3] and shows an EIT-EIA cross-over in the Rb case, as in the experiment[3]. We manage to simulate the interaction effects in such systems that have significant importance, especially for controlling the optical response of these systems. Our proposed method offers a new way of understanding these quantum coherence phenomena deeply, and further investigation on susceptibilities for nonlinear effects might provide insight into quantum technology applications.

**This work is supported by the Scientific and Technological Research Council of Turkey (TUBITAK) under Grant No. 117F372.*

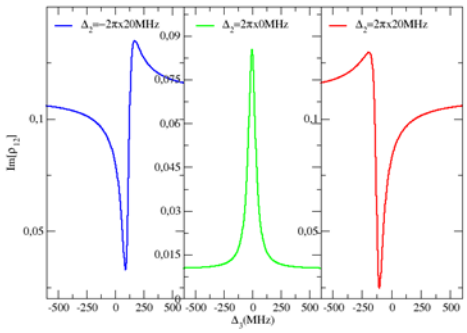

EIT-EIA crossing for different coupling detunings.

References

1. Oyun Y, Çakır Ö and Sevinçli S (2022), J. Phys. B: At. Mol. Opt. Phys. 55, 145502.
2. Šibalić N, Kondo J M, Adams C S and Weatherill K J (2016), Phys. Rev. A 94, 033840.
3. Thaicharoen N, Moore K R, Anderson D A, Powel R C, Peterson E and Raithel G (2019), Phys. Rev. A 100, 063427.

SPEAKERS

S1

Synchrotron Radiation for Structural Biology

B. Sartori*[1], A. Radeticchio[1], R. Haider[2], H. Amenitsch[1]

[1] *Graz University of Technology, Institute of Inorganic Chemistry, Stremayrgasse 9/IV, Graz, Austria*
[2] *MedAuston, Marie Curie-Strasse 5, A-2700 Wiener Neustadt, Austria*

email: barbara.sartori@tugraz.at

Abstract: Biological systems in solution are composed of ensambles of macromolecules, which can be arranged in several conformational states. Synchrotron SAXS can provide insights on their structural features in response to external stimuli, or intermolecular interactions: the low exposure time and the possibility to install dedicated instrumentation for high throughput measurements at the beamline, are remarkably beneficial. We will descibe two setups dedicated mainly to the analysis of biological samples currently available at the SAXS beamline @ Elettra synchrotron, Trieste. The first is the µdrop[1,2,3], a liquid handler coupled with a thermostated fixed observation cell equipped with a wash-and-dry system for hight throughput measurements. The second is the SEC-SAXS system, which combines a liquid chromatography separation column coupled with UV, Multi Angle Light Scattering and Refractiv Index detectors with SAXS, for comprehensive structural analysis of protein samples.

Besides the description of the systems we will show experimental results obtained on biological samples.

References

1. Haider, R., Sartori, B., Radeticchio, A., Wolf, M., Zilio, S.D., Marmiroli, B., Amenitsch, H. µDrop: A system for high-throughput small-angle X-ray scattering measurements of microlitre samples, Journal of Applied Crystallography, 54, (2021), pp. 132-141.
2. Ramírez, M.D.L.Á., Bindini, E., Moretti, P., Soler Illia, G.J.A.A., Amenitsch, H., Andreozzi, P., Ortore, M.G., Moya, S.E., Impact of PEGylation on the degradation and pore organization in mesoporous silica nanoparticles: A study of the inner mesoporous structure in physiologically relevant ionic conditions, Colloids and Surfaces B: Biointerfaces, 219, (2022), art. no. 112797.
3. Quagliarini, E., Renzi, S., Digiacomo, L., Giulimondi, F., Sartori, B., Amenitsch, H., Tassinari, V., Masuelli, L., Bei, R., Cui, L., Wang, J., Amici, A., Marchini, C., Pozzi, D., Caracciolo, G. Microfluidic formulation of dna-loaded multicomponent lipid nanoparticles for gene delivery, Pharmaceutics, 13 (8), (2021), art. no. 1292

S2

Intersection behavior in the forward bias I-V curves and current transport mechanisms (CTMs) in the Al/Al_2O_3/Ge/p-Si heterostructures in temperature range of 90-420 K

A. Hameed Sabreen*[1], Akın Buket[2], Altındal Yerişkin Seçkin[3]

[1*]*Department of Physics, College of Science, University of Diyala, Diyala, Iraq,*
email: sabreenalhameed19@gmail.com
[2]*Department of Physics, Gazi University, 06560, Ankara, Türkiye,*
email: buket.akın1@gazi.edu.tr, bktakn90@gmail.com
[3]*Department of Chemistry and Chemical Processing Technologies, Vocational High School of Technical Sciences, Gazi University, Ankara, Türkiye,*
email: seckinyeriskin@gazi.edu.tr

Abstract: The possible current-transport-mechanisms (CTMs) in the Al/Al_2O_3/Ge/p-Si hetero-structures have been investigated by using the current-voltage (I-V) measurements in wide temperature range of 90-420K as detail. The temperature-response/sensitivities (S), energy dependent profile of surface states/traps (N_{ss}, D_{it}) were also investigated in whole temperature range. Some important electrical parameters of the structure like reverse saturation current (I), ideality-factor (n), zero-bias barrier height (BH), (Φ_{Bo}), series resistance (R_s) values were extracted from the I-V data for each-temperature. The semilogarithmic I-V plot has two different linear-parts which are corresponding to the lower and moderate forward bias voltages. While the value of Φ_{Bo} increases with increasing-temperature, n decreases and also the conventional Richardson-plot deviated from linearity at lower-temperatures. The measurements Richardson-constant (A*) value from the linear part of the Richardson-plot was also found very lower than its theoretical value. Such behavior of them and higher values of n are indicated that a devoted from the TE theory. Therefore, Φ_{Bo}-n, Φ_{Bo}-q/2kT, and n.(kT)/q-(kT/q) plots were drawn to find some evidences to the existence other possible CTMs such as tunneling (TFE and FE) and Gaussian-distribution (GD) BHs., The value of S=dV/dT for 0.01, 0.10, 0.50, and 1μA was found as 2.30, 2.33, 2.34, and 2.35 mV/K which are indicated that the fabricated Al/Al_2O_3/Ge/p-Si hetero-structure is very sensitive to temperature and so it can be used in photo-diodes, solar cells, and temperature-sensor applications. The observed crossing point at 2.4V was explained by an increase of the apparent BH with increasing temperature and the existence of R_s.

Keywords: Current transport mechanisms (CTMs); Intersection behavior in the forward bias I-V; Temperature response/sensitivity; Energy dependent of surface states, Double Gaussian.

S3

Raman OTDR Based Distributed Temperature Sensing for Environmental and Structural Monitoring

Yalçın Buğra*[1], Yıldız Gülşah[1], Kartaloğlu Tolga[1], Özbay Ekmel[1,2,3], Özdür İbrahim[1,4]

[1]Nanotechnology Research Center, Bilkent University, Ankara 06800, Türkiye
[2]Department of Electrical and Electronics Engineering, Bilkent University, Ankara 06800,Türkiye
[3]Department of Physics, Bilkent University, Ankara 06800, Türkiye
[4]Department of Electrical and Electronics Engineering, TOBB University of Economics and Technology, Ankara, Türkiye

email: bugra.yalcin@bilkent.edu.tr

Abstract: Temperature sensing for environmental and structural monitoring is of utmost importance for certain applications, e.g., monitoring of wildfires, gas pipelines, electric lines, temperature of facilities such as nuclear reactors, etc. Conventional devices to measure temperature along many kilometers is not cost effective, and is unpractical to install each measurement device. The solution heralded was to utilize back scattered Raman signal inside the optical fiber to measure temperature, as the Raman scattering is manifestation of interaction of light with optical phonons. Each scattering point along the fiber serves as an individual sensing point, and for that reason this technology is called 'Distributed Temperature Sensing' (DTS). However, problem with Raman OTDR based DTS is originated due to Raman signal being weak as much as 70 dB below the launched optical power, resulting a low signal-to-noise ratio (SNR). Increasing optical power is not viable because of optical nonlinearities. To overcome this problem, advanced noise filtering techniques and interrogation methods should be used. In this study, noise resources of the system is analyzed and extensive approaches are implemented for noise suppression, including wavelet transformation based noise filtering. For the future study, an advanced interrogation method - so called "pulse coding" will be adopted for better system performance. Pulse coding is a method in which involves amplitude modulation of the laser, based on a predetermined code-word. This way, more than one pulse can be present during each interrogation, thus, an increased luminous flux can be achieved accompanied with higher SNR. Optimizing the SNR enables longer sensing distance and higher temperature accuracy performance in Raman OTDR based DTS systems.

S4

Design of All-Fiber Er-Doped ASE Source for Fiber Optic Sensors

Erkut Emin AKBAŞ*[1], Aylin YERTUTANOL[1], Ekmel ÖZBAY[1,2], Yashar AZİZİAN-KALANDARAGH[3,4]

[1] *Nanotechnology Research Center-NANOTAM, Bilkent University, Ankara, Türkiye*
[2]*Department of Electrical and Electronics Engineering, Bilkent University, Ankara, Türkiye*
[3]*Photonics Application and Research Center, Gazi University, 06560 Ankara, Türkiye*
[4]*Department of Photonics, Faculty of Applied Sciences, Gazi University, 06560 Ankara, Türkiye*

email: erkut.akbas@bilkent.edu.tr

Abstract: The area of the Er-doped fiber ASE (Amplified Spontaneous Emission) sources has led to research in the fiber optics technology in the foreground in a relatively short period. ASE sources has increased utility as an important component in many optical areas. ASE source is preferred due to optical wavelength close to 1550 nm provides light-efficient, low-noise in many areas. ASE sources can be used both in digital and analog applications. Rare-earth doped fibers also are used for applications as sensors and broadband sources for fiber gyroscopes [1].

In this study, we measured spectrum of ASE source with 10 m Er-doped fiber and these results compared with commercial 50 nm SLED (Super Luminescent Diode) source for fiber optic gyroscope applications. Wavelength characterization of ASE source depends on temperature is studied. ASE source is analyzed by measuring the wavelength under temperature changes. We investigate the temperature characterization of Er-doped all-fiber ASE source and SLED. Since the all the components which are inside the commercial products, are exposed to heat, the setup is made while all-fiber components were placed inside of the climatic chamber.

In summary, in this paper we have analyzed a temperature characterization of all-fiber Er-doped ASE Source and commercial 50 nm SLED. According the results all-fiber ASE source has shown a more stable attitude in the range of -10 / +60 °C. Although there is no significantly RMS changes in total, the noise of instant RMS changes too much. Due to this huge instant RMS changes it is hard to make an algorithm to compensate this fluctuation. Also after +70 °C SLED is not a good source for industrial application. Thus, we present a stable and algorithm applicable all-fiber Er-doped ASE source with almost maximum 15 % loss in 70 °C temperature range.

References

1. J.F. Digonnet (Ed.); Marcel Dekker Inc., New York, Basel, 2001.

S5

Optimization of photolithography exposure by Lenslets

Mollaei Mina*[1], Mahmoudi Samad[2], Malek Mohammadi Milad[3], Azizian-Kalandaragh Yashar[4,5], Jabbar pour Mahmoud[3], Ahadi Akhlaghi Ehsan[1,2,3]

[1]Department of Physics, Institute for Advanced Studies in Basic Sciences (IASBS) 444 Prof Yousef Sobouti Blvd, Zanjan 45137-66731, Iran
[2]Science and Technology Park, Institute for Advanced Studies in Basic Sciences (IASBS) 444 Prof. Yousef Sobouti Blvd., Zanjan, Iran, Postal Code: 45137-66731
[3]Optics Research Center, Institute for Advanced Studies in Basic Sciences (IASBS), 444 Prof Yousef Sobouti Blvd, Zanjan 45137-66731, Iran
[4]Department of Physics, University of Mohaghegh Ardabili, P.O. Box 179, Ardabil, Iran
[5]Photonics Application and Research Center, Gazi University, 06560 Ankara, Türkiye

email: minamollaei@iasbs.ac.ir, e.a.akhlaghi@iasbs.ac.ir

Abstract: In this paper, we present a method for optimizing the illumination of gradient exposure photolithography using lenslets. The necessity of gradient exposure lithographyis to illuminate uniformly the mask. The use of lenslet in the photolithography setup helped us to improve uniform exposure, optimize the setup, adjust elevation, and create patterns.The implemented method was used to produce microlenses with a more accurate curved surface. The height and distortion of the lenses were measured using a non-contact profilometer.

Keywords: Diffraction, Profilometer, Photolithography, Binary mask, Microlens, Lenslet

S6

Impact of Astigmatism on diffractive features of spiral checkerboard zone plate

Javidi B. *1, Sabatyan A.2

Physics Department, Urmia University,Urmia,Iran
email: Javidibehnaz76@gmail.com, a.sabatyan@urmia.ac.ir

Abstract: In this research work, we aim to study the effect of astigmatism aberration on the diffractive behavior of spiral checkerboard zone plate (SChZP). To this end, the element is tilted with respect to the incident beam. The tilt causes the cylindrical symmetry of the system removed which is because of imposing an astigmatism on the system. Having been mathemathically analyzed, we showed that a ring-liked shaped beam at the focus transformed into Hermite beams of order of topological charge. In the other words, an interference pattern is formed at the focal plane, as the number of dark fringes equals topological charge and its direction gives the sign of the charge. Simulation and the corresponding experiments were carried out for a variety of spiral SChZPs carrying different topological charges

By analyzing the interference patterns, we were able to determine not only the magnitude, but also the sign of the topological charge. It demonstrate that this method provides an easy way to measure the charge of optical vortices.
Our method may also propose and opens a new way to diffractometer or optical metrology base on diffraction.

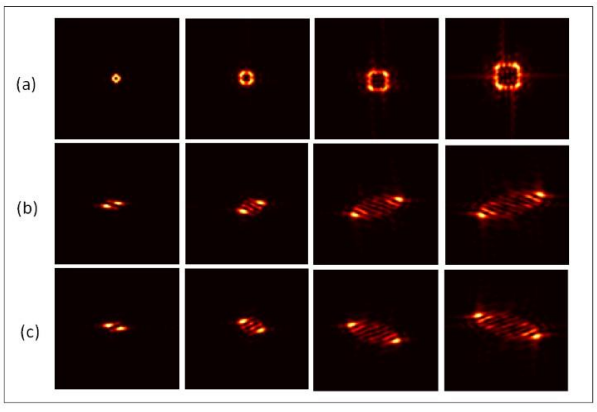

Figure 1. The simulated intensity distribution of four spiral checkerboard zone plates with positive topological charges of 1, 3, 6, and 8, arranged from left to right. a) The intensity distribution without using astigmatism, b) with the implementation of astigmatism, and c) with astigmatism applied to elements with the same charge but negative in sign.

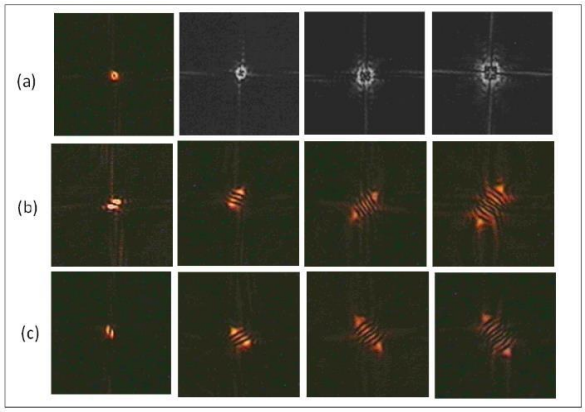

Figure 2. The experimental recorded intensity distribution of four spiral checkerboard zone plates with positive topological charges of 1, 3, 6, and 8, arranged from left to right. a) The intensity distribution without using astigmatism, b) with the implementation of astigmatism, and c) with astigmatism applied to elements with the same charge but negative in sign.

S7

The investigation of frequency dependent electrical parameters and density distribution of interface-traps (D_{it}) of the Au/(ZnO:CeO_2:PVP)/n-Si (MPS) Schottky diodes (SDs) by utilizing impedance spectroscopy model in the frequency range of 2kHz-1MHz

Ozcelik U. [*1,2,3], Altindal S.[1]

[1]*Department of Physics, Graduate School of Natural and Applied Sciences, Gazi University, 06560 Ankara, Türkiye*
[2]*Photonics Department, Applied Science Faculty, Gazi University, 06560 Ankara, Türkiye*
[3]*Photonics Application and Research Center, Gazi University, 06560 Ankara, Türkiye*
email: ugurozcelik@gazi.edu.tr

Abstract: The basic electrical parameters and density-distribution of interface-traps (D_{it}) of the prepared Au/(ZnO:CeO_2:PVP)/n-Si (MPS) type Schottky diodes (SDs) have been investigated by utilizing impedance-spectroscopy model in the frequency range of 2kHz-1MHz and voltage range of ±4.5V. The density of doping donor atoms (N_d), Fermi-energy (E_F), barrier height (Φ_B), and depletion layer width (W_d) were calculated from the reverse bias C^{-2}-V plots as functions of frequency. The energy dependent profile of interface-traps (D_{it}) and their relaxation-times (τ) were extracted from admittance/conductance model which is known to be the most reliable and accurate model when compared with other C-V models. To eliminate the effect of series-resistance (R_s), the measured high frequency capacitance-voltage (C-V) and conductance-voltage (G/w-V) curves were corrected by using Nicollian-Brews method. Experimental results indicated that D_{it} is effective both in weak inversion and depletion regions at low-intermediate frequencies, R_s is effective only at accumulation region at high-frequencies.

Keywords: Frequency dependent electrical parameters; Density of interface traps; voltage dependent profile of resistance (R_i); Low-high frequency capacitance and admittance models.

S8

Improving Illumination and Enhancing the Accuracy of White Light Interferometry Using Array Lenses

Khanjani M. [*1], Hassanzad F.[1], Malek-Mohammadi M.[1], Ahadi Akhlaghi E.[1,2]

[1]*Department of Physics, Institute for Advanced Studies in Basic Sciences (IASBS), Zanjan 45137-66731, Iran*
[2]*Optics Research Center, Institute for Advanced Studies in Basic Sciences (IASBS), Zanjan 45137-66731, Iran*
email: e.a.akhlaghi@iasbs.ac.ir

Abstract: In this research, we introduce a setup to achieve uniform illumination for microscopy applications, as well as enhanced visibility for interferometric measurements. To achieve these goals two array lenses are used, while the emitted light is locally focused by the first array lens to the second one and then the uniform part of the light is selected by a lens and iris. These advancements were successfully implemented and validated in the SSP002 device, underscoring the practical significance and applicability of our findings in optical instrumentation. The results of the comparison show that the minimum visibility is increased from 0.10 to 0.41.

Keywords: array lenses, uniform illumination, White Light Interferometry

S9

Innovative Optical Beam Shaping with One-Dimensional Fresnel-Zone Plates: Novel Complex Structures

Fatehi M. *[1], Sabatyan A.[2], Ebrahimi H.[3]

Physic Department, Urmia University, Urmia,
email: st_m.fatehi@urmia.ac.ir, a.sabatyan@urmia.ac.ir, h.ebrahimi@urmia.ac.ir

Abstract: A Circular Fresnel-Zone Plate (CFZP) is made up of concentric rings of different widths that create constructive interference at a specific focal plane by having a π phase difference between adjacent rings. This results in the formation of a bright spot similar to spherical lenses. Similarly, one-dimensional FZPs consist of linear zones with varying widths and a phase difference of π between them, acting like cylindrical lenses to produce a bright line at the desired focal plane.

FZPs are frequently utilized for laser beam manipulation, leading to numerous research efforts in this area. Conversely, there is a scarcity of studies demonstrating the potential of 1D FZPs in shaping optical beams.

This research aims to showcase, to the best of our knowledge, the capability of 1D FZPs in creating diverse and distinctive 1D beams for the first time. We have demonstrated that it is feasible to achieve novel complex 1D structures by modulating a 1D FZP both transversely and azimuthally. It is also shown that a modulated linear beams are generated whose modulation frequency depends on the transverse manipulation of FZP and the structure of the beam is a function of azimuthal phase of FZP. For instance, chain-like beams are generated where each link has the ability to support topological charges. Also, generating a linear array of optical vortices, as shown at the left side and the right side of the following figure, respectively.

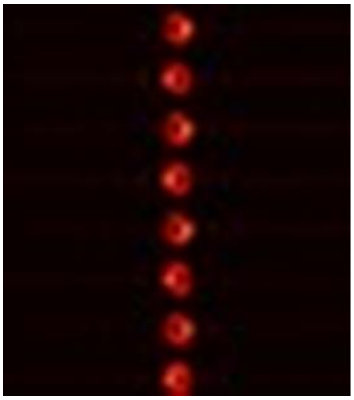

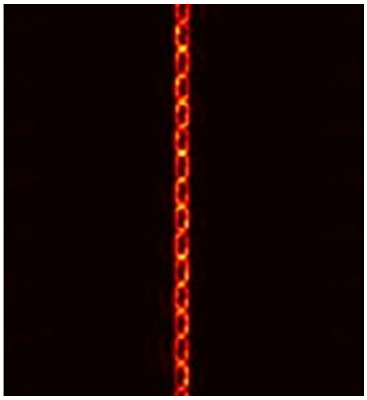

S10

Polarimetric Analysis of Whitefly Larvae on Pomegranate Leaves via Mueller Matrix Imaging

Hashemi Mozhgan*[1], Rasouli Saifollah[1,2]

[1]*Department of Physics, Institute for Advanced Studies in Basic Sciences (IASBS), 444 Prof. Yousef Sobouti Blvd, Zanjan 45137-66731, Iran.*
[2]*Department of Physics, Optics Research Center, Institute for Advanced Studies in Basic Sciences (IASBS), 444 Prof. Yousef Sobouti Blvd, Zanjan 45137-66731, Iran.*
email: mozhganhashemi@iasbs.ac.ir, rasouli@iasbs.ac.ir

Abstract: We report the characterization of a colony of leaf-based whitefly larvae using a dual-rotating retarder polarimeter at the 632.8 nm wavelength. The studied leaves belong to a pomegranate shrub that was held throughout the year in a greenhouse-like location inside the physics department of IASBS. Therefore, the whiteflies studied in this research belong to the Greenhouse Whitefly (Trialeurodes vaporariorum).

The experimental setup for measuring the Mueller matrix of the sample is in a transmission configuration and consists of two main parts: the polarization state generator (PSG) and the polarization state analyzer (PSA). Each part includes a fixed linear polarizer and a rotatable quarter-wave plate. During the experiment, the retarders connected to two step motors rotate incrementally by a 1:5 ratio. For each measurement, the wave plate in the PSG (R1) rotates from 0 to 180° in 6° increments, while the wave plate in the PSA (R2) rotates from 0 to 900° in 30° increments. Consequently, 30 images with specific incident and output polarization states are obtained. Using these 30 images, we can estimate the Fourier coefficients necessary to compute the Mueller matrix elements.

The Mueller matrix is decomposed using the polar decomposition technique originally proposed by Lu and Chipman. This decomposition allows us to obtain linear, circular, and total diattenuation, as well as retardance and depolarization parameters. We calculate these parameters for greenhouse whitefly larvae living on pomegranate leaves and compare them to the results obtained for the clean part of the same leaf. Notably, the presence of larvae on the leaf leads to significant differences in linear, circular, and total depolarization values (3.9%, 4.2%, and 4% more, respectively). The corresponding values for diattenuation are less than 0.5%, while the retardance parameters show differences of 2.8%, 1.1%, and 3.2%, respectively. Therefore, this study shows that whitefly larvae on a leaf change the polarization of light.

S11

SPR simulation of exosome with different drugs

Zeynali S. *[1], Mostafavi Amjad J.[2]

Department of Physics, Institute for Advanced Studies in Basic Sciences (IASBS), 444, Prof Yousef Sobouti Blvd, Zanjan, 45137-66731, Iran
email: [1]S.Zeynali@iasbs.ac.ir, [2] mostafavi@iasbs.ac.ir

Abstract: Exosome are a type of extracellular vesicle (EV) released from cells with nanometer-sized. Nowadays, they are gaining the attention of the physicians due to their unique properties like carry messages between cells in the for proteins, for cancer treatment. Obtaining a reliable and accurate way to identify and detect exosome with different refractive indices is a basic requirement. One of the ways to achieve this accuracy is to use surface plasmon resonance biosensors. The SPR-biosensor is worked based on optical measurement of refractive index changes associated with binding of analyte molecules in a sample to bio-recognize molecules immobilized on the surface of SPR-biosensor. The process of our work was that the EWFD module of COMSOL Multiphysics software was used to design a SPR-biosensor to examine exosome with different refractive indices. This work was done in 3D dimension and scanning on the angle and wavelength. The results show sensitivities of 0.1126, 0.0122 and 0.1064 $\frac{rad}{RI}$ at angle scan (θ-scan) and also sensitivities of 1032, 70.2 and 36.6 $\frac{nm}{RI}$ at wavelength scan (λ-scan) respectively for refractive indices difference 0.0155, 0.1425 and 0.082.

S12

Flexible Interdigital Ag Electrode Fabrication for UV-photodetectors: A Comparative Study of Aerosol Jet Printing and Thermal Evaporation Methods

Pashaei P. *[1,2], Serbest B.[1,2,3], Akman L.B.[1,2], Efkere H. İ.[1,2], Akın Sönmez N.[1,2,3], Özçelik S. [1,2,3]

[1]*Department of Photonics Science and Engineering, Graduate School of Natural and Applied Sciences, Gazi University, Ankara, Türkiye.*
[2] *Photonics Application and Research Center, Gazi University, Ankara, Türkiye.*
[3] *Department of Photonics, Faculty of Applied Sciences, Gazi University, Ankara, Türkiye.*
email: parisa_pashaie@yahoo.com

Abstract: In this research, the fabrication of flexible interdigital Ag electrodes, which play an important role in the production of semiconductor devices such as photodetectors and sensors, is investigated. In the study, both Aerosol jet printing and thermal evaporation methods were used to fabricate interdigital Ag electrodes on three different substrates (ITO, PET, and Kapton). After fabrication, the electrodes were annealed at varying temperatures (150°C, 175°C, and 200°C) for 60 minutes. Subsequently, a comprehensive analysis was performed to evaluate the optical and electrical properties of the fabricated electrodes, using optical microscopy and IV characterization techniques. In addition, the adhesion properties were carefully studied through tape testing to measure the electrode-substrate bond strength. Finally, a comparative evaluation was performed to understand the advantages and disadvantages of the two different fabrication techniques. This study provides useful information to improve our understanding of flexible electrode fabrication processes as well as to optimize the performance of semiconductor devices in various applications using the latest printing method. After annealing, all samples fabricated using both methods exhibited improved resistivity, indicating enhanced conductivity and stability. Such improvement in resistivity suggests better charge transport characteristics within the electrodes, which is crucial for the performance of semiconductor devices like photodetectors and sensors.

Keywords: Aerosol jet printing, Thermal evaporation, flexible electrodes, UV Photodetectors

S13

Using the highly sensitive surface plasmon resonance sensors to accurately determine organic dyes and some inorganic minerals in water

Mahkame Abolfathi*

Department of Physics of Institute for Advanced Studies in Basic Sciences-IASBS, Zanjan, Iran.
email: Mahkameabolfathi@iasbs.ac.ir

Abstract: Nowadays, industrial colors, especially organic colors, threaten human health and environmental safety by contaminating water sources. Therefore, developing a precise method for detecting specific mineral or organic substances in water that are released into natural sources and pose risks to human health and other living organisms is crucial. Methylene blue is one of the organic color pollutants found in the water sources of industrial cities as well as surface waters.

The use of sensors based on surface plasmons, including reliable and widely used methods for determining optical characteristics with high accuracy, is considered crucial. The refractive index is one of the most important optical parameters used to determine the type and amount of density of pollutant substances present in water. The aim of this study is to construct and employ surface plasmon resonance (SPR) sensors for detecting organic colors and mineral substances in water. Furthermore, optimizing the efficiency of the constructed sensor to enhance sensitivity is one of the main objectives of this project. SPR sensors are constructed from a very thin metallic layer placed on a glass substrate. In this project, silver (Ag) has been selected as the metallic layer due to its strong plasmonic properties in the visible region.

To identify organic colors in surface plasmon sensors, an intermediate substance is used to establish a chemical bond between dye molecules and the silver layer surface. Various materials can be used as intermediate substances. Based on studies conducted in similar research, Layered Double Hydroxides (LDHs) have been selected as a suitable receptor layer for detecting organic colors.

The silver layer surface is covered with Layered Double Hydroxides (LDHs) using an electro-deposition method. By establishing a chemical bond between organic dye molecules and Layered Double Hydroxides, the spectral reflection of the produced surface plasmon intensification changes in terms of shape, spectrum width, and peak depth at the metal-dielectric interface. These changes in SPR signals enable the characterization of optical and quantitative parameters of organic dyes. In this project, methylene blue, as a water pollutant, is tested using the proposed method with various concentrations. The improved sensitivity in these sensors will be compared with conventional measurement methods, and parameters such as metallic layer thickness and types of Layered Double Hydroxides (LDHs) will be examined to achieve a highly accurate and effective response.

S14

Periodic SPR Nano-Sensors in Form of a 6-Point Shuriken

Ataii M.R. [*1], Mostafavi-Amjad S.J.[1]

[1]*Department of Physics, Institute for Advanced Studies in Basic Sciences (IASBS), Zanjan 45137-66731, Iran*
email: m.r.ataii@iasbs.ac.ir

Abstract: Surface plasmonic resonance or SPR, was first observed on the verge of the twentieth century. In late 60s and early 70s, simple methods to implement and excite surface plasmons were introduced. Since then, numerous applications have been proposed to utilize SPR, from biosensors to optical switches. This is due to the sensitivity of SPR to fine changes in the conditions of the environment (for example temperature or concentration), and its ability to work in real time.

It is imperative to design and propose structures with different SPR properties to enable the possibility of tailoring devices to meet the needs of science and technology. The purpose of this study was to design periodic nano-structures to excite localized surface plasmons (LSPR), and investigate their characterization. The first step was to simulate different structures. Then, using the efficient parameters obtained from simulation, the SPR sensors are being built.

An interesting structure, is the periodic 6-point shuriken which is a hexagonal structure without the centering node. Using a Kretschmann configuration, silver nano-rods are positioned in the aforementioned pattern on the prism. Here, we limited our investigation to visible spectrum, and simulations were done using COMSOL Multiphysics. The changes in the reflectance dips by varying size of the rods and the shuriken was studied in simulations.

S15

Using optical interference and machine learning to categorize microbeads in water

Genc Sinan*[1,2], Icoz Kutay[2,3], Erdem Talha[2]

[1]*Environmental Photonics Research Group, Middle East Technical University, Ankara, Türkiye*
[2]*Electrical & Electronics Engineering, Abdullah Gül University, Kayseri, Türkiye*
[3]*Biomedical Engineering, University of Delaware, Newark, USA*
email: sinan.genc@agu.edu.tr

Abstract: The exponential increase of microplastics in water resources is a significant concern that humanity has encountered in recent years. According to reports from international authorities, Türkiye consistently ranks among the top three countries in terms of releasing a significant quantity of trash into the Mediterranean. These studies solely take into account the quantity of pollutants, without considering the exact composition or characteristics of such pollutants. This study focuses on the creation of an affordable, portable, and quick-acting device designed to identify, quantify, and categorize various types of microplastics found in water.

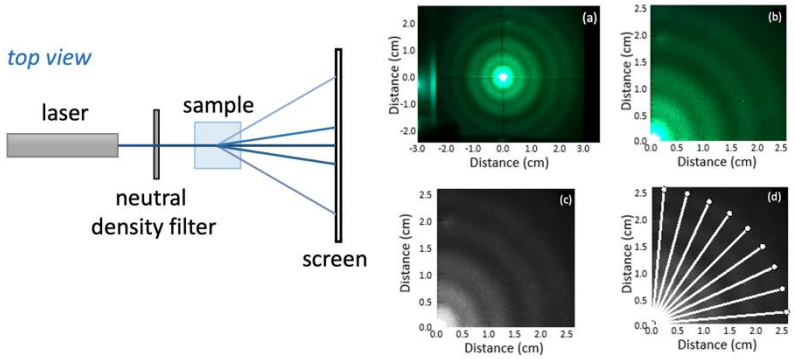

Figure 1. Illustration of the setup and feature extraction from scattering patterns.

Scattering patterns of microplastics are influenced by the refractive index, size, concentration, and the incident light. A code was written in MATLAB to compute numerical solutions of scattering equations, and subsequent tests were conducted using three lasers that emitted light at different wavelengths to investigate the behavior of various microplastics. Next, the Random Forest algorithm was incorporated into the system to achieve rapid and automated responses. The findings of the independent variable t-test indicated that there was no statistically significant difference between the predicted and actual values of refractive index and particle size. Finally, the actual laboratory results were used as test data. 7/9th of the particle size data was accurately acquired, and the largest discrepancy between the actual and anticipated refractive index was 0.13.

Ultimately, we have devised a technique that enables the categorization of microplastics in water based on their dimensions and refractive index. The system can

be customized by incorporating supplementary components to alter specific particle size, shape, and other characteristics. Furthermore, it can be employed for various applications.

S16

Investigating the Mechanical Properties of Biological Cells using Dual-beam Optical Tweezers

Akbarpour Z. [*1], MalekMohammadi M.[2], Hajizadeh F.[3], Maleki M.[4]

Department of Physics, Institute for Advanced Studies in Basic Sciences, Zanjan, Iran.
email: z.akbarpour.ph@gmail.com

Abstract: We are investigating the mechanical properties of 2D cultured breast cancer cells in contrast with 3D cultured breast cancer cells. Dual-beam optical tweezers was employed to investigate cell mechanics by setting up cell deformation as a marker. A dual-beam optical tweezers setup consists of two focused laser beams that could be used to trap two different objects or to trap a large particle like a suspended cell in 3D. Two traps could move independently in solution and this makes it possible to probe the mechanical properties of suspended cells (in 3D). Human breast cancer cell lines with different malignancies [2D-cultured MCF-7 and 3D-cultured MCF-7] were selected for our experiment. Cells were characterized by stretching using dual-beam optical tweezers and compared using the resulting cell diameter difference. We found that invasive cancer cells are softer as compared to noninvasive cancer cells: 2D MCF-7 becomes softer, while 3D MCF-7 exhibits stiffer character. Our results perform to confirm cell elasticity as a possible marker to characterize cell malignancy. The proposed approach will contribute to engage in developing dual-beam optical tweezers for biological application.

S17

SOA-based broadband light source relative intensity noise suppression

Yentur A. *[1], Keskin M.Z.[1] and Ozdur I.[1]

[1]*Department of Electrical and Electronics Engineering, TOBB University of Economics and Technology, Sogutozu Cad. No:43, Ankara, Türkiye.*
email: a.yentur@etu.edu.tr

Abstract: In this work, we present a semiconductor optical amplifier (SOA) based,broadband light source relative intensity noise (RIN) suppression method for fiber opticgyroscope (FOG) applications. Amplified spontaneous emission (ASE) light sources arewidely employed in high-performance FOG navigation systems. A single 980nm backward pumped ASE light source with 65mW output power and 23nm optical spectrum width is used as an initial broadband light source. After the ASE source, a polarizer and apolarization controller (PC) are used for the polarization control before the SOA-basedRIN suppression. The setup of the RIN-enhanced light source can be seen in Fig.1a. TheSOA used in the configuration is working in the saturation region which suppresses theintensity noise caused by non-linear gain saturation. RIN performance of the broadbandlight source is enhanced by more than 16 dB using the SOA-based configuration. RFSAnoise measurement of the light source before SOA and after SOA can be seen in Fig. 1b. For the gyroscope test, we used a navigation-grade FOG and RFSA signal-to-noise ratio (SNR) measurements are compared for both light source configurations. Around 15 dB SNR improvements are obtained using the proposed method which can be seen in Fig.1c.

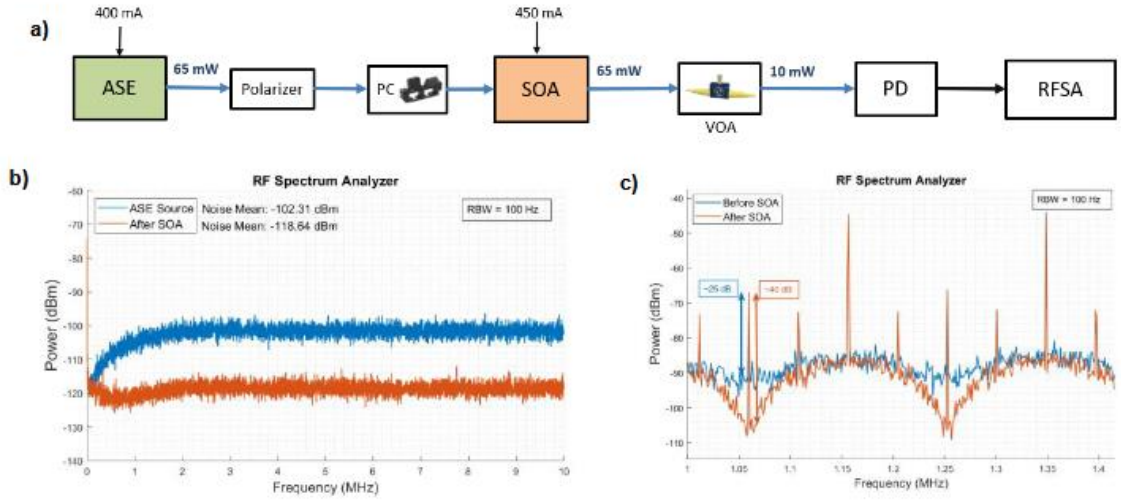

Figure 1. a) Light source test setup b) RFSA light source noise measurement c) FOG SNR measurement

S18

Utilizing Interference Microscopy to Determine Micro-Sized Objects

Hanife F. *[1,2], Azizian-Kalandaragh Y.[1,2]

[1]Gazi University, Photonics Application and Research Center, Ankara, Türkiye
[2]Gazi University, Department of Photonics, Faculty of Applied Sciences, Ankara, Türkiye
email: ferhathanife64@gmail.com

Abstract: Interference microscopy is a powerful technique for determining the size of biological micro-sized objects such as cells, organelles, or nanoparticles. Interference microscopy relies on the interference patterns generated when light waves interact with an object, producing variations in intensity that can be analyzed to derive quantitative information about the object's size and morphology. Utilizing a Mach-Zehnder interferometer microscope for determining micro-sized objects involves exploiting the interference patterns generated by the interaction of light with the specimen to extract information about the object's properties. By taking advantage of interferometry principles, Mach-Zehnder interferometer microscopy offers a powerful platform for quantitative imaging and analysis of micro-sized objects, enabling researchers to explore their structural, morphological, and optical properties in detail. In this study, a Mach-Zehnder interferometer microscope is set up to measure micro-sized samples. The established setup was optimized, interference patterns were created and micro-channels and polystyrene particles of various sizes suitable for the system were measured. In the second stage, a grating was placed in front of the laser light to increase the resolution, and the same samples were measured again. The obtained results were examined in a MATLAB-supported program, and it was observed that the resolution of the system increased. The presentation will give detailed information about the design, testing, and results of the setup.

Keywords: Interference Microscopy, Mach-Zehnder Interferometry, Micro-Sized Objects

Acknowledgements
The authors thanks Dr. Ehsan Ahadi-Akhlaghi and his group for their help for setting up optical interferometry at IASBS, Iran.

References

1. Xiao Yu, Jisoo Hong, Changgeng Liu, Myung K. Kim, Review of digital holographic microscopy for three-dimensional profiling and tracking (optical engineering, vol. 53, issue 1, 112306 (2014).
2. Saghaei H, Elyasi P, Karimzadeh R, Design, fabrication, and characterization of Mach–Zehnder interferometers, Photonics and Nanostructures - Fundamentals and Applications, vol. 37 100733 (2019).

S19

Fabrication and Calibration a Spectral-Domain Optical Coherence Tomography in Infrared Range

Rezaei N.[*1], Zakikhani F.[1], Ebrahimzadeh Kouyakhi A. [*1], Ahadi Akhlaghi E.[*1,2]

[1]Department Physics, Institute for Advanced Studies in Basic Sciences (IASBS), Zanjan, 45137-66731, Iran.
[2]Optics Research Center, Institute for Advanced Studies in Basic Sciences (IASBS), Zanjan, 45137-66731, Iran.
email: nargesrezaei@iasbs.ac.ir, e.a.akhlaghi@iasbs.ac.ir

Abstract: The Optical Coherence Tomography (OCT) technology allows rapid, non-invasive, high-resolution 3D imaging of various samples. Utilizing Michelson interferometer, OCT can be configured in time-domain and Fourier-domain setups for sample examination. 3D imaging requires scanning the sample in the illumination plane, often achieved with a Galvo mirror. This study presents a spectral-domain OCT microscope's construction and its application in sample thickness examination. Experimental setup involved a 439×439 (μm^2) sample. Such advancements in OCT technology hold promise for improved disease diagnosis, non-destructive testing, and scientific research across various fields.

Keywords: Optical Coherence Tomography, OCT, 3D imaging, Fourier-Domain, Galvo mirror.

S20

Fabrication of Different Patterns of Diffraction Grating with Aerosol Jet Printing System

Topcu U. *[1,2], Serbest B. [1,2], Hatipoğlu İ.[2,3], Özçelik S. [2,3], Azizian-Kalandaragh Y.[2,3]

[1] *Department of Photonics Science and Engineering, Graduate School of Natural and Applied Sciences, Gazi University, 06560 Ankara, Türkiye.*
[2] *Photonics Application and Research Center, Gazi University, 06560 Ankara, Türkiye*
[3] *Department of Photonics, Faculty of Applied Sciences, Gazi University, 06560 Ankara, Türkiye.*
email: utkutopcu097@gmail.com

Abstract: Diffractive optical elements (DOEs) are an important component of optical systems for optical communications, biological sensors, imaging systems, data storage systems, optical computing systems, and optical tweezers. [1,2] Also DOEs are used for creating structured light. Traditionally, DOEs are manufactured using lithography techniques. Unlike lithography, more flexible patterns and cheaper patterns can be produced with the help of the Aerosol Jet Printing (AJP) technique. Also, AJP can be produced using gold, silver, and copper ink for different purposes. It can be produced as a passive element with a suitable pattern instead of SLM, which is an active element that provides fast and precise production. This study produced different patterns such as rectangles, isosceles triangles, right triangles, and Laguerre-gauss patterns using the AJP technique for the first time. Additionally, we are testing the quality of our DOEs with the help of atomic force microscopy [1], optical microscopy, and optical setup with MATLAB. We also verify the accuracy of the patterns we produce with MATLAB simulation.

The presentation will give information about the design, testing, and production processes of the DOEs we produce with AJP.

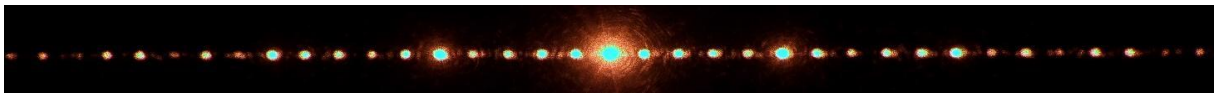

Keywords: Diffractive optical element, Aerosol Jet Printing, Structured Light

Acknowledgment:
The Presidency Strategy and Budget Department supported this study with the project numbered 2019K12-149045.

References

1. O'Shea, D. C., Suleski, T. J., Kathman, A. D. & Prather, D. W. Diffractive Optics: Design, Fabrication, and Test (SPIE Press, Bellingham, WA, USA, 2004).
2. Maragò OM, Jones PH, Gucciardi PG, Volpe G, Ferrari AC. Optical trapping and manipulation of nanostructures. Nat Nanotechnol. 2013 Nov;8(11):807-19.

S21

Refractometry based on reflection phase step spectroscopy

Aminian S.*[1], M. Amjad J.[1,2], A. Akhlaghi E.*[1,2]

[1]Department of Physics, Institute for Advanced Studies in Basic Sciences (IASBS), Zanjan 45137-66731, Iran.
[2]Optics Research Center, Institute for Advanced Studies in Basic Sciences (IASBS), Zanjan 45137-66731, Iran.
email: nader_safari@iasbs.ac.ir, e.a.akhlaghi@iasbs.ac.ir

Abstract: The refractive index is a characteristic parameter of materials, providing information about temperature, pressure, and chemical composition. It is crucial in science and industry. Diffractometry is an easy-to-implement and cost-effective method that is based on Fresnel diffraction (FD) from a phase step. Sabatyan et al. by recording the FD from a cylindrical glass with a certain refractive index that is immersed into a liquid, presented a method for measuring the refractive index of liquids. In addition, Tavassoly et al. did the same thing by using FD from a phase wedge. In this research, we present a diffractometry method to measure the refractive index of liquids using spectroscopy of FD from a phase step. Spectroscopy of a phase step edge produces a fluctuating intensity pattern. This pattern relies on the height of the step and the refractive index of the medium, therefore using a step with a known height and measuring its reflection spectrum, the refractive index of the medium can be determined. By applying Fresnel-Kirchhoff integral, Fresnel approximation, and some mathematics, the intensity of diffracted light from a phase step of height h (Fig. 1a) for an arbitrary observation point is described as follows,

$$I(P) = \frac{I_0}{2}\left[\cos(\varphi) - 2(C_0^2 + S_0^2)\cos(\varphi) + \left(\frac{1}{2} + C_0^2 + S_0^2\right)\right] \quad (1)$$

where for our case $\varphi = 2knh$. $k = 2\pi/\lambda$ and n stand for wave number and refractive index of medium, respectively.

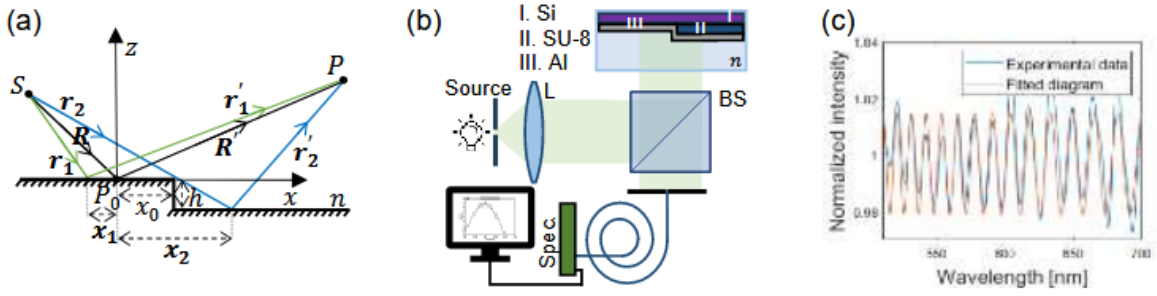

Figure 1. (a) 1D phase step of height h. (b) the schematic experiment. (c) Normalized intensity.

Figure 1(b) shows the schematic of the experiment setup. The emitted white light from the source is collimated by the lens (L) and illuminates the phase stage. The scattered light from the edge of the step is collected by the fiber and recorded by the spectrometer.By fitting Eq. (1) on the recorded data (Fig. 1c) the medium refractive index, n, is obtained. According to the calculations, the refractive index of water is

obtained 1.32 ± 0.02, which the uncertainty was due to the systematic error of step height measurement.

S22

Study of optical properties of asymmetric AgNWs/PVA/Ag_2S nanocomposites by vapor phase sulfidation process

Baghirov M.B.*, Muradov M.B.

Nano Research Laboratory, Baku State University, 23 Academic Zahid Khalilov Street, Baku, Azerbaijan.
email: bmbaghir@gmail.com

Abstract: Presently, asymmetric structures have emerged as a focal point in material science due to their diverse applications in smart systems, sensors, and beyond. However, the fabrication of such structures presents significant challenges. This research introduces asymmetric polymer nanocomposites of silver nanowires/polyvinyl alcohol/silver sulfide (AgNW/PVA/Ag_2S) and investigates their structural properties.The process began with the synthesis of AgNW using a modified polyol method. Subsequently, composite of AgNW/PVA were formed by incorporating PVA at a 2% mass concentration and ensuring even dispersion through ultrasonic treatment. The samples were exposed to different doses of H_2S gas from one direction. Figure 1A shows absorption spectra of AgNWs, revealing peaks at 350 nm (long AgNW plasmon) and 380 nm (transverse plasmon). Successful AgNW synthesis is confirmed. Figure 1B illustrates the UV absorption spectra of both pristine and sulfided AgNWs/PVA nanocomposites. In Figure 1B.a, the absorption spectra of the original AgNWs/PVA sample display characteristic peaks of AgNWs. Upon exposure to H_2S gas, shown in Figures 1B.b, c, and d, a (Increasing concentration of H_2S gas) noticeable decrease in peak intensity associated with these surface plasmons is observed. This reduction stems from the development of a surface layer of Ag_2S on the AgNWs due to interaction with H_2S gas, resulting in the damping of inherent plasmon oscillations of AgNWs. However, not all wires within the nanocomposite undergo sulfidation upon H_2S exposure, leaving observable peaks. The persistence of these peaks indicates unreacted AgNWs within the composite. Furthermore, the effect of H_2S gas induces red shifts in the plasmon peaks, as depicted in Figure 1B. The resonant frequency of plasmons (ω) is intricately related to the density of free electrons (n) within the material. The observed red shift in plasmon peaks signifies a decrease in frequency, attributed to the reduced electron concentration within the material. Thus, the formation of the Ag_2S semiconductor layer on AgNWs under the influence of H_2S gas aligns with the decrease in electron concentration compared to the original, pristine sample configuration.

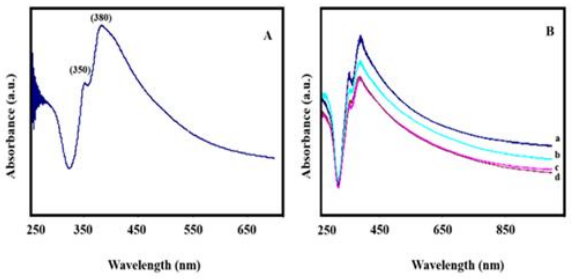

Figure 1. UV-Vis spectrum for A-AgNWs. B) a- AgNWs/PVA, b- AgNWs/PVA-1, c-AgNWs/PVA+2, d- AgNWs/PVA+3.

S23

Pulse Distortion Optimization Caused by EDFA Transient Effect

Dinç, Ö.F.*[1], Uyar, F.[1,2], Kartaloğlu, T. [1], Özdur, İ. [3] and Özbay, E. [1,2,4]

[1]*Nanotechnology Research Center, Bilkent University, Ankara, Türkiye*
[2]*Department of Electrical and Electronics Engineering, Bilkent University, Ankara, Türkiye*
[3] *Department of Electrical and Electronics Engineering, TOBB University of Economics and Technology, Ankara, Türkiye*
[4]*Department of Physics, Bilkent University, Ankara, Türkiye*

Abstract: This research delves into the optimization of pulse distortion induced by transient effects in erbium-doped fiber amplifiers (EDFAs) for distributed acoustic sensing (DAS) applications. DAS systems leverage optical fibers for acoustic signal detection, where EDFA plays a pivotal role in signal amplification. However, transient effects in EDFAs can lead to pulse shape distortion, which can adversely affect the accuracy of acoustic signal measurements [1]. By using the Frantz-Nodvik models we can simulate transient effect-induced temporal pulse and tailor reverse pulse with suitable energy levels to avoid saturation [2]. Through theoretical analysis, numerical simulations, and experimental validation, this study investigates the mechanisms and mitigation strategies for transient-induced pulse distortion in EDFA-based DAS systems. Nonlinear phenomena and transient effects are examined, considering operational parameters to optimize amplifier performance. The findings offer valuable insights into enhancing the reliability and precision of DAS systems by mitigating pulse distortion effects. This research contributes to the advancement of DAS technology for applications such as seismic monitoring and structural health monitoring.

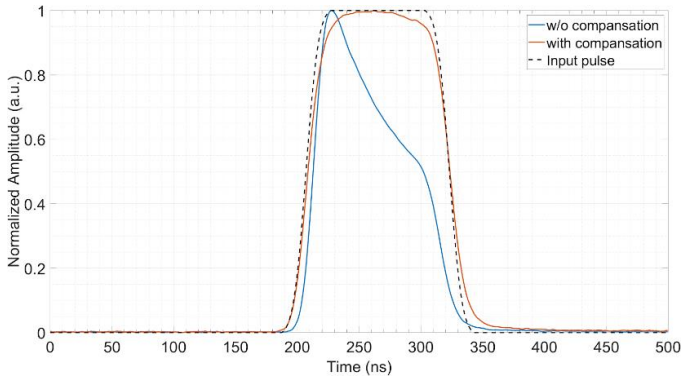

Figure 1. Transient effect compensation result

References

1. Chernutsky, A. O., Zhirnov, A. A., Fedorov, A. K., Nesterov, E. T., Stepanov, K. V., Tezadov, Y. A., ...& Pnev, A. B. (2017, May). Phase-sensitive optical time-domain reflectometry with pulse mode EDFA: Probe pulse preparation. In 2017 Progress In Electromagnetics Research Symposium-Spring (PIERS) (pp. 2231-2236). IEEE.
2. Schimpf, D. N., Ruchert, C., Nodop, D., Limpert, J., Tünnermann, A., & Salin, F. (2008). Compensation of pulse-distortion in saturated laser amplifiers. Optics Express, 16(22), 17637-17646.

S24

Exploring Novel Techniques for Optical Vortex Beam Generation and Detection Using Mach-Zehnder Interferometer and Spiral Zone Plate

Jalali Sh.*[1], Sabatyan A.[2]

Physics Department, Faculty of sciences, Urmia University, Urmia, Iran
email: Shararehjl@gmail.com, a.sabatyan@urmia.ac.ir

Abstract: In this study, the generation of optical vortex beams has been investigated. We demonstrate a new method to detect the optical vortex beams which carries orbital angular momentum (OAM) by using a Mach-Zehnder interferometer. To generate fascinating light modes, we used a spiral zone plate (SZP) and proposed a unique approach involving coaxial superposition of two Laguerre-Gaussian (LG) beams with different azimuthal indexes. We generated these beams using light interference from SPZ within various topological charges.

A variety of beam shapes and light structures such as petals, doughnut, ring lattices, fractional vortex beams and multi-spots beams were generated. The advantage of this technique is that the samples can be moved in order to produce a variety of optical vortex beams at different distances from focal length. Having examined the method theoretically and mathematically, simulation predictions were verified by experimental work and future studies can shed more light on this exploration.

S25

White light spectroscopy of structured surface plasmon resonance biosensors

Fateme Gheibi*[1], Jafar Mostafavi Amjad [2]

Department of Physics, Institute for Advanced Studies in Basic Sciences (IASBS), Zanjan 45137-66731, Iran.
email: fateme.gheibi@iasbs.ac.ir

Abstract: Various optical methods such as ellipsometry, interferometry, spectroscopy, and surface plasmon resonance have recently been employed in the development of different bio-sensors.

Among these, sensors based on surface plasmon resonance have garnered significant interest due to their remarkable precision and sensitivity. Surface plasmons refer to waves that arise from the oscillation of the free electrons at the interface between a metal and a dielectric medium. These waves can be excited by light. Surface plasmons can be exited either by angle or wavelength tuning of the incident light into the metal surface. The sensor is named so because its resonance location is determined by the refractive index of the second medium.

In this particular study, a surface plasmon resonance optical set up utilizing white light was designed and fabricated. The excitation of surface plasmons was achieved through total internal reflection using a cylindrical prism in contact with the metal surface.

To ensure optimal precision, sensors with a coating thickness of 50 nm have been employed, alongside the utilization of a reference laser wavelength of 632 nm. This research assesses the extent of the intensity and phase shift experienced during the excitation of surface plasmons at various wavelengths. By measuring these changes, it becomes possible to determine the electrical property ε of the surrounding medium and explore its applicability in evaluating diverse environments, including chemical, biological, and physical substances.

References

1. Otto, Excitation of nonradiative surface plasma waves in silver by the method of frustrated total reflection, Zeitschrift für Physik A Hadrons and nuclei, Vol. 216, No. 4, pp: 398-410, 1968.
2. J. Homola, Surface plasmon resonance sensors for detection of chemical and biological species, Chemical reviews, Vol. 108, No. 2, pp: 462-493, 2008.

S26

Investigation of Quantum Confinement Effects in Cadmium Sulfide Polymer Nanocomposites and Their Role in Optoelectronic Device Applications

Yiğit Levent Çeçen

Department of Photonics, Gazi University Graduate School of Natural and Applied Sciences, 06560 Ankara, Türkiye
email: yigitcecen@live.com

Abstract: In this research, the energy spectrum of semiconductor CdS nanoparticles prepared by different methods was investigated for changes in nanoparticle sizes and variations in effective mass. The quantum models used in the study were the Effective Mass Approximation (EMA) and the Hyperbolic Band Model (HBM). The comparison of results shows that different models alter the distribution behavior to a certain extent, indicating that this behavior is dependent on the preparation and analysis methods of the samples. Furthermore, this study examined the quantum behavior in nano semiconductor structures with large and small direct bandgaps, along with variations in this behavior with nanoparticle sizes, using HBM and EMA quantum models. The results of the study demonstrate that the size of the energy gap has a direct impact on the quantum behavior in nano semiconductor structures. In these calculations, it was found that the reduced effective mass has an influence, but since it is not very significant in these semiconductor CdS nanostructures, the effective mass does not have a pronounced effect on various quantum parameters and quantum behavior.

S27

Surface Topography Measurement through Fringe Visibility Analysis

Hosseini S. [*1], A. Akhlaghi E.[1,2]

[1]*Department of Physics, Institute for Advanced Studies in Basic Sciences (IASBS), Zanjan, 45137-66731, Iran*
[2]*Optics Research Center, Institute for Advanced Studies in Basic Sciences (IASBS), Zanjan, 45137-66731,Iran,e.a.akhlaghi@iasbs.ac.ir*
email: simahosseini@iasbs.ac.ir

Abstract: Surface topography measurement through interferometry is a non-contact and non-destructive technique which is widely used in various fields for analyzing the surface structures to better understand and characterize surface properties for a wide range of applications. In this paper, a new method for analyzing interference fringes has been introduced which is based on evaluating the visibility changes. In this method, after capturing the interferogram through the interferometer and utilizing the visibility calibrated diagram, the heights of various points on the measured surface are determined. With this method it is possible to measure surface roughness up to 65 micrometers with an accuracy of 3 micrometers.

Keywords: interferometry, visibility, topography

POSTER PRESENTATION

P1

Effect of Buffer Layer Thicknesses on Efficiency of Cadmium Telluride Solar Cell Structures

Ersoy Y. [*1,2], Efkere H.İ.[2], Ozen Y.[2,4], Aydın S.Ş.[2,3], Özçelik S.[2,3]

[1]*Gazi University, Graduate School of Natural and Applied Sciences, Photonics Science and Engineering Department, Ankara, Türkiye*
[2] *Gazi University, Photonics Application and Research Center, Ankara, Türkiye*
[3]*Gazi University, Faculty of Applied Sciences, Department of Photonics, Ankara, Türkiye*
[4]*Gazi University, Science, Department of Physics, Ankara, Türkiye*
email: yukselersoy@msn.com

Abstract: With its ideal band gap (~1.45 eV) and wide absorption coefficient (>10^4 cm^{-1}), CdTe has stood out among solar cells with a recorded efficiency of 21.5% [1]. Improvements in short-circuit current (J_{sc}) and fill factor (FF) enabled the CdTe solar cell to achieve this efficiency. Despite some modifications, it appears that the values of open-circuit voltage (Voc) have remained largely stable [2]. High Voc requires good ohmic contact with CdTe, however this is hard because to the poor doping and high work function of the material [3]. To overcome this difficulty, researchers have concentrated their research on the back contact buffer layer.

In this study, the effect of absorber layer thickness on the energy conversion efficiency of Glass/ITO/ CdS/CdTe/ZnO/NiO solar cell was examined. CdS, CdTe, ZnO and NiO layers were deposited on ITO-coated glass, respectively, using the Co-Sputtering System. ZnO buffer layers were coated with thicknesses of 50, 100 and 150 nm, and the samples were named Sample1, Sample2 and Sample3, respectively. Structural and optical measurements of the samples were made with X-ray diffraction (XRD) system and UV-Vis Spectrometer. Fabrication processes of the samples for electrical analyzes were carried out using the Thermal Evaporation System. Electrical output parameters were obtained using the Solar Simulator. By analyzing the measurement results, the sample with the highest energy conversion efficiency was determined.

Acknowledgements: This work was supported by the Presidency of Strategy and Budget (Türkiye) under project numbers of 2019K12-149045.

References

1. Green M.A., Emery K., Hishikawa Y., Warta W., Dunlop E.D., "Solar cell efficiency tables (Version 46). Progress in Photovoltaics Research and Applications", 23, 805 (2015).
2. Gloeckler, M., Sankin I., Zhao Z., "CdTe solar cells at the threshold to 20% efficiency", IEEE Journal of Photovoltaics, 3(4), 1389-1393 (2013).
3. Hall R., Lamb D., Irvine S., "Back contacts materials used in thin film CdTe solar cells", Energy Science & Engineering, 9 (2021).

P2

Solar Sail Development

Kılıç K.A. *[1,2], Özçelik S.[1,2,3]

[1]Gazi University, Graduate School of Natural and Applied Sciences, Photonics Science and Engineering Department, Ankara, Türkiye
[2]Gazi University, Photonics Application and Research Center, Ankara, Türkiye
[3]Gazi University, Faculty of Applied Sciences, Department of Photonics, Ankara, Türkiye
e-mail: kenananilk@gmail.com

Abstract: Solar sails are photonic devices in which propulsion is provided by the momentum change of photons reflected from the sail surface and no fuel is used for propulsion. Propulsion is provided by solar radiation pressure (SRP). The sail surface, which is lightweight and highly reflective, converts the momentum of photons into a propulsive force. The momentum carried by individual photons is extremely small (9 N/km^2 in Earth orbit). Therefore, the sail must have a large surface area and a low mass to ensure a momentum transfer of the appropriate magnitude. The speed of the sail increases with time and can reach very high values (~400 km/s). With the continuous nature of photon pressure and the absence of fuel requirements, solar sails have significant potential for space exploration.

The first successful demonstration of solar sail technology in the interplanetary space was the IKAROS project (JAXA, 2010). In line with its objectives, the sail's guidance and navigation test was completed with the closest approach to Venus. The next solar sail to be flown was NanoSail-D2 (NASA, 2011). NanoSail-D2 is a sail deployment demonstration that could lead to an atmospheric drag system to de-orbit defunct satellites at the end of their operational lifetime. Another important study is the LightSail 2 project (Planetary Society, 2019). The aim of this project is to successfully demonstrate the use of a controllable solar sail on a cubesat.

The aim of this study is the design, modelling and development-production of a small-scale solar sail. The main basis of the sail is the development of a thin film coating, 0.1 µm thick, capable of reflecting sunlight over a wide spectral range, on a substrate with a thickness of 2.5 µm. Experimental studies will be carried out using the PVD coating systems (Magnetron sputtering) and characterization infrastructure available at G. U. Photonics Application and Research Center. The development of new materials and the development of coatings with high area/mass ratio are important R&D studies that distinguish the studies from others.

In this context, previous studies were examined and the calculations and modelling on the subject were evaluated. As a result of these investigations, the necessary formulations were developed and the design of the system in which the experimental production will be carried out was made.

P3

Investigation Of Optical Properties and Wetability In Anti-Reflective Film

Yunus Emre KOÇ*[1,2], Yashar AZIZIAN-KALANDARAGH[3,4]

[1]*Department of Photonics Science and Engineering, Graduate School of Natural and Applied Sciences, Gazi University, 06560 Ankara, Türkiye.*
[2]*TÜBİTAK SAGE Optical Systems Group Thin Film Coating and Lithography Unit.*
[3]*Photonics Application and Research Center, Gazi University, 06560 Ankara, Türkiye*
[4]*Department of Photonics, Faculty of Applied Sciences, Gazi University, 06560 Ankara, Türkiye.*
email: emre.koc@tubitak.gov.tr

Abstract: Frost may occur on the surfaces of the protective windows in various ammunition under cold weather conditions. The operating performance of imaging systems is negatively affected due to accumulated water vapors. These effects can be controlled thanks to the coating applied to these optical parts that act as windows. The wettability of coatings is directly related to the amount of icing. Within the scope of this study, the wettability of various coating materials will be examined, taking into account their optical properties, and will be improved by integrating them into anti-reflective coatings.

In this study, thin film layers produced from HfO_2 material on glass were examined in terms of permeability and wettability. Using the DC Sputter method, HfO_2 thin film layers were coated on the glass substrate from a Hafnium metal source using the DC magnetron sputter method. The materials coated at low temperatures were produced at different pressures and oxygen amounts and the most appropriate production parameters were determined. The produced thin film coatings were then dropped onto the coating surface with a Hamilton glass injector, and the connection between the contact angle of the drop and the surface was examined.

P4

Photocapacitance/conductance Characteristics of Si-based Heterostructure Interlaid with P(EHA) Functional Polymers Depending on Illumination Intensity

Ulusoy M., Balıkçı L.M., Güçlü Ç.Ş.

Gazi University, Department of Physics, 06560 Ankara, Türkiye
email: ulusoymurat@gazi.edu.tr

Abstract: In this study, poly (2-ethylhexyl acrylate) (PEHA) homopolymer was coated as an interlayer onto n-type Si by initiated chemical vapor deposition (iCVD), which provides much better deposition control and homogeneity [1]. The capacitance/conductance-voltage (*C*/(*G*/*ω*-*V*) characteristics were investigated both in the dark and under illuminations with a reference sample. The basic electrical parameters and the illumination-induced variation of surface state (N_{ss}) were obtained for two samples with different methods. The formation of the polymer interlayer resulted in a reduction in N_{ss} values, both in the inversion and forward biases. Furthermore, while the photocapacitance sensitivity due to the light effect at constant *C* values (for 1.2 nF) was 6.3 Vcm^2/W for the reference structure, this value was obtained as 12.1 Vcm^2/W in the interlayered structure. Consequently, the findings are suitable for optoelectronic applications, given the significant changes in *C* and *G* values that occur depending on voltage and illumination levels.

Keywords: P(EHA) interlayer; *C*/*G*-*V* photo-characteristics; Structural, optical and electrical parameters

References

1. Şakalak, H.; Karaman, M. All-Dry Synthesis of Poly(2-Ethylhexyl Acrylate) Nanocoatings Using Initiated Chemical Vapor Deposition Method. *Prog Org Coat* 2019, *132*, 283–287. https://doi.org/10.1016/j.porgcoat.2019.03.044.

P5

Analysis of the effects of photonic crystals on the optical properties in low-dimensional materials

Yaqub M.A. [*1,2], Gupta H.[1,2], Contino T.[1,2], Ashraf M. W. [1], Tamagnone M.[1]

[1]*Nano-Photonic Devices, Istituto Italiano di Tecnologia, via Morego 30, 16163 Genova, Italy*
[2]*Dipartimento di Chimica e Chimica Industriale, Università degli Studi di Genova, Via Dodecaneso, 31, 16146 Genova, Italy*
email: muhammad.yaqub@iit.it

Abstract: Because of their strong light-matter interaction, two-dimensional materials have been investigated and shown to be attractive options for designing highperformance photodetectors (PDs). Yet, the efficiency of 2D material PDs remains deficient, with flaws including slower response speed and a sensitive contact interface impeding their swift growth in the field of optoelectronics. In our present work, we integrate photonic crystals into 2D and vdW materials (in particular GaTe and InSe) to enhance their optical properties, such as photoconductivity and photoluminescence. These materials were selected owing to their direct bandgaps. We optimized the design of photonic crystals so that they resonate at the target wavelength to maximize the absorption and photoluminescence characteristics. The same approach can be used at the photoluminescence wavelength to maximize it. Ansys HFSS was used to design the structure of GaTe/InSe-based photodetectors and for the numerical simulations. The maximum absorption peaks were found at ~500 THz (600 nm), depicting the application of the photodetectors in the visible spectrum, as shown in Figure 1(a) [square photonic crystal not shown]. Some changes were made in the design to optimize our structure for the PL characteristics and numerical simulations were carried out for GaTe as shown in Figure 1(b). For GaTe, the dip was observed at ~403 THz (1.67 eV) and for InSe dip was observed at 308 THz (1.27 eV), in consistent with the existing literature (InSe not shown.)

We will present more details and numerical and experimental results (measurements are currently in progress). In the future, we will also explore substrate effects to induce changes in the material's band structure and enhance the performance further.

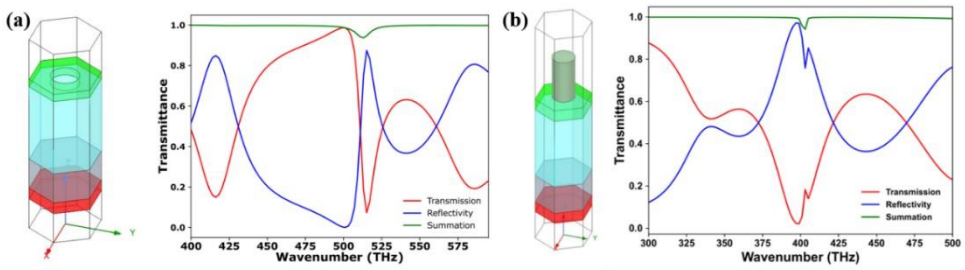

Figure 1. Design and simulation for **(a)** Hexagonal photonic crystal for photodetector for InSe, and **(b)** simulations for PL analysis for GaTe

Acknowledgements:
We acknowledge the financial support of the European Research Council (ERC) under Grant Agreement No. ERC-2020-STG 948250 (SubNanoOptoDevices).

P6

Study of the role of Strontium in tunning structural, electric, optical and dielectric properties of Zinc Cobalt Spinel Ferrites

Parveen Iqra*[1], Hafeez Anwar[2]

Department of Physics, University of Agriculture Faisalabad, Pakistan, 38000
email: iqraparveen57@gmail.com

Abstract: $Zn_{0.5}Co_{0.5}Sr_xFe_{2-x}O_4$ spinel ferrites with varying Sr^{+2} concentrations (x = 0.00, 0.02, 0.04, 0.06, and 0.08) were synthesized using the co-precipitation technique. Multiple characterization methods, including X-ray diffraction (XRD), scanning electron microscopy (SEM), energy dispersive X-ray analysis (EDX), Fourier-transform infrared spectroscopy (FT-IR), UV-Vis spectroscopy, and dielectric analysis, were employed to comprehensively evaluate their structural, morphological, elemental, vibrational, optical, and dielectric properties. XRD analysis revealed a decrease in crystallite size from 20.9 nm to 10.4 nm and a reduction in lattice constant from 8.46 to 8.39 Å as the Sr^{+2} concentration increased. SEM images depicted a decrease in particle size and the formation of agglomerates with increasing strontium content. The presence of spinel ferrites was confirmed by sharp peaks at 430 cm^{-1} and 534 cm^{-1} in the FT-IR spectra. UV-Vis spectroscopy indicated a decrease in the optical band gap from 3.02 to 2.21 eV with increasing dopant concentrations. Dielectric analysis showed a decreasing trend in both dielectric constant and dielectric loss due to doping. The AC conductivity exhibited an increasing trend with frequency, reaching a maximum value of 0.33×10^{-7} $[ohm\ cm]^{-1}$ at higher frequencies. Moreover, the dielectric analysis revealed the material's frequency dependency, suggesting potential applications in microwave and frequency-dependent devices.

Keywords: co-precipitation technique, dielectric analysis, agglomerates, AC conductivity,

P7

The Investigation of basic electrical parameters, photosensitivity, and energy dependent profile of interface traps (D_{it}) in the Au/n-Si (MS) type photodiodes with and without (ZnO-CeO_2:PVP) interlayer by utilizing current-voltage (I-V) characteristics

Oray Üstün[1], Yashar Azizian-Kalandaragh[2]

[1]*Department of Photonics Science and Engineering., Graduate School of Natural and Applied Sciences, Gazi University, Ankara, TÜRKİYE*
email: oray.ustun@gazi.edu.tr
[2]*Department of Photonics Science and Engineering., Graduate School of Natural and Applied Sciences, Gazi University, Ankara, TÜRKİYE*
email: yasharazizian@gazi.edu.tr

Abstract: (ZnO-CeO_2:PVP) interfacial-layer was grown at Au/n-Si interface to perform MS and MPS type photodiodes were fabricated onto same n-Si wafer and then their current-voltage measurements were performed both in dark and 100mW.cm^{-2} illumination intensity. The basic electrical parameters of them such as the leakage current (I_o), ideality-factor (n), barrier-height (Φ_{Bo}), and rectification-ratio (RR=$I_{forward}/I_{reverse}$ at ±5V) were obtained as 5.97x10^{-7}A, 5.545, 0.64eV, and 2.74x10^5 for MS and 2.72x10^{-8}A, 4.36, 0.72eV, and 1.85x10^7 for MPS photodiodes, respectively in dark condition. On the other hand, they were found as 5.54x10^{-6}A, 5.88, 0.59eV, and 8579 for MS and 7.14x10^{-7}A, 5,18, 0.64eV, and 76065 for MPS photodiodes, respectively under illumination. The value of photosensitivity (S=I_{dark}/I_{ph}) was found as 700 for MPS which is 19 times higher than the MS. All obtained these parameters for MS and MPS when compared each other, the used (ZnO-CeO_2:PVP) interlayer leads to an important improve performance of the MS photodiode.

Keywords: Au/n-Si and Au/(ZnO-CeO_2:PVP)/n-Si photodiodes; A comparison of MS and MPS; Current-voltage characteristics; Basic electrical parameters and photosensitivity

P8

Quantum Tip-Enhanced Raman Spectroscopy (QUTERS)

Özge Demirtaş[1], Batuhan Balkan[*2], Taner Tarık Aytaş[3], Ramazan Şahin[3], Mehmet Emre Taşgın[4], Alpan Bek[1,2,5,6]

[1]Micro and Nanotechnology Program, Middle East Technical University, 06800 Ankara, Türkiye
[2]Department of Physics, Middle East Technical University, 06800 Ankara, Türkiye
[3]Department of Physics, Akdeniz University, 07058 Antalya, Türkiye
[4]Institute of Nuclear Sciences, Hacettepe University, 06800 Ankara, Türkiye
[5]Nanomagnetics Instruments Inc., ODTÜ-Teknokent, 06800, Ankara, Türkiye
[6]The Center for Solar Energy Research and Applications (ODTÜ-GÜNAM), 06800, Ankara, Türkiye

Abstract: A combination of Raman spectroscopy and scanning probe microscopy has shown great potential as a nanoscale resolved detection tool called tip-enhanced Raman spectroscopy (TERS)[1]. TERS is a non-destructive, label-free technique that provides highly sensitive spectral information and surface topography characterization. One method to improve the performance of TERS probes is by fabricating a metal grating on probe shaft to facilitate the excitation of surface plasmon polaritons (SPP). Plasmon nanofocusing[2] enables efficient coupling of far-field radiation to the near-field zone by propagation of SPPs through the probe apex. In this study, we aim to further increase the TERS signal by modifying atomic force microscopy (AFM) probes to form grating on the probe shaft using femtosecond (fs) laser pulses. To determine the optimal parameters, we investigated the formation of ripples on flat substrates and tips under varying fs laser power, velocities, and hatch distances of the galvoscanner head. Our TERS device design is based on the epi-illumination and collection configuration, allowing characterization of both opaque and transparent samples and minimizing the residual background signal that arises from side illumination. Additionally, we propose a practical implementation utilizing interference of multiple conversion paths (Fano)[3], which is promising on Raman-active molecule imaging with larger tip-surface spacing, lower laser or hot-spot intensities without causing damage or inducing modifications in the vibrational modes. By selectively decorating the AFM probe with quantum emitters, the TERS signal can be increased without increasing the near-field intensity.

Keywords: Plasmonics, TERS, probe fabrication, quantum path interference.

Acknowledgement
Ö.D. and A.B. thank The Scientific and Technological Research Council of Türkiye (TÜBİTAK) for their partial financial support under the 2211-C, TEYDEB 1501 programs and grant nr 119F101. The authors thank Dr. Ihor Pavlov and Dr. Arian Goodarzi for assisting with the fs laser structuring.

References

1. Stöckle, R. M., Suh, Y. D., Deckert, V. & Zenobi, R. Nanoscale chemical analysis by tip-enhanced Raman spectroscopy. Chem. Phys. Lett. 318, 131–136 (2000).

2. Berweger, S., Atkin, J. M., Olmon, R. L. & Raschke, M. B. Adiabatic Tip-Plasmon Focusing for Nano-Raman Spectroscopy. J. Phys. Chem. Lett. 1, 3427–3432 (2010).
3. Postaci, S., Yildiz, B. C., Bek, A. & Tasgin, M. E. Silent enhancement of SERS signal without increasing hot spot intensities. Nanophotonics 7, 1687–1695 (2018).

P9

Color Rendering Properties of Quantum Dot Embedded Glasses: Evaluation with IES TM-30-18

Balaban, M. [*1], Yükselici, M. H. [*1]

[1]*Yıldız Technical University, Department of Physics, 34220 Esenler, İstanbul, Türkiye*
email: mesut.balaban@std.yildiz.edu.tr

Abstract: Quantum dots (QDs) offer unique luminescent properties, enabling their use as colorants in various mediums. Integrating semiconductor QDs into glass matrices (QDGMs) enhances their stability for demanding applications. Evaluating the colorimetric properties of QDGMs is crucial for their successful implementation. This study assesses the color rendering characteristics of QDGMs using the advanced IES TM-30-18 standard, which surpasses the limitations of the traditional Color Rendering Index (CRI).

We prepare QDGMs using commercial Cd, S, and Se doped RG695 Schott filter glass. Systematic thermal treatments are introduced to control QD size. A monochromator setup (360-830 nm) with a tungsten lamp source is employed for optical characterization. The results demonstrate that the IES TM-30-18 metrics (R_f and R_g), along with color vector graphics, provide a more comprehensive and informative picture of QDGMs' color rendering capabilities compared to CRI.

Importantly, this study reveals a direct correlation between the size of CdSSe quantum dots formed in the glass matrix and the color rendering properties of the QDGMs. This finding has significant implications for the tailored design of QDGMs for specific color rendering needs across a variety of applications.

Keywords: quantum dots, glass, colorimetry, IES TM-30-18, color rendering index

P10

Estimation of the Reduced Effective Mass of Charge Carriers in PbS Nanostructures using the Effective Mass Approximation (EMA) and Hyperbolic Band Model (HBM)

Rabia Şahin[*1], Ali Barkhordari[*2], Yashar Azizian-Kalandaragh[*1,3]

[1] *Department of Photonics, Faculty of Applied Sciences, Gazi University, 06560, Ankara, Türkiye*
[2]*Faculty of Physics, Shahid Bahonar University of Kerman, Kerman, Iran*
[3]*Photonics Application and Research Center, Gazi University, 06560, Ankara, Türkiye*

Abstract: This study investigates the synthesis of lead sulfide (PbS) nanoparticles using ultrasonic waves to elucidate their structural and optical properties. Through X-ray diffraction (XRD), UV-visible spectroscopy (UV-Vis), and scanning electron microscopy (SEM), a comprehensive examination of the structural and optical features of the synthesized nanostructures was characterized. Analysis of SEM images and XRD of the prepared nanostructures confirmed the nanocrystalline PbS structures. Furthermore, UV-Vis spectroscopy was utilized to determine the band gaps of the PbS nanostructures, revealing a significant blue shift compared to bulk PbS material. This shift was attributed to alterations in the effective masses of electrons and holes within the nanostructures, arising from the quantum confinement effect inherent in PbS semiconductor nanostructures. To quantitatively evaluate the effective mass, the Effective Mass Approximation (EMA) and the Hyperbolic Band Model (HBM) were employed, incorporating experimental data on band gap energies and nanocrystal dimensions [1,2]. The findings from this study indicate that the reduced effective mass of charge carriers in PbS nanostructures is higher than that in bulk crystals. Additionally, the investigation reveals instances where the band gap of the nanoparticles is narrower than that of bulk crystals, which can be elucidated by variations in lattice parameters from the core to the surface of the nanoparticles. In summary, this research sheds light on the impact of synthesis methods on the optical properties and effective masses of charge carriers in PbS nanocrystals. The study underscores the paramount importance of comprehending these properties for the customized design and implementation of semiconductor nanomaterials in a wide array of applications.

Keywords: Quantum confinement effect, effective mass, PbS semiconductor nanocrystals, EMA, HBM.

References

1. Brus, L. Electronic wave functions in semiconductor clusters: experiment and theory. The Journal of Physical Chemistry,1986, 90(12), 2555–2560.
2. Ella L. Wassweiler, Melany Sponseller, Anna Osherov, Joel Jean, Moungi G. Bawendi, and Vladimir Bulovic, Metal Oxide Interlayers Enable Lower-Cost Electrodes in PbS QD Solar Cells, ACS Appl. Energy Mater. 2023, 6, 11, 5646–565.

P11

Effect of Hole Transport Layer Thicknesses on Efficiency of CdTe/CdS Solar Cell

Varol B. *[1,2], Efkere H.İ.[2], Ozen Y.[2,4], Aydın S.Ş.[2,3], Özçelik S.[2,3]

[1]*Gazi University, Graduate School of Natural and Applied Sciences, Photonics Science and Engineering Department, Ankara, Türkiye*
[2] *Gazi University, Photonics Application and Research Center, Ankara, Türkiye*
[3]*Gazi University, Faculty of Applied Sciences, Department of Photonics, Ankara, Türkiye*
[4]*Gazi University, Science, Department of Physics, Ankara, Türkiye*
email: beyzavarol09@gmail.com

Abstract: Due to its excellent absorption coefficient and almost ideal band gap of 1.47 eV, cadmium telluride is used as a thin-film photovoltaic material. Since CdTe absorbs more than 90% of accessible photons (hυ > 1.44 eV) at a thickness of 1 μm, films of 1-3 μm are sufficient for thin-film solar cells. CdS thin films are most frequently employed as a window layer in CdS/CdTe solar cells. Cadmium sulfide (CdS) has a wavelength of 514 nm for its absorption maximum peak, meaning that it can absorb UV and visible light with a band gap of 2.42 eV. The higher efficiency of CdTe/CdS solar cells in the superstrate configuration over the substrate configuration sets them apart from other types of cells. High-performance solar cells can be produced by inserting a hole transfer layer (HTL) to restrict carrier recombination at the interface between CdTe and a back contact electrode. This will provide an interfacial dipole effect [1-2].

In this study investigated at how the thickness of the hole transport layer affected the glass/ITO/CdS/CdTe/ZnO/NiO solar cell's efficiency. Using Co-Sputtering System, layers of CdS, CdTe, ZnO, and NiO were deposited on ITO-coated glass. NiO layers were deposited with thicknesses of 50, 100, 150 nm and the samples were named as S1, S2 and S3, respectively. The samples were subjected to structural and optical investigations using X-ray diffraction (XRD) and UV-Vis spectrometer systems. The samples were fabricated for electrical measurements, and a Solar Simulator was used to determine the electrical output parameters. Upon analysis of the results, the most efficient solar cell structure was identified.

Acknowledgements: This work was supported by the Presidency of Strategy and Budget (Türkiye) under project numbers of 2019K12-149045.

References

1. Ferekides C., Britt J., “CdTe solar cells with efficiencies over 15%”, Solar Energy Materials and Solar Cells, 35, 255-262 (1994).
2. Jiang Y., Pan Y., Wu W., Luo K., Rong Z., Xie S., Zuo W., Yu J., Zhang R., Qin D., Xu W., Wang D., Hou L., “Hole Transfer Layer Engineering for CdTe Nanocrystal Photovoltaics with Improved Efficiency”, Nanomaterials, 10(7), 1348 (2020)

P12

Developing Anti-Reflective Thin Films on GaAs Substrate for Infrared Applications

Sayın B.*[1,2], Özçelik S.[1]

[1]*Photonics Application and Research Center, Gazi University,06560 Ankara, Türkiye*
[2]*Transvaro Electron Devices, HAB Saray OSB Mah. G5 Cad. No:40-11 Kahramankazan, Ankara, Türkiye*
email: sayinn.bengisu@gmail.com; sozcelik@gazi.edu.tr

Abstract: The scattering and reflection of light reaching the detector surface are significant factors that reduce the detection efficiency and sensitivity in infrared detectors. The aim of this study is to develop suitable anti-reflection thin films to reduce scattering and reflection in GaAs-based detectors. The high refractive index of GaAs material (n=3.3) is considered a fundamental factor increasing reflection. Therefore, the reduction of reflection and enhancement of detector sensitivity are targeted by coating the detector surface with an anti-reflection film with a lower refractive index. In this study, original multilayer coating designs were developed on GaAs substrates to achieve 95% optical transmittance in the 3-5 micrometer band (MWIR) through design and film coating efforts. The developed anti-reflection thin film structures were modeled using Essential Macleod software as three-layers (Si3N4/SiO2/Si3N4). Thin films designed with Essential Macleod were produced using sputtering technique, and the structural properties of the anti-reflection layers were determined by X-ray diffraction (XRD), optical properties by Fourier Transform Infrared Spectroscopy (FTIR), and surface morphology properties by Atomic Force Microscopy (AFM) measurements. The XRD analysis results are shown in Figure 1, FTIR (Fourier Transform Infrared Spectroscopy) spectra are shown in Figure 2, and 2D and 3D AFM images with a size of 5μm2 are displayed in Figure 3. This study represents a significant step towards enhancing the performance of GaAs infrared detectors, and it is believed to have the potential to substantially improve the performance of other infrared detection systems in the industry.

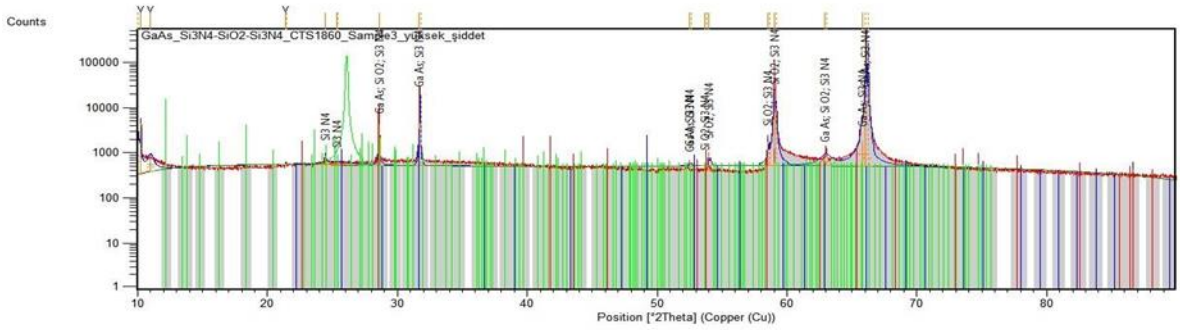

Figure 1.

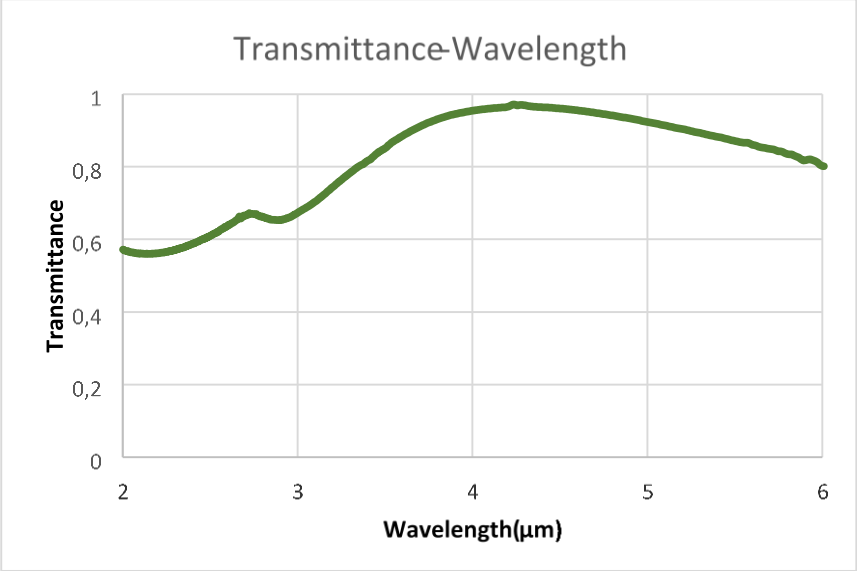

Figure 2.

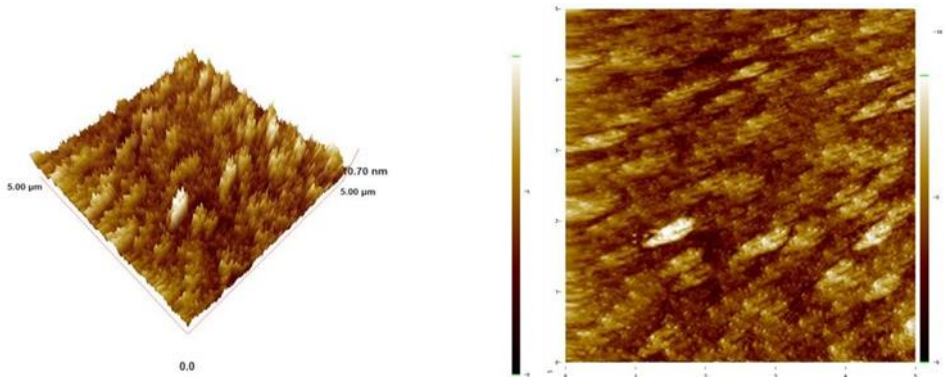

Figure 3.

Keywords: GaAs, Antireflection, Coating, Thin Films, Infrared, Essential Macleod

This study was supported by T.R. Presidency Strategy and Budget Office under Project number 2019K12-149045

P13

High-Precision Measurement of Refractive Indices of Liquids and Thin Films Using the Fresnel Diffraction Method

KARAKAYA G.C. [*1], AZIZIAN-KALANDARAGH Y.[1,2]

[1]*Department of Photonics, Faculty of Applied Sciences, Gazi University, Ankara, Türkiye, 06560*
[2]*Photonics Application and Research Center, Gazi University, Ankara, Türkiye, 06560*
email: gcan.karakaya@gazi.edu.tr, yasharazizian@gazi.edu.tr

Abstract: This study investigates the high-precision measurement of refractive indices of liquids, solutions, and transparent thin films using the Fresnel diffraction method from an abrupt phase step formed by a transparent wedge. Refractive index is of critical importance in the optical and lens industry, in the design of optical and imaging systems, and in photonics applications. Based on theoretical studies, it is known that a change in medium causes a phase shift in light, which is proven to be related to the refractive index by Snell's law. In traditional measurement methods, the precision level of the measurement is around 10-2 to 10-3, and these precision levels are becoming inadequate today. This study aims to develop a diffraction refractometry study that operates with high precision using the Fresnel diffraction method. It is anticipated that this study will be successful considering that there is no limitation in the measurement of refractive index and the real limitation is the methods we use and the technological developments we have. The targeted precision level is in the order of 10-5. It is aimed to make a significant contribution to the science of optics and photonics with this experimental study, which will enable the measurement of refractive index with higher precision, and to encourage future studies in this field.

Keywords: Refractive Index, High-Precision Measurement, Fresnel Diffraction, Diffraction Refractometry

P14

Anti-Reflective Layer Design Using Scattering Matrix Method for P3HT:PCBM Organic Solar Cell

Dereli T. [*1], Dilek E.[1], Durgun A.[1], Hatipoglu I. [*1,2,]

[1]*Department of Photonics, Faculty of Applied Sciences, Gazi University, Ankara, Türkiye, 06560*
[2]*Photonics Application and Research Center, Gazi University, Ankara, Türkiye, 06560*
email: talha.dereli@gazi.edu.tr, isahatipoglu@gazi.edu.tr

Abstract: As the global population escalates, so does the energy demand. Solar cells provide a sustainable solution, converting sunlight into electricity and fostering a cleaner environment. While silicon-based cells dominate, organic variants like P3HT:PCBM are gaining ground for their enhanced efficiency and cost-effectiveness.[1,2] Yet, achieving higher efficiency for organic solar cells necessitates integrating critical anti-reflection layers. Despite P3HT:PCBM being a prevalent polymer in organic solar cell research, there remains a notable gap in the literature concerning efforts to mitigate optical losses. Previous studies often employed multilayer structures without thorough consideration of cost and practicality.[3] In this study, we address this gap by employing the S-Matrix Method to theoretically determine optimal material properties, considering the numerical stability required for structures containing absorbing materials.[4] Subsequently, the material closest to these theoretically calculated properties was selected, thereby identifying the most cost-effective single-layer material. Our findings demonstrate a significant enhancement in efficiency, with the classical design yielding 84% transmission to P3HT:PCBM film compared to 98% achieved through the implementation of an anti-reflection layer design.[5] This 14% increase in efficiency directly tackles a primary concern in P3HT:PCBM solar cell performance, while also preserving cost-effectiveness. The implications of this study extend beyond mere efficiency improvements; it offers valuable insights for researchers engaged in the study of organic solar cells, showcasing potential avenues for advancing the field.

Keywords: Scattering Matrix Method, anti-reflective coating, organic solar cells, P3HT:PCBM

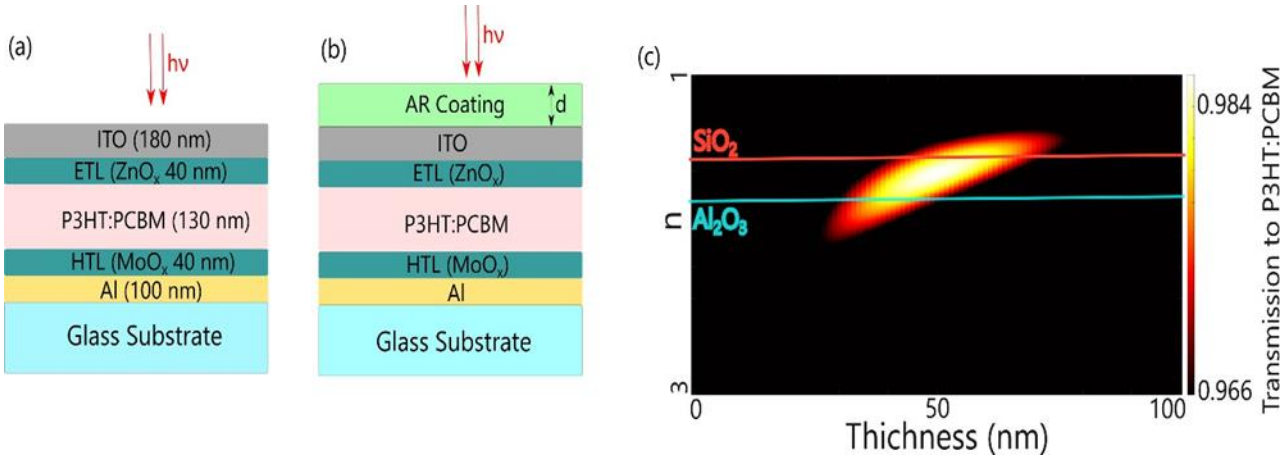

References

1. Li, Gang, Rui Zhu, and Yang Yang. "Polymer solar cells." Nature photonics 6.3 (2012): 153-161.
2. Berger, P. R., and M. Kim. "Polymer solar cells: P3HT: PCBM and beyond." Journal of Renewable and Sustainable Energy 10.1 (2018).
3. Kubota, Shigeru, et al. "Robust design method of multilayer antireflection coating for organic solar cells." IEICE transactions on electronics 96.4 (2013): 604-611.
4. Moharam, M. G., et al. "Formulation for stable and efficient implementation of the rigorous coupled-wave analysis of binary gratings." JOSA a 12.5 (1995): 1068-1076
5. Çetinkaya, Ç. et al. Design and fabrication of a semi-transparent solar cell considering the effect of the layer thickness of MoO3/Ag/MoO3 transparent top contact on optical and electrical properties. Scientific Reports 2021 11:1 11, 1–17 (2021).

P15

Investigation of Optical, Structural and Morphological Properties of Zirconium Oxide Thin Films

Selim Y.N. [*1,2], Toprak B.Ç. [1,2], Efkere H.İ.[2], Tataroğlu A.[2,4], Aydın S.Ş.[2,3], Özçelik S.[2,3]

[1]*Gazi University, Graduate School of Natural and Applied Sciences,* Photonics Science and Engineering Department*, Ankara, Türkiye*
[2] *Gazi University, Photonics Application and Research Center, Ankara, Türkiye*
[3]*Gazi University, Faculty of Applied Sciences, Department of Photonics, Ankara, Türkiye*
[4]*Gazi University, Science, Department of Physics, Ankara, Türkiye*
email: yareenseliim@gmail.com

Abstract: Zirconium oxide (ZrO_2) is crucial for many industries due to its strong mechanical properties and thermal stability. ZrO_2 thin films show promise in various applications, such as optical coatings and electronics, thanks to their high refractive index and chemical stability. Research aims to improve deposition methods and explore new uses for ZrO_2 thin films [1].

In this study, ZrO_2 thin film was deposited on n-Si and glass substrates with an RF magnetron sputtering system at room temperature with a thickness of 100 nm at an operating pressure of 5 mTorr. Structural, optical and morphological properties of the produced ZrO_2 thin film were examined using X-ray diffraction (XRD), UV-Vis Spectrometry and Atomic Force Microscope (AFM) systems. ZrO_2 thin film surface morphology was examined from Atomic Force Microscope (AFM) measurements. The root mean square (RMS) values of the surface roughness of the thin films were found to be 0.80 nm. When the XRD pattern of the ZrO_2 thin film was examined, diffraction peaks were observed at 30.07° (111), 44.15 ° (211), 52.60° (220) and it was determined that these peaks had a cubic crystal structure. Using the optical transmittance spectrum obtained from UV-Vis measurement, the Tauc curve was obtained and the energy band gap of the thin film was found to be approximately 4.1 eV.

Acknowledgements: This work was supported by the Presidency of Strategy and Budget (Türkiye) under project numbers of 2019K12-149045.

References

1. Qi H.J., Huang L.H., Tang Z.S., Cheng C.F., Shao J.D., Fan Z.X., “Roughness evolution of ZrO_2 thin films grown by reactive ion beam sputtering”, Thin Solid Films, 444, 146-152 (2003).

P16

Electric and Optic Properties of B1-xAlxN Alloys Using Ab Initio Calculation

Bayal Özlem*[1], Öztürk M. Kemal [2]

Department of Physics, Gazi University, Ankara, Türkiye
email: [1]ozlembayal@gmail.com, [2]ozturkm@gazi.edu.tr

Abstract: In this study, electronic, optical, elastic, dynamical and structural properties of B1-xAlxN structure are investigated. During this investigation, density functional theory (DFT) in CASTEP code, local density approximation (LDA) and generalized gradient approximation (GGA) are employed. B/G ratio, Bulk module (B), Scherar module (G), Poisson's ratio (v), Kelinman parameters (ξ), Cauchy pressure (P), compressibility are gained by using elastic constants for the mentioned structure. B1-x Alx N structure showed epitaxial semiconductor behaviour with well crystallized and brittle characteristics. It also showed cubic structure behaviour for 0.25 and 0.75 Al content and tetragonal structure for 0.50 Al content. With increasing Al ratio, band gap values showed decreasing behaviour as 4.06, 3.56 and 3.34 eV respectively. It is noticed that compressibility is affected by increasing Al contents. It is also found out that real part of refraction constant (RPRF) is in accordance with real part of Dielectric function (RPDF). Peak center of losing function is gained as 27.75 eV for %25 Al content. This value corresponds with maximum Plasmon frequency.

P17

Diffractive beam shaping element for generating multiple structured beams with distinct spatial structures

Ebrahimi H. *[1], Sabatyan A.[2]

Physics Department, Faculty of sciences, Urmia University, Urmia, Iran .
Email[1]: h.Ebrahimi@urmia.ac.ir.
Email[2]: a.sabatyan@urmia.ac.ir.

Abstract: This study introduces a new method for creating multiple beams using a forkgrating-based spiral zone plate (FSZP). The FSZP is modified by a forked grating, resulting in a multi-beam element that generates various optical vortices and structures at the focal plane. The characteristics of the FSZP are examined through theoretical, mathematical, simulation, and experimental analyses, using different samples with varying parameters, including the topological charge of the SZP and coefficients related to trigonometric functions. These parameters have a significant impact on the output beam structure, leading to the creation of multiple distinct structures at the focal point. In particular, the FSZP produces two sets of off-axis focal spots with different topological charges. The findings demonstrate that this innovative element offers a flexible and effective approach to producing structured light in a customized array with specific properties, facilitating applications in optical communication, imaging, and manipulation. This method has the potential to pave the way for further research and advancements in the realm of structured light.

To illustrate the approach, we show the process of creating several samples and their respective point spread functions in the figure below.

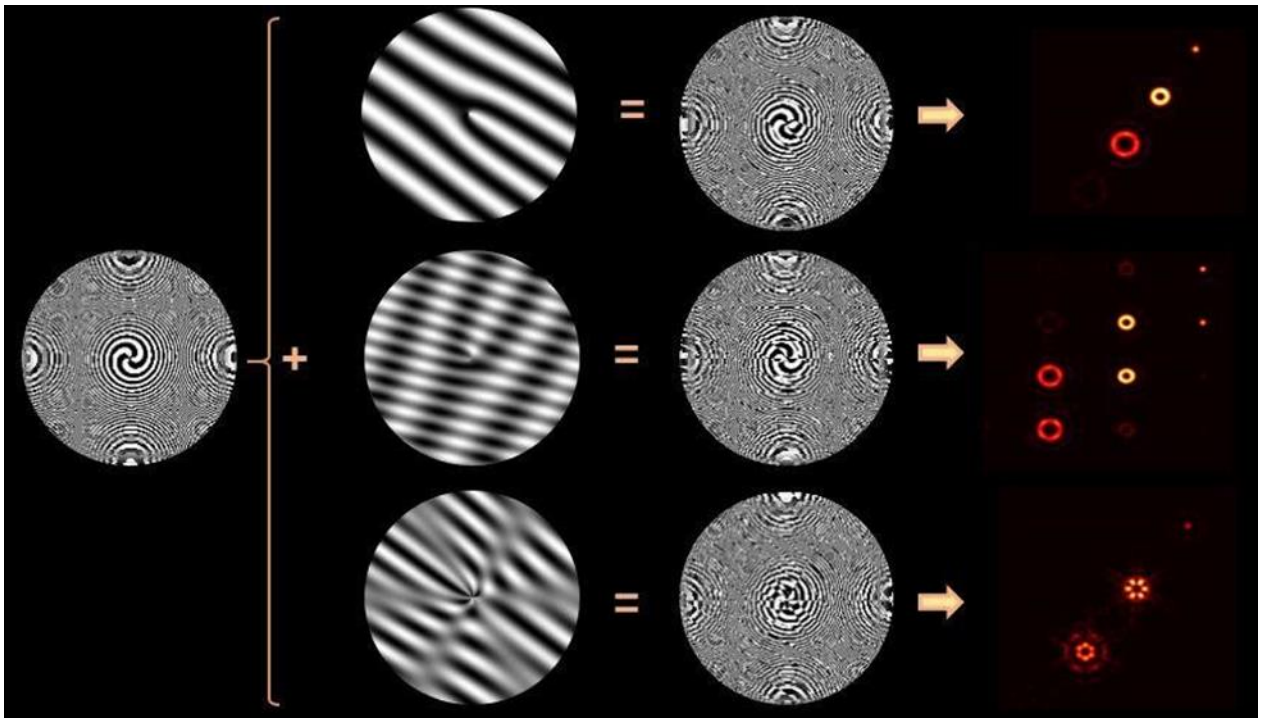

P18

Novel Optical Arrays using a Multi-Focusing Complex Sinusoidal Grating-Based Spiral Zone Plate

Ebrahimi H. [*1], Sabatyan A.[2]
Physics Department, Faculty of sciences, Urmia University, Urmia, Iran .
email: [1]h.Ebrahimi@urmia.ac.ir. , [2] a.sabatyan@urmia.ac.ir.

Abstract: This paper presents a novel composite diffractive element that can be precisely adjusted to create a variety of impressive beam patterns and structures. Specifically, we have enhanced the spiral zone plate by integrating a complex sinusoidal grating into its design, significantly expanding the range of available parameters to shape different light beams. This means increasing the variety of options for adjusting various factors that determine the characteristics of light beams, allowing for a wider range of customization and control over how the light beams look and behave. Thus, this element serves as a multi-focusing device, allowing for the generation of optical arrays in various forms, from simple spots and grids to complex and innovative beam shapes. Our study includes thorough mathematical analysis and related simulations, along with experimental confirmation of the mathematical results. To demonstrate the approach, we present the process of generating multiple samples and their corresponding point spread functions in the figure below.

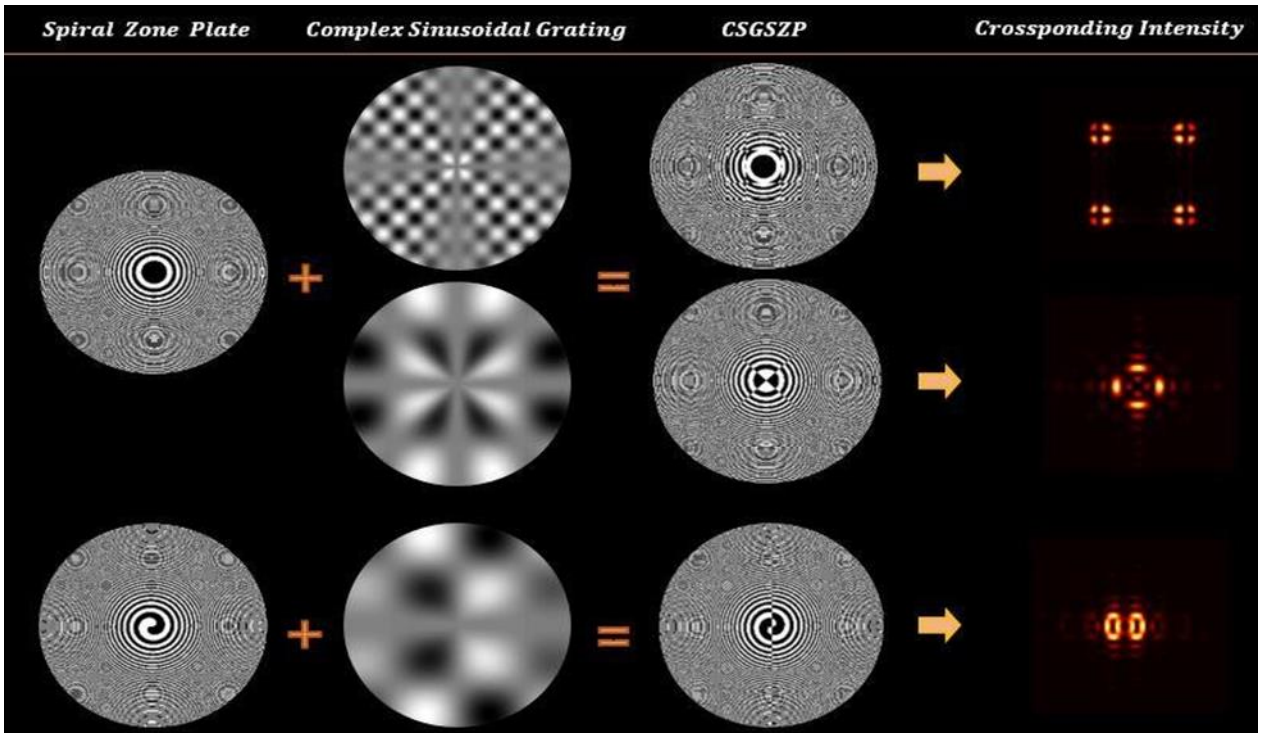

P19

Object Detection with Deep Learning A in Microscopy Applications

Farazin J. [*1], Rahmani M.[1], Hajizadeh F.[1], Ahadi Akhlaghi E. [1]

[1]*Department of Physics, Institute for Advanced Studies in Basic Sciences (IASBS), Zanjan 45137-66731, Iran.*
email: javidfarazin@gmail.com

Abstract: The integration of artificial intelligence (AI) in microscopy has revolutionized the field of image analysis, enabling rapid and accurate object detection in various microscopy applications. This review summarizes the current state of AI-powered object detection in microscopy, highlighting the applications of deep learning techniques in microscopy and other microscopy modalities. We discuss the principles of deep learning, including convolutional neural networks (CNNs) and generative adversarial networks (GANs), and their applications in Microscopy, such as denoising and image restoration. We also explore the challenges and limitations of object detection in microscopy, including the need for high-quality training datasets and the importance of evaluating object detection models in real-world scenarios. Furthermore, we examine the potential of AI-powered object detection in microscopy to enable automated image analysis, improve diagnostic accuracy, and enhance research productivity. Finally, we outline future directions for research in this field, including the development of more robust and efficient object detection models and the integration of AI with other microscopy techniques.

P20

Improving Spatial Resolution in Point-Scanning Fluorescence Microscope Using Bessel Beams

Hajipoor Z. [*1], *Shadafrooz H.*[1], *Fazlalizadeh Z.*[1] A. Akhlaghi E.[1,2]

[1]*Department of Physics, Institute for Advanced Studies in Basic Sciences (IASBS), Zanjan 45137-66731, Iran,*
[2]*Optics Research Center, Institute for Advanced Studies in Basic Sciences (IASBS), Zanjan, 45137-66731, Iran,*
email: e.a.akhlaghi@iasbs.ac.ir

Abstract: Advancing progress across scientific fields such as medicine, biology, and technology relies heavily on enhancing resolution in optical imaging. Precision instruments, like optical microscopes, play a crucial role in accelerating advancements in various research domains. To optimize their performance, improving and developing two parameters - resolution and contrast - are essential. For observing biological processes by labeling transparent specimens, fluorescence microscopy is a commonly used imaging technique. To identify intracellular structures, this system requires a spatial resolution of 100 (nm) and adequate temporal resolution for studying the dynamics of cellular processes. One promising method for improving fluorescence microscopy is the point scanning technique, a three-dimensional imaging method that enhances spatial resolution, eliminates out-of-focus light, and improves image contrast.

By solving the Helmholtz equation, we reach the complex amplitude corresponding to the Bessel functions:

$$E_n(r,\phi,z) = Ae^{ik_z z}J_n(k_r r)e^{\pm in\phi} \qquad (1)$$

Optical beams with such a complex amplitude are known as Bessel beams. In Eq. (1), If n=0, we will have the Bessel beam of order zero and the complex amplitude becomes Eq. (2)

$$E_0(r,\phi,z) = Ae^{ik_z z}J_0(k_r r) \qquad (2)$$

Our research goal are to design and implement a setup based on the point scanning technique using Bessel structured lighting to improve spatial resolution.

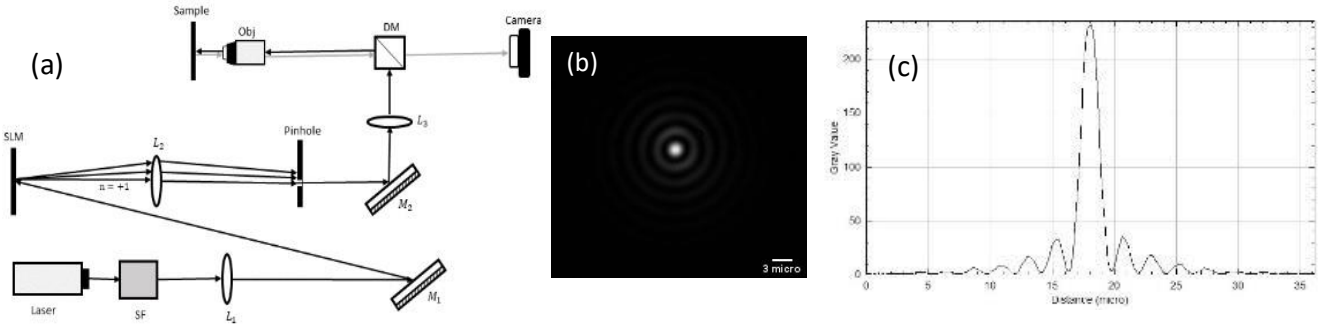

Figure 1. a) Schematic setup for **fluorescence microscope** (**laser**, laser diode; **SF**, spatial filter; **L_1**, lens; **M_1**, flat mirror; **SLM**, spatial light modulator; **L_2**, lens; **M_2**, flat mirror; **L_3**, lens; **DM**, dichroic mirror; **Obj**, objective). (b) The experimental intensity profile of a Bessel beam has been measured.

P21

Investigation of Surface Roughness by Scattering Method

Atefeh Sadeghi

Institute for Advanced Studies in Basic Sciences Department of Physics, Gava Zang, Zanjan, Iran
email: atefehsadeghi@iasbs.ac.ir

Abstract: It has been about a century that level mapping has been taken into consideration in a wide range of different basins. The statistical behavior of surfaces has many applications in various fields such as storing information on surfaces, making thin layers and producing quality optical parts.

In industries, there may be a need to use the properties of rough surfaces, or to eliminate the degree of roughness of the surfaces. Undoubtedly, the most widely used optical tool is a lens, and in fact, we also see the world through the lens of a pair of them. Lenses are made through abrasion, which causes scratches on their surface. The presence of scratches on the lens causes the white light reflected from the surface of the lens to appear gray due to scattering in different directions at the location of the scratches.

At the same time as the first optical surfaces were made about four hundred years ago, the examination of these surfaces was limited to visual inspection. In this way, after shaping these surfaces in the polishing stage, they continued the smoothing operation until the gray lines were completely removed. In the industry, the roughness of the produced parts was checked visually or by touching the surface with the tips of the fingers to understand the feeling of roughness or smoothness. Due to the importance of roughness measurement, in 1940, the first National Institute of Standards and Technology was established in America, with the aim of monitoring the quality and controlling the quality of manufactured parts.

There are many methods for measuring rough surface parameters, which generally fall into two categories of contact and non-contact methods. For example, mechanical profilers are in the category of contact roughness measurement methods, and interferometry and scattering are in the non-contact category. In addition to being destructive, contact methods have a lower data transfer rate than non-contact methods.

In my project, I have measured the roughness of surfaces with different degrees of roughness using the scattering pattern with several different methods. In the first chapter, the simulation of uneven surfaces was done by the scattering method in two dimensions. The second chapter of the examination of surfaces with different degrees of roughness (uneven glasses with different mesh numbers), the analysis of the roughness measurement pattern of glass surfaces has been done by the scattering method in the laboratory and using an optical setup. In the third chapter, the smooth glass is roughenedusing powder sandpapers and the spectrum of the rough glass is measured by the spectrometer in the available length of 400 to 800 nm. Spectrometer

reflection accessory has been used to capture the spectrum of the samples, and some samples have been converted to 50 nm silver by the coating device and tested. In the fourth chapter, samples with different degrees of roughness are drawn.

P22

Novel 1D Helico-Conical Optical Beam Generation via Restructured Linear Zone Plates

Fatehi M. [*1], Sabatyan A.[2], Ebrahimi H.[3]

Physic Department, Urmia University, Urmia,
email: st_m.fatehi@urmia.ac.ir, a.sabatyan@urmia.ac.ir , h.ebrahimi@urmia.ac.ir

Abstract: Helical-Conical beams are a specialized 2D type of optical beams produced by utilizing a phase element with helico-conical properties, that exhibit a helical phase front with a conical shape. The helico-conical nature of these beams makes them particularly useful for applications such as optical tweezers, optical communications, and optical data storage, optical trapping, and micromanipulation.

Our objective is to modify a 1D Fresnel-Zone Plate by incorporating a helico-conical phase function to investigate its potential in producing 1D helico-conical optical beams for the first time. Following the specification of the phase, we analyzed its focusing characteristics using Fresnel-Kirchhoff diffraction integration. By adjusting the specified parameters of the helico-conical phase, we have showcased the development of a variety of innovative structured optical beams. Additionally, altering the conical phase both normally and parallel to the linear zones of the FZP resulted in the generation of distinct structured beams. This facilitates the easy management of their characteristics. The simulation outcomes are supported and confirmed through corresponding experimental validation. Some of the generated unique beams have been shown in the following.

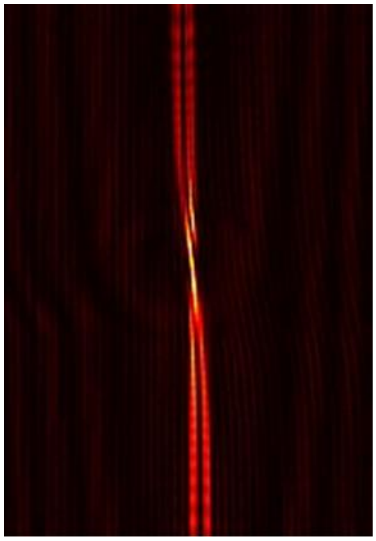
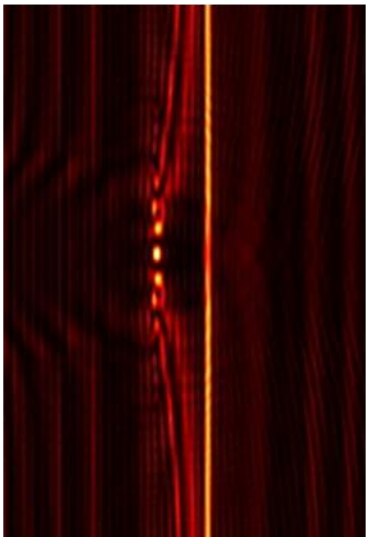
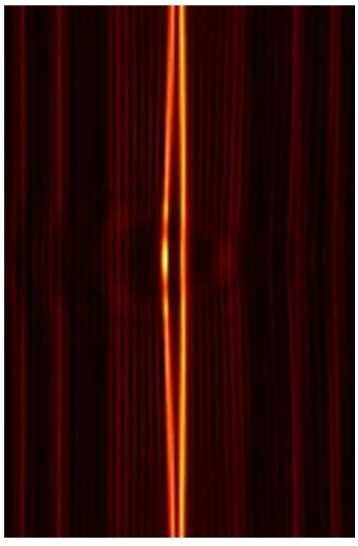

P23

Investigating the relationship between the induced current in the excitation of surface plasmon sensors with the reflection optical spectrum

Mollaha Maryam*

Department of Photonics, Faculty of Physics, Institute for Advanced Studies in Basic Sciences (IASBS), Zanjan, Iran.

Abstract: Surface plasmon resonance (SPR) sensors have emerged as a sensitive and precise method for detecting molecules and chemical changes in various environments. This technique is based on the absorption of light by surface plasmons, which changes in response to alterations in the surrounding environment.

In investigating the relationship between the induced current in SPR sensors and the reflected optical spectrum, the sensors are first excited using a specific light source. The induced current in the sensors generated by surface plasmons leads to changes in the reflected optical spectrum.

By analyzing the reflected optical spectrum, detailed information about the changes in the induced current in the sensors and the results of exciting surface plasmons can be obtained. This non-destructive and sensitive method can aid in the detection and identification of molecules and chemical changes in various environments, serving as a powerful tool in fields such as medicine, food identification, and industry.

The interaction between the induced current and the optical spectrum in SPR sensors provides valuable insights into the molecular interactions occurring at the sensor surface. By monitoring the changes in the optical spectrum, researchers can gain a deeper understanding of the binding events between analytes and receptors immobilized on the sensor surface. This real-time monitoring capability makes SPR sensors a versatile tool for studying biomolecular interactions, drug discovery, and environmental monitoring.

Overall, the correlation between the induced current in surface plasmon resonance sensors and the reflected optical spectrum offers a valuable approach for studying molecular interactions, detecting analytes, and monitoring chemical processes with high sensitivity and specificity. This technology holds great promise for advancing research in various scientific disciplines and applications.

P24

Polarization-Dependent Modulation of Surface Plasmon Resonance with Highly Focused Gaussian Beams

Delgoshaei S. [*1], Abdollahpour D.[1], Mostafavi Amjad J.[1]

[1] *Department of Physics, Institute for Advanced Studies in Basic Sciences (IASBS), Zanjan, 45137-66731, Iran.*
email: simindelgoshaei@iasbs.ac.ir dabdollahpour@iasbs.ac.ir mostafavi@iasbs.ac.ir

Abstract: In this study, we explore the dynamics of Surface Plasmon Resonance (SPR) influenced by linear and circular polarizations using Gaussian beams. We investigate how these polarization states affect SPR at the nano-bio interface. By examining the SPR responses under linearly and circularly polarized light, we understand how polarization impacts the behavior of Transverse Magnetic (TM) and Transverse Electric (TE) modes. Our approach simplifies the optical setup, making it easier to see how SPR responds to different polarizations. This helps us see polarization as a tool to fine-tune SPR, potentially transforming SPR-based sensing technologies. We also introduce SPR microscopy (SPRM), which combines the high-resolution of optical microscopy with the capabilities of SPR. SPRM enhances the benefits of both methods, allowing for direct visualization of samples and real-time analysis of binding affinity and kinetics. The findings from this research not only advance optical diagnostics but also improve the design of SPR sensors. This marks an important advance in plasmonics, connecting basic understanding with practical uses, and highlights the role of polarization in improving optical sensing and material characterization.

Keywords: Surface Plasmon Resonance Microscopy, Polarization Effects, Gaussian Beams, Optical Sensing, Plasmonic Modulation

P25

The Influence of Azimuth Phase on the Diffractive Behavior of Axilens

Javidi B.[*1], Sabatyan A.[2]

Physics Department, Urmia University,Urmia,Iran
email: Javidibehnaz76@gmail.com, a.sabatyan@urmia.ac.ir

Abstract: Herein, we are about to introduce a novel diffractive element base on axilens. Axilens is an optical element which is combination of axicon and focusing lens. So, axilens is a long focal depth optical element. By incorporating a modulating azimuthal phase into its structure, we have developed a spiral axilens. When illuminated by a plane beam, the spiral axilens is expected to create a nondiffractive vortex beam.

Our examination of the focusing behavior of the spiral axilens has shown that it produces a non-diffractive optical vortex which is azimuthally modulated. Surprisingly, it is very practical in measuring topological charge, as the number of the modulated arcs determines the topological charge of the vortex beam.

However, a very long hollow optical cylinder carrying topological charge is generated by the element that could be implemented in many applications, such as optical trapping, lidar and particle guiding.

Additionally, this diffractive element produces some kind of Pearcey beams very simply.

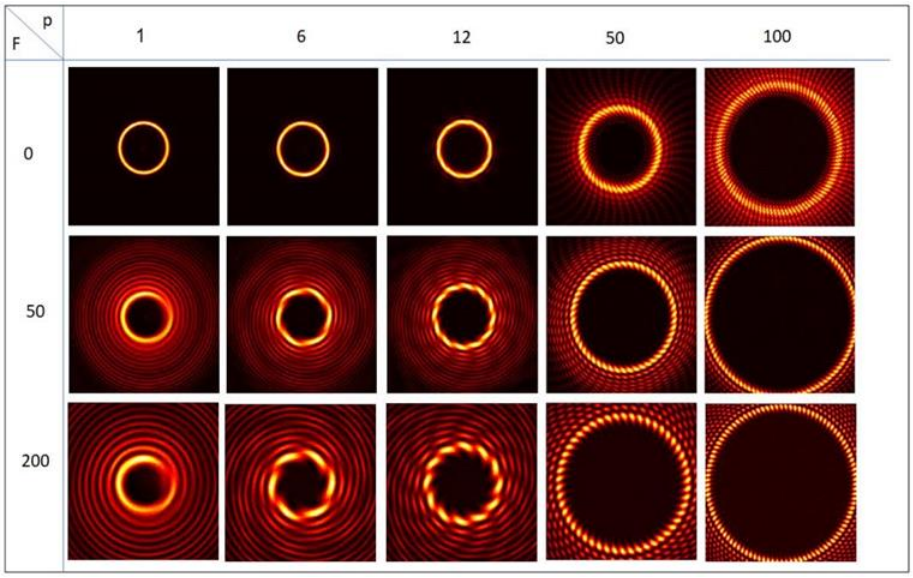

Figure 1. The simulated intensity distribution of spiral axilens with topological charges of 1, 6, 12, 50, and 100, arranged from left to right. The first, second, and third rows correspond to F=0, 50, and 200, respectively.

P26

Frequency and voltage dependence of complex dielectric, coelectric modulus and ac conductivity (σ_{ac}) in the Al/DLC/p-Si structures in wide range frequency and voltage

Balcı E.[*1,3], A. Feizollahi Vahid A.[2], Altındal Ş.[3]

[1]*Department of Physics, Polatlı Faculty of Sciences and Arts, Ankara Hacı Bayram Veli University, Ankara, Türkiye*
[2]*Department of Nanotechnology Engıneering, Zonguldak Bulent Ecevit University, Zonguldak, Türkiye*
[3]*Department of Physics, Faculty of Sciences, Gazi University,06560, Ankara, Türkiye*
email: *balci.esra@hbv.edu.tr*

Abstract: In this study, Al/DLC/p-Si structures were fabricated instead of traditional metal/insulator/semiconductor (MIS) structures and then frequency and voltage dependence properties of real and imaginary components of the complex dielectric ($\varepsilon^*=\varepsilon'-j\varepsilon''$), complex electric modulus ($M^*=M'+jM''$), loss-tangent ($\delta=\varepsilon''/\varepsilon'$), and ac conductivity ($\sigma_{ac}$) have been investigated in wide frequency range of 2kHz/1MHz and ±5V, respectively. All these values were calculated from the measured capacitance and conductance values. The increase of ε' and ε" with decreasing frequency were explained by the existence of surface-states (N_{ss}), surface and dipole-polarizations especially at low and moderate frequency in depletion region. The observed an anomalous-peak in the ε'-V plot at accumulation was attributed to the existence of series-resistance (R_s) especially at high frequencies. The observed changes in the ε' and ε" with frequency was attributed to the Maxwell-Wagner type polarization. The observed peak in the M''-V plot almost for each frequency and shifts its position was explained by the relaxation-process and N_{ss} effects at low-moderate frequencies. The value of ε', even at 2 kHz, is about 4.28 times higher than the maximum value of traditional SiO_2 (3.8), and hence, it can be successfully used instead of traditional insulators to more storage electronic charges or energy.

Keywords: Diamond Like Carbon (DLC) interlayer Frequency and voltage dependence; Dielectric and relexation properties; Al/DLC/p-Si Schottky structures

P27

Analysis of Pore Sizes in Porous Glasses Produced Using HF, HNO_3 and H_2SO_4 Acids

Yener N.N. [*1], Elmas M.F.[1], Seymen O.K.[1], Erenler B.[1,2], Sönmez N.A.[1,2]

[1]*Department of Photonics, Gazi University 06560, Ankara, Türkiye,*
[2]*Photonics Application and Research Center, Gazi University, 06560 Ankara, Türkiye,*
email: nnur.yener@gazi.edu.tr; nihanakin@gazi.edu.tr

Abstract: Glass is a non-crystalline material widely used in decorative and technological applications. Its hardness, transparency, and stability, electrical, chemical, and thermal have increased its popularity. Porous glass, characterized by voids, channels, or slits, is notable for its transparency in the visible light spectrum and excellent mechanical stability [1,2]. In this study, commercial sodium borosilicate glass substrates with compositions of 81% SiO_2, 13% B_2O_3, 4% Na_2O/K_2O, and 2% Al_2O_3 by weight were used. Each piece was cleaned with soap, acetone, alcohol, and deionized water in an ultrasonic cleaner, then dried with high-purity nitrogen. The cleaned glass pieces were subjected to phase separation in a diffusion furnace. They were annealed at different times and with various accessories. Post-annealing, the glass pieces, now combined into two phases (alkali-borate and silicate), were immersed in hot dilute acid solutions. Gradually, HF, HNO_3, and H_2SO_4 acids were tested in different ratios and processes. This process, also known as filtering, involved varying times and temperatures to create a series of samples for comparison. In the final production stage, the glass parts were dried in an annealing oven, completing the production of porous glasses under different conditions and durations. Phase separation enables control of macropores sizes in the glass, ranging from nanometers to micrometers. The physical properties and pore size of the porous glass formed by phase separation depend on three main parameters of the production process: (i) composition of the starting glass, (ii) heat treatment conditions (time and temperature), and (iii) acid type and leaching conditions.

Keywords: porous glass, phase separation, acid leaching.

Acknowledgements This work was supported by TUBITAK (2209-A) under Project No:1919B012203984.

References

1. Addanki, S., Nedumaran, D. (2017). Fabrication of ozone sensors on porous glass substrates using gold and silver thin films nanoislands. Optik, 150, 11-21.
2. Balaguer, A., Chisvert, A., Salvador, A., Herraez, M., & Diez, O. (2008). A solid-phase extraction and size-exclusion liquid chromatographic method for polyethylene glycol 25 p-aminobenzoic acid determination in urine: Validation for urinary excretion studies of users of sunscreens. analytica chimica acta, 611(2), 220-225.

P28

Development of Full Reflective Reflector for Solid-State Lasers

Mahmut Çağlayan[1], Rabia Şahin[1], Elif Temel[1], Utku Yaman Can Aslan[1]
Süleyman Özçelik [1,2,3]

[1]Photonics Department, Gazi University, 06560, Ankara
[2]Photonics Application and Research Center, Gazi University, 06560, Ankara
[3]ASENTEK Defense and Energy Technologies, OSTIM Technopark 06374, Ankara

Abstract: Solid-state lasers are an important sub-branch of laser technology and are widely used in industrial and scientific applications. These lasers have advantages such as high energy efficiency, long lifetime, stable operation, and wide wavelength range. To increase the performance of solid-state lasers, reflector systems used in pumping lasers in the form of solid-state rods are of great importance. These systems increase the efficiency of the laser by reflecting and focusing the laser light. The main purpose of this study is to design a silver-coated reflector by electroless coating method to improve the performance of solid-state lasers. The electroless plating method is a technique that enables the application of metal layers to surfaces without relying on chemical or electrochemical reactions [1,2]. In this study, silver plating was applied to glass samples using the electroless method. It is evaluated that the developed coating technology can make a significant contribution to the domestic production of fully reflective reflectors for solid-state lasers supplied from abroad in our country. As a result of the experiments, around 99.1% reflectance was achieved in the 500-900 nm range. This work has the potential to improve the performance of solid-state lasers using the electroless coating technique, an economical technique that can be expanded to industrial mass production.

Keywords: Solid-state lasers, reflector systems, electroless plating, silver coating, performance enhancement

References

1. Muench F., (2021) “Electroless Plating of Metal Nanomaterials” Chem. Electro. Chem. 8, 2993–3012
2. Smith, J., & Johnson, A. (2023). "Optimizing Silver Thin Films for Enhanced Infrared Reflection and Visible Range High Reflectivity." Journal of Materials Science and Technology, 45(2), 215-230. doi:10.1234/jmst.2023.1234567

P29

Synthesis and Characterization of FTO Thin Films Coated by Sol-Gel Method

Ali Mert GÜNDOĞDU[1], Gamze Altun[1], Kaan YILMAZ[1], Süha Gül KARA[2], Betül SATILMIŞ[2], Tuğçe ATAŞER[1,2]

[1]Department of Photonics, Faculty of Applied Sciences, Gazi University, 06560, Ankara, Türkiye
[2]Photonics Application and Research Center, Gazi University, 06560, Ankara, Türkiye

Abstract: Transparent conductive oxide films have attracted significant attention because of their potential applications in optoelectronic devices. SnO_2 thin films exhibit high optical transparency ($T \geq 85\%$) and a large n-type electrical conductivity that can be tailored by doping with foreign atoms. The most favored doping atoms are indium (In) and antimony (Sb) which substitute tin cations or fluorine (F) substituting the oxygen. Among them, fluorine-doped tin oxide (FTO) films show rather low resistivity and highly chemical and thermal stable [1]. Recently, FTO films have been extensively used optoelectronic devices such as solar cell [2], sensor devices [3], touch panels, light emitting diodes [4]. The FTO films are deposited using a variety of coating techniques including chemical vapor deposition [5], magnetron sputtering [6] and sol-gel method [7]. Sol-gel process is more advantageous than the other methods due to its cost-effective and the possibility of films deposition onto large and complex shaped substrates. In this study, the structural and optical properties of FTO thin films coated using solutions aged for different periods of time on soda lime glass (SLG) substrate by the sol-gel method in a spin coating device were examined by UV-Vis spectrometer and atomic force microscope (AFM) measurements. It was concluded that different aging times in solutions affected the optical and surface morphology of the film. It is suggested that FTO thin films coated on SLG substrate can be used as transparent conductive electrodes in optoelectronic devices such as gas sensors and solar cells.

P30

Investigation on Electrical Properties of MIS SDs with Cu-doped Diamond Interlayer

Feizollahi Vahid A. [*1], Urgun N.[2], Avar B.[3], Altındal Ş.[4]

[1]Department of Nanotechnology Engineering, Zonguldak Bülent Ecevit University, Zonguldak, 67100, Türkiye, E-mail: aylarfeyzi8@gmail.com
[2]Department of Mechatronics Engineering, Faculty of Engineering, Karabük University, Karabük, 78050, Türkiye, E-mail: nuray1erkutlu@gmail.com
[3]Department of Metallurgy and Material Engineering Faculty of Science, Zonguldak Bülent Ecevit University, Zonguldak, 67100, Türkiye, E-mail: barisavar@beun.edu.tr
[5]Department of Physics, Faculty of Sciences, Gazi University, Ankara, 06560, Türkiye, E-email: altundal@gazi.edu.tr

Abstract: This study presents the deposition of a Cu-DLC (copper-containing diamond-like carbon) thin film on p-type silicon using an electrochemical method, followed by detailed characterization of its chemical and surface properties through X-ray photoelectron spectroscopy (XPS) and scanning electron microscopy (SEM). XPS analysis confirms the successful formation of sp^2 and sp^3 carbon-carbon bonds at 283.83 eV and 285.05 eV, respectively, along with the presence of C-OR(H) and C-O bonds at 286.22 eV and 289.82 eV, respectively. Cu 2p XPS results reveal the incorporation of copper atoms as metallic nanoparticles within the DLC matrix. SEM imaging demonstrates uniform film coverage across the entire surface with distinct features and topographic contrasts. To evaluate the Cu-doped thin film as a Schottky diode interface, an Au/(Cu-DLC)/p-Si structure is fabricated. Subsequently, both C-V (capacitance-voltage) and G/ω-V (conductance-voltage) analyses are conducted at low frequencies of 5 kHz and high frequencies of 5 MHz within the voltage range of -1 to 3 volts, revealing frequency and voltage-dependent behaviors. Key electrical parameters, including diffusion potential (V_D), acceptor doping concentration (N_A), Fermi energy (E_F), maximum electric field (E_m), depletion layer width (W_D), and barrier height (Φ_B), are extracted from the C^{-2} plot. Interfacial states (N_{ss}) are characterized using voltage and frequency-dependent high-low frequency capacitance method. Overall, this study highlights the exceptional performance of the Cu-DLC thin film as an intermediate layer in electronic devices, offering a superior alternative to oxide or other insulating layers for reducing interface states (N_{ss}) and defects. The integration of copper into the DLC matrix significantly contributes to mitigating undesirable electrical effects in semiconductor devices.

P31

Investigation of evolution in surface plasmon resonance for Escherichia coli bacteria in the vicinity of silver nanoparticles

Mahdis Mirabioun*[1], Jafar Mostafavi Amjad[1]

[1]*Department of physics, Institute for Advanced Studies in Basic Sciences (IASBS), 444 Prof Yousef Sobouti Blvd, Zanjan, Iran email: Mahdis.Mirabioun@iasbs.ac.ir*

Abstract: The surface plasmon resonance is a phenomenon that occurs at the interface of a metal and a dielectric, resulting from the excitation of free electron oscillations. This phenomenon is widely used in the identification and detection of biological materials and molecules. Changes in wavelength and absorption intensity and reflection intensity are observed due to the response of free electrons in the presence of electromagnetic fields with biological molecules, allowing for the measurement of the concentration of materials and/or biological molecules. Escherichia coli bacteria are a common type of bacteria found in the human gut and are widely used in scientific research. Escherichia coli is a rod-shaped, gram-negative, facultative anaerobic. The size of Escherichia coli bacteria is 2-1 micrometers in length and 0.5 micrometers in diameter. It has 10 flagella that are located in a rotary structure. Nowadays, there are various studies and methods for the detection and measurement of biological cells. However, in other methods, a lot of time is consumed for the detection of different types of biological cells, and the measured samples are not reusable, so they cannot be used multiple times. For this reason, the surface plasmon resonance method can minimize these problems. In this study, we obtain the bacterium image using microscopy as well as spectroscopy of bacteria in the vicinity of silver nanoparticles and using modeling of the received data, we obtain the refractive index and concentration of bacteria.

P32

Analysis of Nb_2O_5 Films Coated on PI Substrates by Sol-gel Technique Which can be ETL Layer in Solar Cells

Ramazan Alpay[*1,2], Süha Gül Kara[1,2], Berk Serbest[1,2,3], Tuğçe Ataşer[1,2,3], Barış Kınacı[1,2,3], Nihan Akın Sönmez[1,2,3], Süleyman Özçelik[1,2,3]

[1]Gazi University, Graduate School of Natural and Aplied Sciences, Division of Photonics Science and Engineering, 06560, Ankara
[2]Gazi University, Photonics Application and Research Center, 06560, Ankara
[3]Gazi University, Faculty of Applied Sciences, Photonics Department, 06560, Ankara
email: rmzn_alpay@hotmail.com

Abstract: The electron transport layer (ETL) functions to collect electrons and prevent the transport of holes to the electrode in the PSC. Nb_2O_5 has been reported to be a good electron transport layer for improving the efficiency of leaded perovskite solar cells [1]. Niobium pentoxide (Nb_2O_5) has been demonstrated as an ideal electron transport layer (ETL) material for solar cells due to its excellent optical transmittance and high carrier mobility.

Transparent conductive electrodes (anodes) are also an important component for solar cells. AgNW has recently attracted great interest as a transparent conductive electrode due to their excellent optical transparency (>80%), low sheet resistivity (< 50 ohms/sq) and vacuum-free fabrication options.

In this study, Nb_2O_5 solution was spin-coated on uncoated PI (Polyimides) and AgNW-coated PI. Firstly, within the scope of optimization studies, optical transmittance measurements of uncoated PI samples coated with Nb_2O_5 solution at (2500-3000-3500-4000-4500-5000 rpm) were taken. XRD spectra showed that Nb_2O_5 films were amorphous as expected. As the next study, Nb_2O_5 solution was coated on AgNT/PI in spin coating by sol-gel technique. Electrical, optical and structural analysis of Nb_2O_5/AgNW/PI samples coated at different rpm were performed. The resistivity and carrier density for the Nb_2O_5/AgNW/PI sample are $5.6x10^{-3}$ ohm cm and $1.6x10^{+21}$ cm^{-3}, respectively. Moreover, an average optical transmittance of 80% in the visible region and an optical band gap > 3.4 eV were achieved. This result shows that our Nb_2O_5 film obtained at low temperature can be used as ETL layer in solar cells.

Keywords: Niobium pentoxide (Nb_2O_5) Films, Electron transport layer(ETL), Polyimides(PI), Solar cells

Acknowledgments: This study is supported by TUBITAK under Project No: 121F379.

References

1. Byungil Hwang, Youngseo An, Hyangsook Lee, Eunha Lee, Stefan Becker, Yong-Hoon Kim & Hyoungsub Kim, “Highly Flexible and Transparent Ag Nanowire Electrode Encapsulated with Ultra-Thin Al_2O_3: Thermal, Ambient, and Mechanical Stabilities”, Scientific Reports **7,**41336 (2017).

P33

Comparing Illusory Movement Perception in Dyslexic and Typically Developing Children

Rasouli Z. [*1], Rasouli S.[2,3], Salehi J.[1]

[1]*Department of Psychology, University of Zanjan, Zanjan, Iran, email:*
[2]*Department of Physics, Institute for Advanced Studies in Basic Sciences (IASBS), Zanjan 45137-66731, Iran*
[3]*Optics Research Center, Institute for Advanced Studies in Basic Sciences (IASBS), Zanjan 45137-66731, Iran*
email: z.rasouli57@gmail.com

Abstract: Dyslexia, a prevalent learning disorder, poses significant challenges for affected children, impacting their educational, social, and psychological well-being. Visual perception and processing difficulties are common among children with dyslexia. Leveraging illusory motion patterns, we investigated the neurobiology of vision indirectly and non-invasively.

In this research, we present a pattern-driven approach by leveraging illusory motion designs for early dyslexia diagnosis in preschool children. Our descriptive study focused on dyslexic and normal students aged six to nine years in Zanjan city during the 2020-2021 academic year. The dyslexic group (n = 19) comprised students from four learning disorder centers, while the normal group (n = 35) included students from selected schools in districts 1 and 2. We employed 11 illusory motion designs as research tools. Data analysis revealed significantly lower illusory motion perception in dyslexic children compared to their normal peers.

Notably, our study introduces an illusory motion stimulus with high potential for early dyslexia diagnosis. It successfully identified illusory movement in 94% of healthy children and 32% of dyslexic children. This innovative approach holds promise for predicting reading disorders during education and serves as a valuable screening tool for vulnerable children before entering school.

The results reveal that dyslexic children achieved lower average scores compared to their normal peers across all illusory stimuli. Specifically, for a given illusory movement stimulus, healthy children demonstrated a 94% detection rate of illusory movement, while dyslexic children exhibited only 32% detection. This significant 62% difference underscores the potential of this stimulus for early dyslexia diagnosis. Additionally, another stimulus, which did not induce an illusion of movement, showed intriguing results. Among normal students, 83% accurately recognized the absence of motion, whereas dyslexic students exhibited a lower percentage (58%). These findings highlight variations in the perception of illusory movement and suggest potential applications for assessing and screening dyslexia in children before school entry.

P34

Investigation of Structural, Morphological and Optical Properties of ZnGa2O4 Thin Films Produced by Rf Magnetron Sputtering Method

Karakaya K.[*1,2], Efkere H.İ.[2], Sönmez A.N.[2,3], Özçelik S.[2,3]

[1]*Gazi University, Graduate School of Natural and Applied Sciences,* Photonics Science and Engineering Department*, Ankara, Türkiye*
[2]*Gazi University, Photonics Application and Research Center, Ankara, Türkiye*
[3]*Gazi University, Faculty of Applied Sciences, Department of Photonics, Ankara, Türkiye*
email: kubra.karakaya1@gazi.edu.tr

Abstract: Due to its wide band gap (~4.5-5.2 eV), $ZnGa_2O_4$ thin films are a promising semiconductor oxide [1]. It is an ideal candidate for the production of novel photodetectors due to its lack of sensitivity to light with a wavelength above 280 nm. In order to contribute to the research on the development of high-performance deep ultraviolet photodetectors and their use in many other technological researches, the structural, morphological and optical properties of $ZnGa_2O_4$ thin films with high crystal quality were analyzed in the laboratory environment.

In this study, $ZnGa_2O_4$ thin films were grown on Corning Glass, Glass and Silicon substrates at 400 °C substrate temperature using RF Magnetron sputtering technique with Nanovak brand NVTS-500 device within Gazi Photonics at 100 W, 150 W and 200 W power and 5 mTorr process pressure in Ar gas atmosphere. Our film thickness was determined to be minimum 200 nm. And as a result, films in the 200-250 nm range were obtained. Structural, morphological and optical measurements of the samples were made using X-ray diffraction (XRD) system, Atomic Force Microscope (AFM) and Ultraviolet and Visible Region (UV-VIS) Spectrometer, respectively.

The value of the band gap energy was calculated using the Tauc plot method embedded in the Origin software, using the experimental data of the UV-VIS absorbance spectrum.

$ZnGa_2O_4$ UV-VIS measurements were made in the wavelength range of 200-1100 nm. As a result of the calculation, 92.1% for CTS 1887, which represents our thin film coated at $ZnGa_2O_4$ 100 W 400 °C process values; Optical transmittance values of 88.8% were found for CTS 1888, which represents our thin film coated at $ZnGa_2O_4$ 150 W 400 °C process values, and 88.3% for CTS 1889, which represents our thin film coated at $ZnGa_2O_4$ 200W 400 °C process values. It is seen that the optical transmittance values of these efficiently produced $ZnGa_2O_4$ samples are close to the values in the literature (average 70-93% for 400-800 nm wavelength) [2].

Acknowledgements

This work was supported by the Presidency of Strategy and Budget (Turkey) under project numbers of 2019K12-149045.

References

1. Aleksandrova, M.; Ivanova, T.; Hamelmann, F.; Strijkova, V.; Gesheva, K. Study of Sputtered ZnO: Ga2O3 Films for Energy Harvesting Applications. Coatings 2020, 10, 650. [CrossRef]
2. J. K. Kim, J. M. Lee, J. W. Lim, J. H. Kim, and S. J. Yun, “High-performance transparent conducting Ga-doped ZnO films deposited by RF magnetron sputter deposition”, Jpn. J. Appl. Phys., vol. 49, no. 4, 2010.

FULL TEXTS

FT1

White light spectroscopy of the structured surface plasmon resonance biosensors

Fateme Gheibi*[1], Jafar Mostafavi Amjad[2]

Department of Physics, Institute for Advanced Studies in Basic Sciences (IASBS), Zanjan 45137-66731, Iran.
email: fateme.gheibi@iasbs.ac.ir

Abstract: Optical methods such as ellipsometry, interferometry, spectroscopy, and surface plasmon resonance (SPR) have recently been used in developing biosensors. SPR sensors have attracted attention due to their accuracy and sensitivity. Surface plasmons are waves created by the oscillation of free electrons between a metal and a dielectric medium that can be excited by light. Sensors rely on the refractive index of the second medium to determine the resonance location. This study uses white light and total internal reflection through a cylindrical prism to focus on a SPR optical setup. Sensors with 50 nm coverage and 632 nm reference laser wavelength were used. This study evaluates the intensity and phase shift of surface plasmon excitation at different wavelengths to determine the electrical property ε of the surrounding medium and its application in assessing different materials.

Keywords: Surface Plasmon Resonance, White light spectroscopy, Biosensors

1.1 Introduction

SPR is widely used in chemical and biosensor applications. Surface plasmons are electron oscillations along a metal interface with a dielectric medium. Total internal reflection occurs when incident light passes through a prism coated with a thin metal layer at angles greater than the critical angle. Then the photon transfers its energy to the oscillating electrons and when Ki is equal to Ksp, SPR occurs and an SPR sensor generates a dark band profile in the reflected light at a specific wavelength and angle [1]. The light source is crucial for overall performance, and when designing an SPR sensor, the key to achieving high performance lies in the resonance of surface plasmons. Methods to stimulate surface plasmons include angle and wavelength scanning. This research has used white light spectroscopy to investigate the excitation of surface plasmons which has developed a technique that combines wavelength and angle scanning and provides comprehensive information in one scan [2].

1.2 White light spectroscopy of SPR

White light spectroscopy is a method for analyzing light across a wide range of wavelengths. Unlike traditional methods, this method uses a light source that emits a broad spectrum. When electromagnetic radiation interacts with a material, it can be absorbed, transmitted, or reflected. Spectroscopy measures the amount of radiation absorbed or transmitted by a sample. The extent of absorption and transmission varies depending on the material and its optical properties, which are influenced by the wavelength of light.

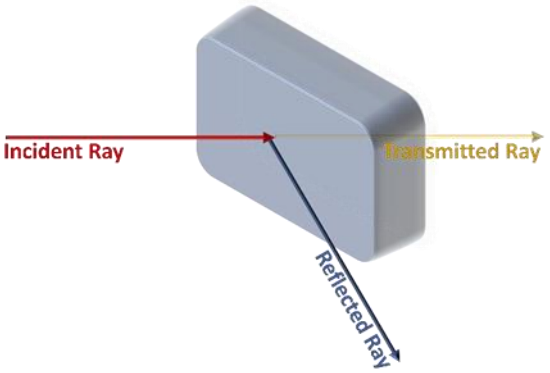

Figure 1. Transmission, reflection caused by incident light hitting matter

The radiation of materials with dielectric function $\tilde{\varepsilon} = \varepsilon r + i\varepsilon i$ is influenced by the type of material (conductive or non-conductive), which provides insights into optical properties.

2. Theoretical investigation

SPR can be achieved by either wavelength or angle scanning. Angle scanning involves altering the incident angle of light on the sensor surface, whereas wavelength scanning involves changing the wavelength of light. Both techniques provide valuable insights into the sample's properties.

The goal of this project is to create an optical setup that combines angle scanning and wavelength scanning techniques. In this setup, each wavelength from the white light spectrum has its own angle, indicating the interconnectedness between wavelength and angle. However, it should be noted that every wavelength is not in resonance with every angle we send to the SPR arrangement. By directing light at a 45° angle onto the prism, different wavelengths with different angles are present in the input and reflection spectra, leading to SPR at specific angles for each wavelength. Therefore, a unique SPR diagram was created for each wavelength (Fig. 2(a)).

By rotating and radiating the prism at different wavelengths, extinction and resonance can be observed at certain angles. Resonance occurs at specific angles for different wavelengths, but spectroscopic data show a spectrum that includes multiple SPRs. The minimum point indicates the wavelength and resonance angle of the surface plasmon (Fig. 2(b)).

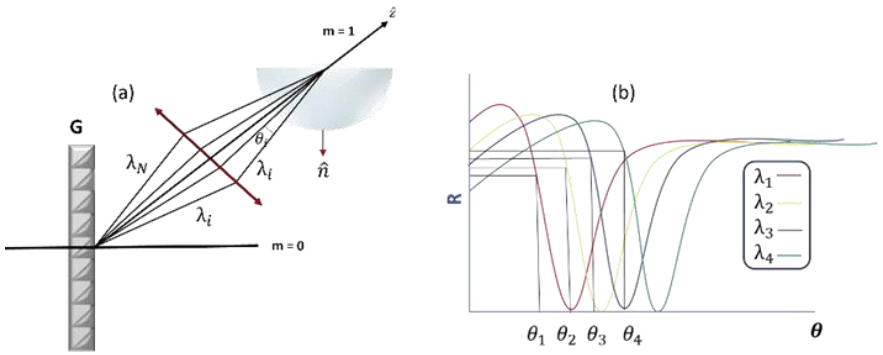

Figure 2. (a) The spectrum of white light that passes through G (the diffraction grating) and has different wavelengths hits the prism at different angles and is reflected. (b) SPR occurs at certain angles for different wavelengths. For wavelengths 1, 2, 3, and 4, the resonance angle is specified in height.

3. Experimental configuration

The white light spectroscopy setup is shown in Figure 3. The broad white light source is converted into a point light source by an aperture and directed to a non-polarized beam splitter by a collimator lens, on the other hand, the laser light, whose intensity is reduced by ND, enters the beam slit. arrive The beam splitter directs the incoming light toward the optical axis. After passing through the lenses, these two lights pass through the polarizer to be polarized to the p polarization and are directed to the diffraction grating and separated by themselves. Continue setup according to the first command set. The output lights are focused by a lens in the Krechman structure, which consists of a prism and a sensor, because this angle of incidence is greater than the critical angle, total internal reflection occurs, and the output lights are parallelized by the next lens, and with the lenses Imaging, after passing through the polarizer with p polarization, they reach the ccd to record the phenomenon of SPR. We analyze the data recorded with CCD using MATLAB and obtain the required information.

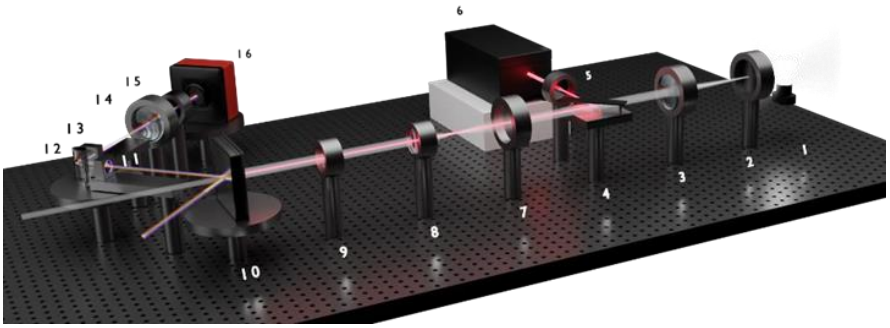

Figure 3. (1) Wide white light source to produce white light in the visible spectral width (2) Aperture to convert the wide light source to a point light source, (3) Collimator lens, (4) Beam splitter, (5) Nd for reducing intensity of laser light, (6) He-Ne laser, (7) lens, and (8) lens to magnify and extend the focal length, (9) Polarizer to have light with tm mode or p polarization, (10) Diffraction grating separates (disperses) light into its component wavelength., (11) lens to focus the light in the Kirschmann structure, (12) krechmann config. (prism & biosensor), (13) Collimator lens, (14) imaging lens, (15) p-polarizer and (16) CCD.

4. Results

After adjusting the settings for both the laser and the white light source, the laser light (632.8 nm) came very close to matching the red color of the white light spectrum. At a specific angle, SPR occurred. The figure below shows the data recorded from both light sources under the same condition.

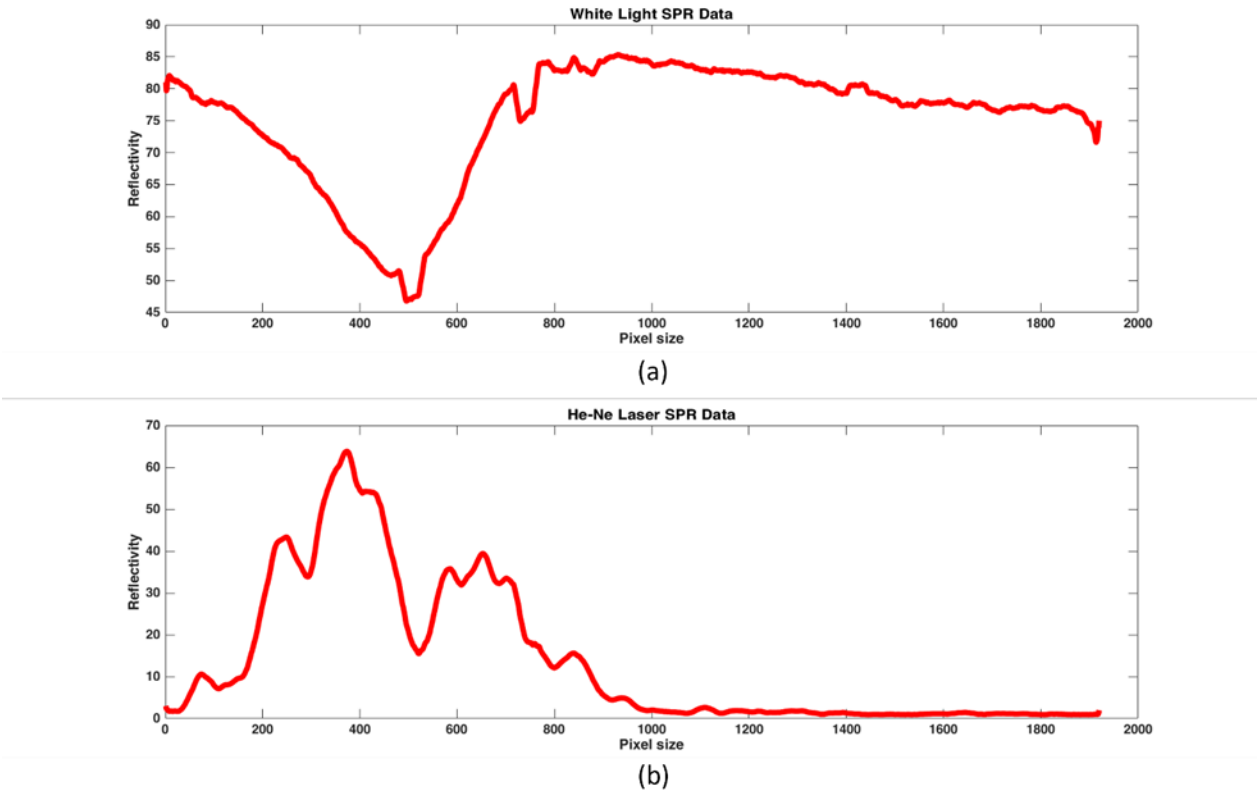

Figure 4. (a)white light surface plasmon resonance data with silver-coated biosensors. (b) Helium-neon laser surface plasmon resonance data with silver-coated biosensors.

5. Conclusion

According to the laboratory setup and recorded data, we were able to provide a technique that instead of setting up angle scan and angle scan setups, with one scan, information can be obtained that includes both, and having this information helps us to Obtain about material properties such as refractive index and phase information. The future work that we are considering is to write MATLAB code to automate the analysis of this data.

6. References

1. J. Homola, Surface Plasmon Resonance Based Sensors, Springer Series on Chemical Sensors and Biosensors (Springer-Verlag, 2006).
2. M. Piliarik, and J. Homola, “SPR (SPR) sensors: approaching their limits?” Opt. Express17(19), 16505–16517 (2009).
3. Yamamoto, Masahiro. "SPR (SPR) theory: tutorial." Review of Polarography 48.3 (2002): 209-237.

FT2

Improving Illumination and Enhancing the Accuracy of White Light Interferometry Using Array Lenses

Khanjani M.[*1], Hassanzad F.[1], Malek-Mohammadi M.[1], Ahadi Akhlaghi E.[1,2]

[1]*Department of Physics, Institute for Advanced Studies in Basic Sciences (IASBS), Zanjan 45137-66731, Iran*
[2]*Optics Research Center, Institute for Advanced Studies in Basic Sciences (IASBS), Zanjan 45137-66731, Iran*
email: e.a.akhlaghi@iasbs.ac.ir

Abstract: In this research, we introduce a setup to achieve uniform illumination for microscopy applications, as well as enhanced visibility for interferometric measurements. To achieve these goals two array lenses are used, while the emitted light is locally focused by the first array lens to the second one and then the uniform part of the light is selected by a lens and iris. These advancements were successfully implemented and validated in the SSP002 device, underscoring the practical significance and applicability of our findings in optical instrumentation. The results of the comparison show that the minimum visibility is increased from 0.10 to 0.41.

Keywords: array lenses, uniform illumination, White Light Interferometry

1. Introduction

Optical topography measurement is dependent on illumination quality. Essential to achieving reliable measurements is the uniformity and stability of illumination across the measurement field. In these systems employing a single LED, lasers, or lamps, the resulting light gradient profile from the center to the edge regions [1]. Non-uniform illumination can lead to variations in the intensity of light falling on the surface being measured. Furthermore, bright spots may saturate the camera sensors, while the other areas illuminate with insufficient light. This inconsistency affects the accuracy of 3D topography measurements [2]. To overcome this issue some methods have been suggested and developed. Wang and et. al. developed a flexible LED light source with carefully tuned parameters tailored to various features of cutting tools [3]. Adaptable Scanning for Tunable Excitation Regions (ASTER), a versatile illumination technique is introduced by Mau and et. al. [4]. Zhou and et. al. considered that dual lens arrays can shape the non-uniform beam into a flat-field beam [5].

Alternatively, all these methods are used for non-interferometric optical topography measurement systems. Interferometric optical topography measurement systems are advanced tools used for non-contact surface profiling and measurement. These systems utilize the principles of interferometry to accurately measure the topography of a surface by analyzing the interference patterns created by reflected or transmitted light waves from the sample [6, 7]. For interferometric optical topography measurement systems, the illumination beam coherency degree should be considered to impact the visibility of interferometry fringes and also the effective dynamic range. High fringe visibility is essential for accurate phase extraction, and achieving this depends on the

ability of the camera to handle a broad range of light intensities while maintaining a favorable Signal-to-Noise Ratio (SNR) [8].

In this paper, we present a novel approach aimed at overcoming existing challenges in surface profilometry non-uniform Illumination. Our method, implemented on the SSP002 WLI system developed by Fathoptic Co. utilizes array LED technology and array lenses to improve illumination uniformity. This enhancement maintains a high degree of coherency to guarantee precise nano-profilometry measurements.

2. Methodology

One of the aspects affecting measurement accuracy in nano-profilometry is the analog-to-digital conversion (ADC) process, which introduces quantization errors. These errors result from the discretization of continuous analog signals into a finite number of digital levels. The accuracy of phase measurements in interferometry is highly dependent on minimizing these quantization errors, which is dependent on ADC resolution [9]. When a non-uniform illumination is applied the impact of these errors will be noticeable. To address these challenges, we consider the use of an array LED with two array lenses. These arrays consist of multiple small lenses arranged in a grid pattern. By directing light through an array of lenses, we can spatially multiplex the incoming rays. Each LED in this array source and lens focuses light onto a specific region of the sensor. As a result, we effectively divide the image sensor into smaller sub-regions, each corresponding to a pixel. With lens arrays, the light distribution becomes more uniform across the sensor. This reduces the impact of quantization errors because each lens contributes to a distinct pixel value. As a result, the intensity distribution becomes more uniform, and visibility throughout the image becomes more uniform and increased.

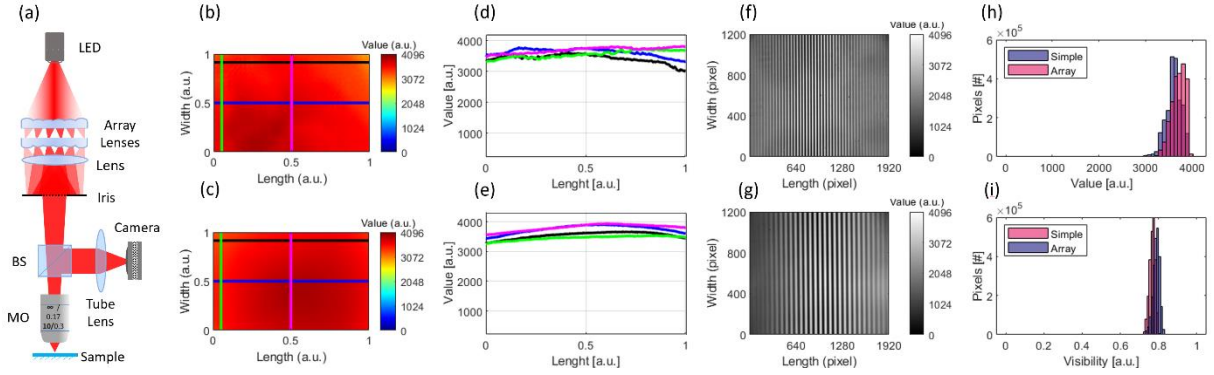

Figure 1. (a) Mirau interferometer system consist of array LED source, two array lenses, (b) Intensity image recorded using single LED, (c) Intensity image recorded using array LED, (d) Intensity profile of four divided areas from image 1(b) of single LED, (e) Intensity profile of four divided areas from image 1(c) of array LED, (f) hologram of interference fringes from single LED, (g) hologram of interference fringes from array LED, (h) histogram comparing intensity distribution of images obtained from single LED and LED array, and (i) histogram comparing visibility of fringes obtained from single LED and LED array.

Fig. 1(a) illustrates the SSP002 WLI Mirau-based system arranged by the flat-top illumination using an array lenses setup. The light emitted from the array LED source is focused by the first array lens to the second one and then the uniform part of the

light is selected by the Lens and the Iris. The images and holograms are recorded by a camera (Basler acA2500-60um, at 5 MP resolution) equipped with a Mirau microscope objective (MO) (10X Nikon CF IC Epi Plan DI) and the tube-lens (f=200 mm, ϕ=25 mm). Figs. 1(d) and 1(e) show the four intensity profiles of the captured images (Figs. 1(b) and 1(c)), by four color-coded lines. Comparison Fig. 1(d) and Fig. 1(e) shows that the use of array lenses makes the intensity distribution uniform in all areas. The performance of the interferometry system when using traditional methods and our proposed design of array lenses are consistent with Figs. 1(f) and 1(g). In addition, the profile intensity histogram is presented in Fig. 1(h), which shows that in the case of using the array of lenses the intensity dispersion is reduced. The histogram also shows distinct interference fringes in Fig. 1(i), indicating similar results. The minimum and maximum visibility values of the various points of the field of view for the traditional method were found to be 0.10 and 0.81, respectively, as well as for the array lenses system 0.41 and 0.83.

3. Conclusion

In conclusion, our study demonstrates the efficacy of employing an array lens setup in optical systems, showcasing notable improvements in light diffusion uniformity and visibility for microscopy and interferometry applications. By integrating this innovative configuration, we effectively addressed challenges associated with light scattering and non-uniformity, resulting in enhanced performance and accuracy. The successful implementation of these advancements in the SSP002 device underscores the practical relevance of our research, offering tangible benefits for optical instrumentation and enabling advancements in various fields reliant on precise light control and measurement.

References

1. İ. Celebi, M. Aslan, and MS. Unlu, “A spatially uniform illumination source for widefield multi-spectral optical microscopy,” PLoS ONE, vol. 18, 2023, pp. 1-12.
2. A. Cao, H. Pang, J. Wang, M. Zhang, L. Shi, and Q. Deng, “Center Off-Axis Tandem Microlens Arrays for Beam Homogenization,” IEEE Photonics Journal, vol. 7, 2015, pp. 2400207- 2400210.
3. W. Wang, W. Liu, Y. Zhang, P. Zhang, L. Si, and M. Zhou, “Illumination system optimal design for geometry measurement of complex cutting tools in machine vision,” International Journal of Advanced Manufacturing Technology, vol. 125, 2023, pp. 105–114.
4. A. Mau, K. Friedl, C. Leterrier, N. Bourg, and S. Leveque-Fort, “Fast widefield scan provides tunable and uniform illumination optimizing super-resolution microscopy on large fields,” Nature Communications, vol. 12, 2021, pp. 1-9.
5. X. Zhou, M. Wei, Y. Wang, Zh. Xu, Y. Han, J. Lian, “Effect of light source uniformity for imaging ellipsometry measurements,” Optics Communications, vol. 545, 2023.
6. C. Taudt, Development and Characterization of a Dispersion-Encoded Method for Low-Coherence Interferometry, Springer Vieweg, Wiesbaden, 2022, pp. 39-88.
7. Ch. Ch. Lai and I. J. Hsu, “Surface profilometry with composite interferometer,” Optics Express, vol. 15, 2007, pp. 13949-13956.

8. Sh. Chen, Sh. Xue, D. Zhai, and G. Tie, “Measurement of Freeform Optical Surfaces: Trade-Off between Accuracy and Dynamic Range,” Laser Photonics Review 2020, pp. 1900365-1900285.
9. L. Zaworski, D. Chaberski, M. Kowalski, and M. Zielinski, “Quantization Error in Time-to-Digital Converters,” Metrology and Measurement Systems, vol. XIX, 2012, pp. 115-122.

FT3

Optimization of photolithography exposure by Lenslets

Mollaei Mina*[1], Mahmoudi Samad[2], Malek Mohammadi Milad[3], Azizian-Kalandaragh Yashar[4,5],Jabbar pour Mahmoud[3], Ahadi Akhlaghi Ehsan[1,2,3]

[1]*Department of Physics, Institute for Advanced Studies in Basic Sciences (IASBS) 444 Prof Yousef Sobouti Blvd, Zanjan 45137-66731, Iran*
[2]*Science and Technology Park, Institute for Advanced Studies in Basic Sciences (IASBS) 444 Prof. Yousef Sobouti Blvd., Zanjan, Iran, Postal Code: 45137-66731*
[3]*Optics Research Center, Institute for Advanced Studies in Basic Sciences (IASBS), 444 Prof Yousef Sobouti Blvd, Zanjan 45137-66731, Iran*
[4]*Department of Physics, University of Mohaghegh Ardabili, P.O. Box 179, Ardabil, Iran*
[5]*Photonics Application and Research Center, Gazi University, 06560 Ankara, Türkiye*
email: *minamollaei@iasbs.ac.ir, e.a.akhlaghi@iasbs.ac.ir*

Abstract: In this paper, we present a method for optimizing the illumination of gradient exposure photolithography using lenslets. The necessity of gradient exposure lithography is to illuminate uniformly the mask. The use of lenslet in the photolithography setup helped us to improve uniform exposure, optimize the setup, adjust elevation, and create patterns. The implemented method was used to produce microlenses with a more accurate curved surface. The height and distortion of the lenses were measured using a non-contact profilometer.

Keywords: Diffraction, Profilometer, Photolithography, Binary mask, Microlens, Lenslet

1. Introduction

In recent decades, with the increasing demand for miniaturization, advanced lithographybased fabrication techniques have been used to fabricate optical and photonic devices with small dimensions and high precision. Micro and nano elements such as waveguides, gratings, and microlenses are used in the fields of optics and photonics, high-resolution imaging, spectrometers, and miniature interferometers. However, the presence of limitations such as precise surface control, high cost, precise molds, etc. in the development and production process of these devices have limited their progress. New technologies in the field of lithography have led to grayscale lithography which different intensities of light are used to differently expose separate areas of a substrate [1,2]. Using a relatively low light intensity can mean that only a certain depth of light is resistant and the rest remains unchanged. The result of this can be the creation of a three-dimensional structure in photoresist simply by using lithography techniques. Therefore, it is very important to have a uniform mask illumination to create a three-dimensional structure [3, 4]. In this paper, we present the optimization of UV-LED photolithography layout with lenslet combined to have a uniform mask illumination. This setup is used to fabricate microlens with a binary mask and the gradient exposure based on the diffraction phenomenon. In this method, by controlling the degree of defocus of the mask pattern on the surface of the sample, a

gradient illumination is created, and as a result, a gradient of thickness in the photoresist and a three-dimensional structure is implemented.

2. Experimental Setup and Method

Figure 1 shows the photolithography optical setup with a 365 nm UV light source. Lenses are used for precise adjustment and uniform illumination of the mask.
The optical mask was prepared with the desired structural pattern, in this work, we used a pinhole, which was placed at a distance of 2f from the lens. The position where the visualized image shows the best edge sharpness is the focus position. To adjust and move the position of the mask, a holder connected to the positioner is used, and a quartz lens with a focal distance of 75 mm, which does not absorb ultraviolet rays, is used to image the design of the mask on the feather cyst. Then, after passing through the mask, the light is reflected parallel to the second lens, after which a part of the light shines in the beam splitter on the substrate coated with light resist. Due to the substrate material, it is reflected from the surface and radiated to a third lens located between the quartz beam splitter and the detector camera. The second arm is for checking the settings of the exposure system and the mask adjustment section so that the second lens and camera capture the lightsensitive surface of the sample. Figures 1(b) and 1(c) show the traditional photolithography output intensity distribution and the profile for the unmasked state, respectively. The difference between the setup without and with the lens can be seen in Figures 1(d) and 1(e).

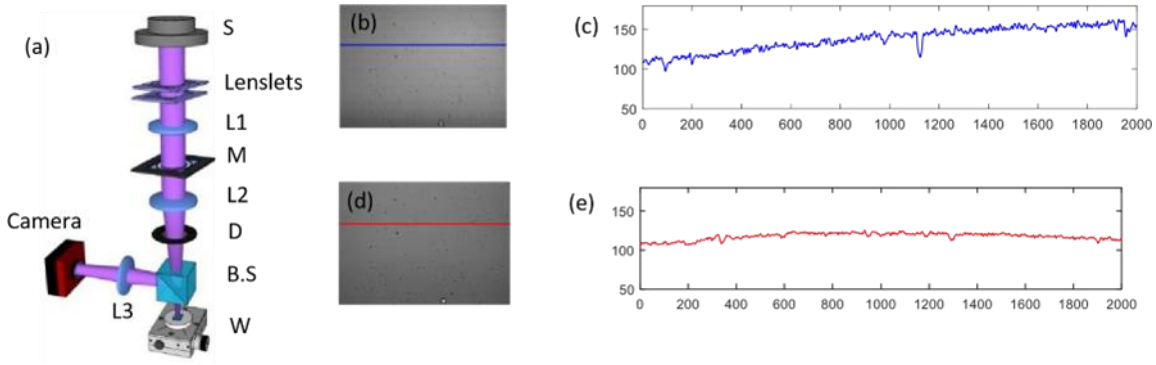

Figure 1. (a). Schematic of photolithography optical setup that includes S: UV light source, M: a binary mask made using micromachining on a steel plate with a thickness of 100 microns and a diameter of 170 µm, lenslet: microlens array, L1: lens, L2: quartz lens, D: diaphragm, B.S.: Beam splitter, W: is the Wafer, L3: is the imaging lens and CCD is camera. (b) Recorded image of photolithography layout without lenslet. (c) Intensity profile of image without lenslet. (d) Recorded image of photolithography layout image with lenslet and (e) Intensity profile of image with lenslet.

After designing the mask with micromachining and photolithography with a microlens, checking and measuring the physical and appearance characteristics of the manufactured microlens was done using a white light interference microscope and non-contact profilometer (Fath-Optics, SSP001). Figure 2 shows a typical image of an interference pattern of the manufactured sample.

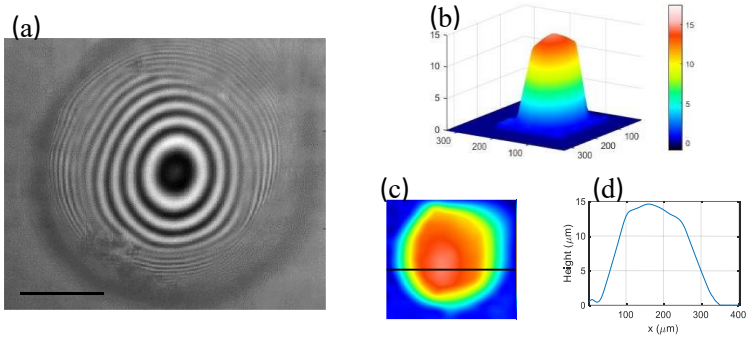

Figure 2. (a) Recorded image of microlens made by white light interference microscope. The concentric circles represent the geometrical distribution of the collocation points. (b) 3D image of a microlens .The image was recorded using an interference microscope (Fath-Optics, SSP001) with a depth resolution of 5 nm. (c) 2D image of microlens height distribution (d) microlens height profile on the line marked in figure (b). The scale bar in the pictures is 50 microns.

According to the measurements, the diameter of the microlens is 173 μm and the height of the convex part of the microlens is 4.1 microns. In addition, according to the refractive index of the photoresist material, which is equal to 1.59, the focal length of the manufactured microlens was equal to 1.5 mm.

3. Conclusion

In this paper, an optimization method for photolithography layout and microlens fabrication using gradient exposure is presented. The final optimization leads to an increase in the accuracy and quality of the manufactured microlenses. Then, by using a binary mask placing the light-sensitive surface of the substrate outside the image plane, and creating a defocused gradient intensity distribution, the results have been improved. The advantages of using this method are overcoming the lack of uniform exposure and the limitations in photolithography with Binary and gradient masks that provide the possibility of easy and controllable manufacturing of microlenses with diverse physical and appearance characteristics and with desirable quality.

References

1. Zheng, Lei, et al. "UV-LED projection photolithography for high-resolution functional photonic components." Microsystems & nanoengineering 7.1 (2021): 64.
2. Dill, Frederick H. "Optical lithography." IEEE transactions on electron devices 22.7 (1975): 440-444.
3. Allouti, Nacima, et al. "Grayscale lithography process study for sub 5μm microlens patterns." Novel Patterning Technologies for Semiconductors, MEMS/NEMS, and MOEMS 2019. Vol. 10958. SPIE, 2019.
4. Deng, Qinyuan, et al. "Fabrication of micro-optics elements with arbitrary surface profiles based on one-step maskless grayscale lithography." Micromachines 8.10 (2017): 314.

FT4

Fabrication and Calibration a Spectral-Domain Optical Coherence Tomography in Infrared Range

Rezaei N.[1], Zakikhani F.[1], Ebrahimzadeh Kouyakhi A.*[1], Ahadi Akhlaghi E.[1,2]

[1]Department Physics, Institute for Advanced Studies in Basic Sciences (IASBS), Zanjan, 45137-66731, Iran,
email: nargesrezaei@iasbs.ac.ir.
[2]Optics Research Center, Institute for Advanced Studies in Basic Sciences (IASBS), Zanjan, 45137-66731, Iran,
email: e.a.akhlaghi@iasbs.ac.ir

Abstract: The Optical Coherence Tomography (OCT) technology allows rapid, non-invasive, highresolution 3D imaging of various samples. Utilizing Michelson interferometer, OCT can be configured in time-domain and Fourier-domain setups for sample examination. 3D imaging requires scanning the sample in the illumination plane, often achieved with a Galvo mirror. This study presents a spectraldomain OCT microscope's construction and its application in sample thickness examination. Experimental setup involved a 439×439 (μm^2) sample. Such advancements in OCT technology hold promise for improved disease diagnosis, non-destructive testing, and scientific research across various fields.

Keywords: Optical Coherence Tomography, OCT, 3D imaging, Fourier-Domain, Galvo mirror.

1. Introduction

Optical Coherence Tomography (OCT) is an innovative imaging technology that enables rapid, noninvasive, and high-resolution three-dimensional imaging of biological and non-biological samples. With a depth sampling range of several millimeters and axial resolution in the micrometer range, OCT is positioned between ultrasound and confocal microscopy in terms of axial and depth resolution. This makes it a precious tool for a wide range of applications [1,2].

In OCT, the Michelson interferometer is commonly used to examine samples through time-domain and Fourier-domain configurations. In the time-domain setup, a point on the sample is probed by moving the reference mirror and recording the acquired information with a detector. In the Fourier-domain setup, the detector captures all depth information for a point on the sample with a single data acquisition, without the need to move the reference mirror. For three-dimensional imaging, the sample must be scanned in the illumination plane to record depth information for all points on the surface. However, this scanning motion can be impractical or noisy for certain samples, such as the human eye. To address this, many setups use a Galvo mirror to laterally scan the sample while keeping it fixed on the illumination plane. The Galvo mirror moves the illumination to different parts of the sample, allowing depth information to be obtained for each momentary data acquisition. After processing with a data analysis algorithm, a three-dimensional image of the sample is generated [1-4].

In this article, the results of constructing and classifying a spectral-domain optical coherence tomography microscope are presented. Using this setup, the thickness of a sample is examined to assess the accuracy of the constructed OCT.

2. Theory

If an almost heterogeneous medium is irradiated by a Gaussian beam, the Gaussian beam waist in this case can be approximated as a flat wave. By considering the flat wave equation and utilizing the Green's function $G_H(r, r')$, the scattered wave can be approximated as a solution to the Helmholtz equation, as follows [1-3]:

$$V_{(s)} = V^{(i)} + \frac{1}{4\pi}\int_{vol(r')} G_H(r,r')d^3r' \times \int_{vol(r')} F_s(r',k)V'^{(i)}d^3r' \quad (1)$$

where $V(s)$ represents the scattered wave. Integration is performed over a volume of the sample irradiated. The relative domain of the scattered waves is determined by the scattering potential $F_s(r, k)$:

$$F_s(r,k) = k^2[m^2(r,k) - 1] \quad (2)$$

In Eq. (2), m is the complex refractive index of the sample. The scattered radiation from the homogeneous volume inside the sample, at a distance d much greater than the coherence length of the light source used, is recorded. In this case, using the far-field approximation for the scattered wave domain, we have:

$$A^{(s)} = \frac{A^{(i)}}{4\pi d}\int_{V'} F_s(r')\exp(-iK.r')\,dr^3 \quad (3)$$

In Eq. (3), $K = k^{(s)} - k^{(i)}$, is the vector difference between the incident and scattered waves. This equation is a simplified form of the scattering cross-section theory, which allows the calculation of the sample scattering potential via inverse Fourier transform of the scattered waves. The intensity of the scattered wave in the spectral domain, $I_S(t)$, is represented in Eq. (4) [2]:

$$I_{(s)}(\tau) = I_0\begin{bmatrix}\sum_i |R_R|^2 + |R_i|^2 \\ +2\sum_{i,j,i\neq k} R_i R_j^* \Gamma[\tau \mp (\tau_i - \tau_j)] \\ +2\sum_i R_R^* R_i \Gamma[\tau \mp (\tau_i - \tau_R)]\end{bmatrix}. \quad (4)$$

In Eq. (4), R_R is the complex reflection coefficient from the reference arm, R_i and R_j are the complex reflection coefficients from different layers of the sample, I_0 is the incident wave intensity, and $\Gamma(\tau)$ is the coherence function of the light source as a function of time delay (τ). In Eq. (4), the first term is a constant value representing the scattered waves at τ = 0. The second term is the interference between scattered waves from different layers. The third term is the interference between scattered waves from different layers and the reference wave reflected from the reference mirror. The axial resolution of optical coherence tomography can be calculated with Eq. (5):

$$\Delta z = \frac{2ln2}{\pi}\frac{\lambda_0^2}{\Delta\lambda}. \quad (5)$$

In Eq. (5), λ_0 is the central wavelength of the light source and $\Delta\lambda$ is the spectral bandwidth of the light source. Lateral resolution, similar to confocal microscopy, can be calculated with Eq. (6) [1]:

$$\Delta x = \frac{2\lambda_0}{\pi}\frac{f_{obj}}{d}. \qquad (6)$$

In Eq. (6), f_{obj} is the focal length of the lens and d is the beam waist. For the analysis of the obtained information, first, to eliminate the constant term in Eq. (4), the intensity of the reference and sample beams is recorded. Then, the recorded intensities are subtracted from the interference spectrum intensity. By converting the wavelength to wave number and using interpolation, the interference intensity will be obtained as a function of wave number, which, by applying the Fourier transform, will yield the depth information of the sample [4-6].

3. Experimental Setup and Method

Fig. 1 illustrates the schematic arrangement employed in optical coherence tomography (OCT). An SLD source with 840 (nm) central wavelengths, with a coherence length of 15.4 (µm), serves as the light source. The light beam is introduced into the OCT setup via a single-mode fiber and then directed towards the interferometer through an 4 × objective lens. Subsequently, a beam splitter divides the light into two arms, one directed towards the reference mirror and the other towards the sample. At the terminus of these arms, two 10 × objective lens microscopes are symmetrically positioned. In the sample arm, a galvo mirror laterally scans the light beam across the sample surface. Eventually, the

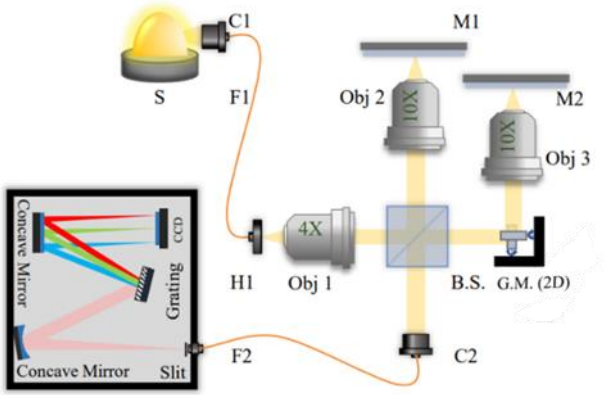

Figure 1. Schematic design of optical coherence tomography setup.

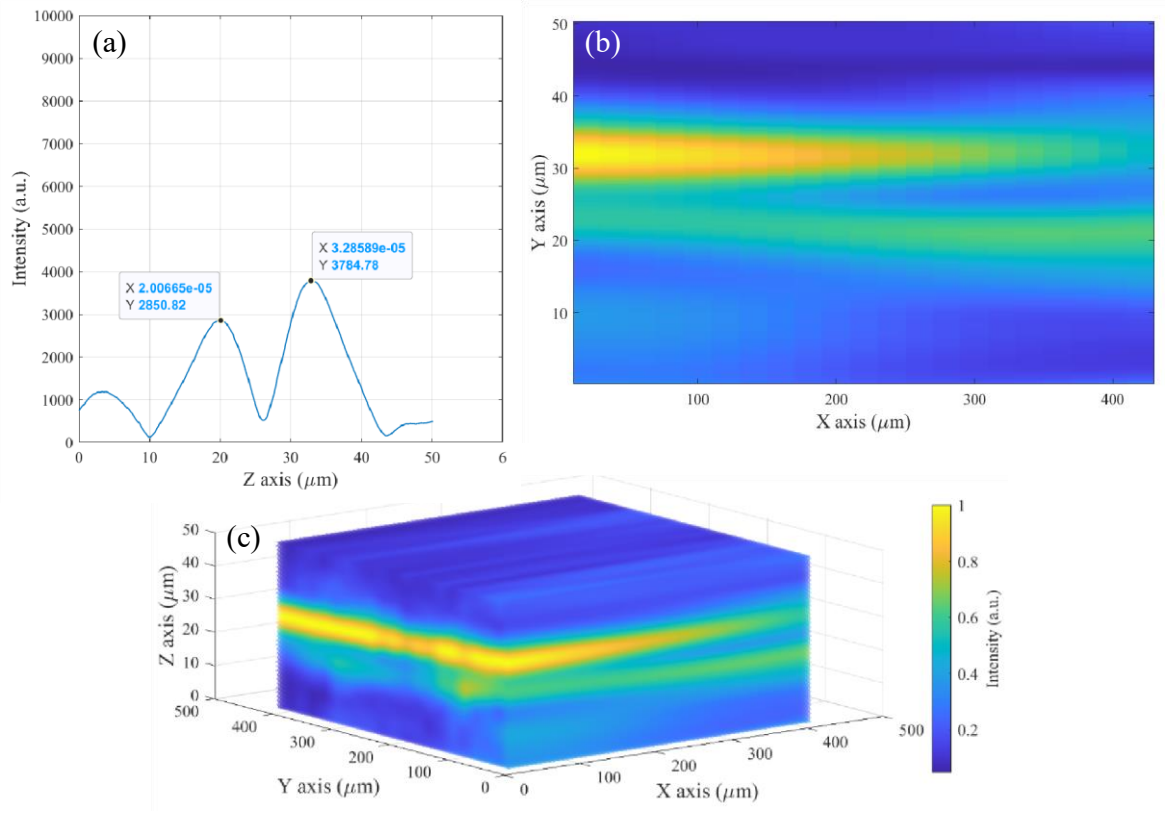

Figure 2. (a) A-Scan of sample. (b) B-Scan of sample. (c)3D image obtained from the sample by OCT.

reflected light beams from both the sample surface and the reference mirror surface interfere, creating an interference pattern directed towards the input of the spectrometer.

In this study, a 439×439 (μm^2) hole was employed as the sample for optical coherence tomography. The sample was analyzed with an axial resolution of 7.7 (μm) and a lateral resolution of 7 (μm). Data acquisition from the sample lasted for 2 (min). Subsequently, after signal processing, a 3D image of the sample was generated, as depicted in Fig. 2.

Fig. 2 exhibits peaks corresponding to two internal layers of the sample, which determine the thickness of a specific part of the sample. Utilizing OCT, the thickness of this section, closely aligning with the thickness measured by the Mirau microscope.

4. Conclusion

In this study, a Fourier-domain optical coherence microscope was constructed using an SLD source as a broadband light source in the infrared spectral range, with an axial resolution of 7.7 (μm). A sample with dimensions of 439×439 (μm^2) was examined three-dimensionally as the sample, showing good agreement between the measured results and both theoretical values and those obtained by a Mirau microscope. Finally, the results of hole thickness measurement and 3D sample imaging are presented.

References

1. A. F. Fercher, W. Drexler, C. K. Hitzenberger, and T. Lasser "Optical coherence tomography —principles and application," IOP Publishing, 2003.
2. W. Drexler, J. G. Fujimoto, "Optical Coherence Tomography Technology and Applications," Springer reference, 2016.
3. J. A. Izatt and M. A. Choma, "Theory of Optical Coherence Tomography," Springer Berlin Heidelberg, 2003, page 47 -72.
4. Z. Yaqoob, J. Wu, and C. Yang, "Spectral domain optical coherence tomography: a better OCT imaging," Bio Techniques, 2005.
5. A.F.Fercher, C. K. Hitzenberger, M. Sticker, E. Moreno - Barriuso, R. Leitgeb, W. Drexler, H. Sattmann, "A thermal source technique for optical coherence tomography," Optics Communications , page 57-64, 2000.
6. Y. W. Qin, H. Zhao, Z. Q. Zhuang, "High resolution spectral-domain optical coherence tomography using thermal light source," Springer science, 2011.

FT5

Surface Topography Measurement through Fringe Visibility Analysis

Hosseini S.[1*], A. Akhlaghi E.[1,2]

[1]*Department of Physics, Institute for Advanced Studies in Basic Sciences (IASBS), Zanjan, 45137-66731, Iran*
[2]*Optics Research Center, Institute for Advanced Studies in Basic Sciences (IASBS), Zanjan, 45137-66731, Iran*
*email: e.a.akhlaghi@iasbs.ac.ir *simahosseini@iasbs.ac.ir*

Abstract: Surface topography measurement through interferometry is a non-contact and non-destructive technique which is widely used in various fields for analyzing the surface structures to better understand and characterize surface properties for a wide range of applications. In this paper, a new method for analyzing interference fringes has been introduced which is based on evaluating the visibility changes. In this method, after capturing the interferogram through the interferometer and utilizing the visibility calibrated diagram, the heights of various points on the measured surface are determined. With this method it is possible to measure surface roughness up to 65 micrometers with an accuracy of 3 micrometers.

Keywords: interferometry, visibility, topography

1.Introduction

Surface topography measurement has numerous applications in industry and science. In the industry, devices such as CMM and Stylus are typically used to scan a probe over the surface of a sample. However, these methods are considered destructive and have low measurement speeds. Optical methods offer a non-destructive and more accurate alternative for surface topography measurements.

Interferometry is one of the optical methods used for measuring surface roughness, utilizing the wave properties of light and the superposition of at least two light beams. There are several methods for analyzing recorded interference intensities such as White Light Interferometry (WLI), Phase Shifting Interferometry (PSI) and Fourier method. WLI is a method that requires a precise piezoelectric transducer. However, data capturing through WLI is time-consuming and not suitable for dynamic samples and also it is not a cost-effective method. PSI and Fourier method work based on analyzing the phase modulation. Phase analyzing based methods are conventional and accurate, they are unsuitable for measuring surfaces with discrete roughness greater than λ/2.

To address this issue, we introduce a new method that allows for the measurement of sample roughness up to 65 μm by capturing only one interferogram. This method involves calibrating the linear part of the visibility diagram and measuring visibility changes through the sample. In a comparison with WLI and Fourier methods, our method showed promising results. The 3D profile of the sample calculated using our

method differed from that calculated using WLI, with our method reporting a height of 13±3μm compared to WLI's reported height of 17μm.

2. Method

To evaluate the quality of captured interferograms, visibility is utilized by analyzing the darkness or brightness of the fringes,

$$V = \frac{2|E_1 E_2 g_{12}(\tau)|}{|E_1|^2 + |E_2|^2}, \qquad (1)$$

here, E_1 and E_2 are two interfered electromagnetic fields and $g_{12}(\tau)$ is the mutual coherence degree. Visibility changes depend on two parameters, mutual coherence degree and the intensity difference between the two beams. In this method, we assumed a constant intensity distribution on the viewing plane, which prevents the effect of intensity difference in the interference pattern from appearing in the brightness distribution and thus in the final data. Therefore, by calibrating the coherence degree based on the light path, the roughness of surfaces can be measured.

2.1 Visibility Calibration

To utilize this method, an interferogram captured using an almost ideal mirror as a sample, which is shown in fig 1 (a). then as shown in fig 1(b), the visibility changes of the captured interferogram evaluated. According to the fig 1(c), only the linear part of the visibility diagram is used to measure the height from the visibility. And finally, as shown in fig 1(d) the slope of the visibility diagram changes was measured with the surface height changes.

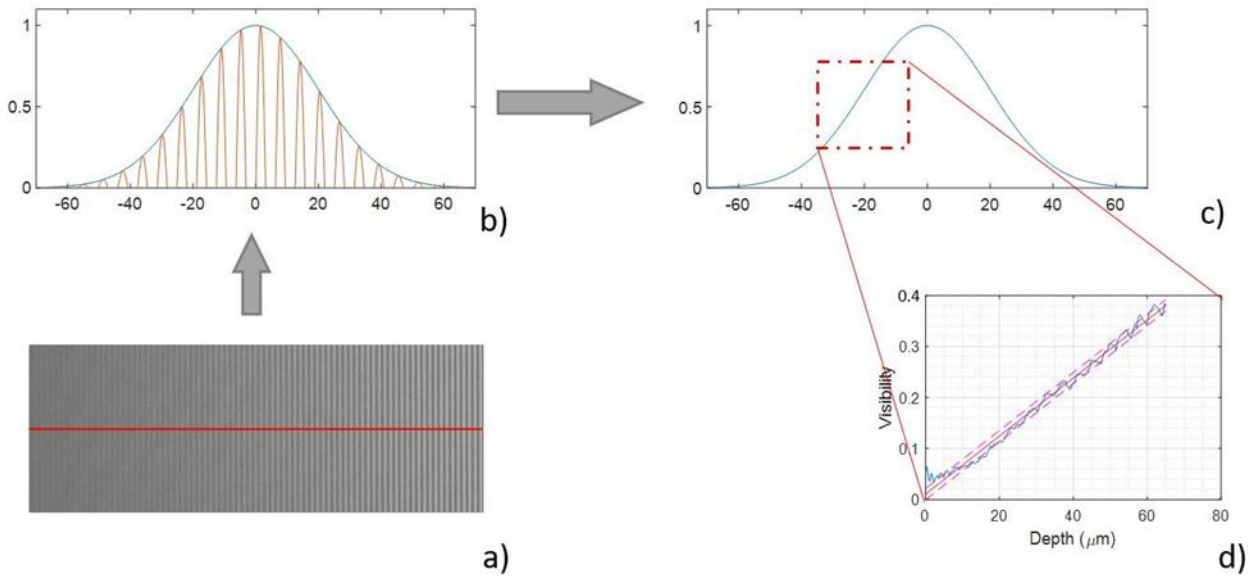

Figure 1. a) Captured interferogram using a clean mirror as a sample. b) The variations in fringe intensity resulting from the coherence length restriction. c) Visibility changes from 0 to 1. d) Linear part of the visibility diagram.

3. Results

Here, we have introduced a novel fringe analysis method that relies on visibility variations. The precision of this technique is $\pm 3\ \boldsymbol{\mu m}$ for a measurement range of $65\ \boldsymbol{\mu m}$. A comparison between the results obtained using this method and white light interferometry (WLI) was conducted for a stepped height sample which is shown in fig 2(a).

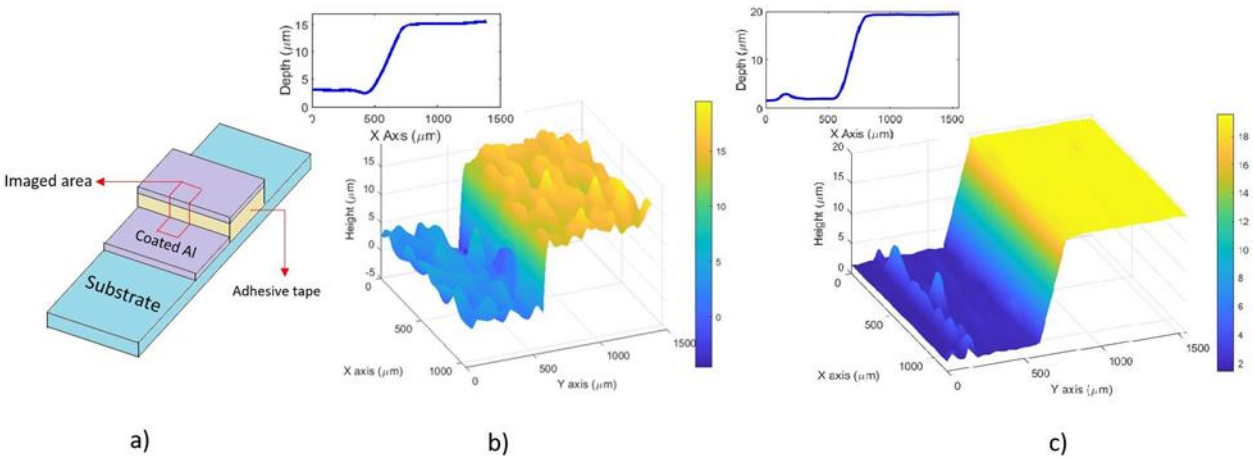

Figure 2. a) The sample that is made using adhesive tape as a discrete step and a layer of coated aluminum on it. b) 3D surface topography result of the sample by visibility-based method. c) 3D surface topography result of the same part of the sample by WLI method. In this comparison, according to fig 2(b), the visibility-based method yielded a measured height of $\mathbf{13 \pm 3}\ \boldsymbol{\mu m}$, while WLI indicated a height of $\mathbf{17}\ \boldsymbol{\mu m}$ for the same sample according to fig 2(c).

4. Conclusion

In this project, following the adjustment of the Mirau interferometer, the coherence length of the light source was fine-tuned. Subsequently, the resulting changes in visibility were carefully evaluated. In order to assess the accuracy and precision of this method, a discrete step was made, and the 3D surface topography results obtained from this method were compared to those from the white light interferometry (WLI).

References

1. A. Fisher, D.Stobener, G. Behrends, “A Lateral-scanning white-light interferometer for topography measurements on rotating objects in process environments,” CIRP Annals, 71(1), pp.437-440.
2. Malacara, Daniel, ed. “Optical shop testing.” Vol.59. John Wiley & Sons, 2007.
3. De Groot, Peter. “Phase shifting interferometry in Optical measurement of surface topography,” pp. 167–186. Springer, 2011.
4. Langenbeck, Peter. “Interferometry for precision measurement.” 2014.

FT6

Polarization-Dependent Modulation of Surface Plasmon Resonance with Highly Focused Gaussian Beams

Delgoshaei S.*[1], Abdollahpour D.[1], Mostafavi Amjad J.[1]

[1]*Department of Physics, Institute for Advanced Studies in Basic Sciences (IASBS), Zanjan, 45137-66731, Iran.*
email: simindelgoshaei@iasbs.ac.ir dabdollahpour@iasbs.ac.ir mostafavi@iasbs.ac.ir

Abstract: In this study, we explore the dynamics of Surface Plasmon Resonance (SPR) influenced by linear and circular polarizations using Gaussian beams. We investigate how these polarization states affect SPR at the nano-bio interface. By examining the SPR responses under linearly and circularly polarized light, we understand how polarization impacts the behavior of Transverse Magnetic (TM) and Transverse Electric (TE) modes. Our approach simplifies the optical setup, making it easier to see how SPR responds to different polarizations. This helps us see polarization as a tool to fine-tune SPR, potentially transforming SPR-based sensing technologies. We also introduce SPR microscopy (SPRM), which combines the high-resolution of optical microscopy with the capabilities of SPR. SPRM enhances the benefits of both methods, allowing for direct visualization of samples and real-time analysis of binding affinity and kinetics. The findings from this research not only advance optical diagnostics but also improve the design of SPR sensors. This marks an important advance in plasmonics, connecting basic understanding with practical uses, and highlights the role of polarization in improving optical sensing and material characterization.

Keywords: Surface Plasmon Resonance Microscopy, Polarization Effects, Gaussian Beams, Optical Sensing, Plasmonic Modulation

1. Introduction

Surface Plasmon Resonance (SPR) stands at the forefront of optical sensing technologies, offering unrivaled sensitivity in the detection of biomolecular interactions and material characterization at the nanoscale[1]. SPR is a phenomenon that arises when polarized light interacts with a metal-dielectric interface, leading to the excitation of coherent electron oscillations known as surface plasmons at the interface[2]. This interaction is highly sensitive to changes in the refractive index near the metal surface, making SPR an invaluable tool in various scientific fields, including biosensing, material science, and photonics[3].

The fundamental principle of SPR can be captured by the dispersion relation, which links the wavevector of the surface plasmon (k_{sp}) to the incident light's wavevector (k_0) and the dielectric constants of the metal (ε_m) and the surrounding medium (ε_d)[4]:

$$k_{sp} = k_0 \sqrt{\frac{\varepsilon_m \varepsilon_d}{\varepsilon_m - \varepsilon_d}}$$

This relation highlights the dependency of SPR on the optical properties of the materials involved and the conditions under which surface plasmons are excited. It is precisely this sensitivity that our research seeks to exploit by examining how different polarization states of incident light, specifically linear and circular polarizations, affect the excitation and propagation of surface plasmons[5].

Utilizing Gaussian beams, this study delves into the interplay between polarization and SPR, shedding light on how the orientation and nature of the electric field component of light influence surface plasmon excitation. Polarization, representing the orientation of the light's electric field, plays a pivotal role in SPR phenomena[6]. Linear polarization, characterized by a constant electric field direction, and circular polarization, where the electric field rotates creating a helical wavefront, are expected to differentially modulate the efficiency of SPR excitation due to their distinct interaction with the metal surface[7,8 and 9].

Our study uses a detailed experimental approach to observe Surface Plasmon Resonance (SPR) in silver-coated samples when exposed to Gaussian beams with different polarizations. We aim to understand how polarization affects SPR, which helps broaden our knowledge of plasmonic behavior and leads to better optical sensors. In this research, we not only look at the basic principles of SPR but also show how controlling polarization can improve SPR-based sensors. By exploring how light polarization interacts with SPR, we're developing new, more sensitive, and specific methods for detecting tiny phenomena.

2. Experimental Investigations

Experimental Investigations
This section delves into the empirical exploration of Surface Plasmon Resonance (SPR) phenomena under varying polarization states. Our comprehensive experimental setup aimed to meticulously capture the SPR behavior across a spectrum of linear polarization angles (0°, 45°, 90°, and 135°) and a circular polarization condition.

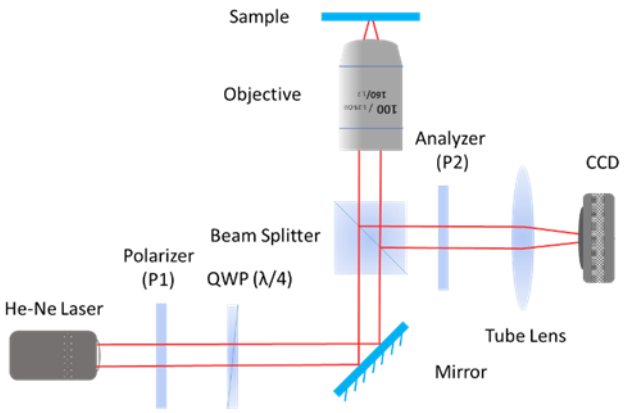

Figure 1.

Experimental Setup
Our laboratory setup comprised a sophisticated optical arrangement designed to illuminate the specimen with polarized light at specific orientations. A schematic diagram of this setup Fig.1 provides a visual representation of the components

involved, including the light source, polarization filter, specimen stage, and imaging system. This setup was instrumental in generating highly focused Gaussian beams with the desired polarization characteristics, enabling us to investigate the SPR effects with precision.

SPR Observations

Observations were made for each polarization state, capturing the resultant SPR effect on microscopic images. These images (Fig. 2) reveal the SPR patterns for linear polarizations at 0°, 45°, 90°, and 135°, alongside an image for circular polarization. Each polarization angle offered a unique insight into the SPR phenomena, with variations in the intensity and distribution of the plasmonic waves.

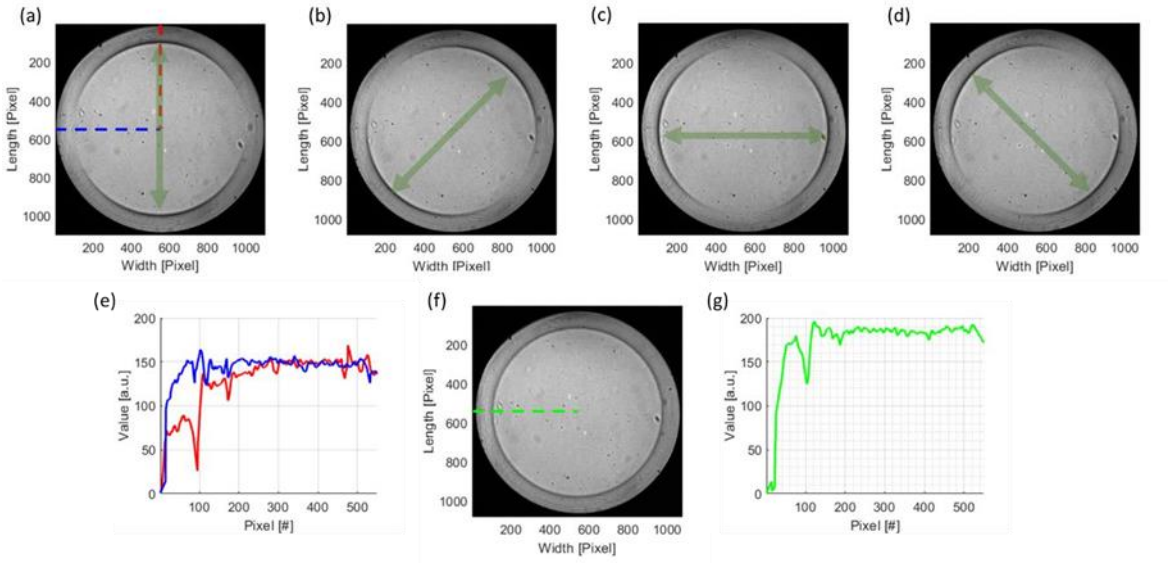

Figure 2 SPR Microscopic images for linear polarizations at (a) 0°, (b) 45°, (c) 90°, (d) 35°, (e) Intensity profiles for linear polarizations at 0° (red and blue lines at fig.2 (a)), (f) SPR Microscopic images for circular polarizations, (g) Intensity profiles for circular polarizations (green line at fig.2 (f)).

To further refine our investigation, we applied a coverslip atop the specimen for each polarization condition. This modification aimed to mitigate the background noise, thereby enhancing the clarity of the SPR signals.

Results Discussion

Our experiments show how polarization affects Surface Plasmon Resonance (SPR) behavior. Different angles of linear polarization create unique SPR patterns, highlighting the crucial role of the electric field's orientation in exciting surface plasmons. Specifically, the intensity profiles at 0°, displayed in Figure 2(e) with red and blue lines, reveal distinct SPR characteristics. The blue profile shows a pronounced valley where SPR occurs, indicating the presence of Transverse Magnetic (TM) modes. Conversely, the red profile does not display any peak, suggesting the influence of Transverse Electric (TE) modes. Additionally, the profiles for circular polarization, shown by the green line in Figure 2(f) and analyzed in Figure 2(g), demonstrate a weaker SPR valley compared to the blue plot from Figure 2(e), and this weaker valley remains consistent across different plots. This evidence confirms that polarization significantly modulates SPR, influencing its potential for improved sensing

applications. Our findings also emphasize the importance of controlling experimental conditions, like using a coverslip, to reduce noise and enhance the reliability of optical sensing.

3. Conclusion

This investigation has shed light on the intricate dynamics of Surface Plasmon Resonance (SPR) under varying states of polarization, providing valuable insights into how linear and circular polarizations influence SPR phenomena. Through meticulous laboratory experiments, we observed SPR patterns across different polarization angles and under circular polarization. The application of a coverslip to the specimen notably enhanced the clarity of SPR signals by effectively mitigating background noise, thus enabling a more precise visualization of SPR phenomena.
Our findings emphasize the significant role of polarization in modulating SPR, with linear and circular polarizations each inducing unique SPR patterns. This underscores the potential of polarization control in optimizing SPR-based sensing applications. The improvement in SPR signal clarity with the use of a coverslip further highlights the importance of experimental conditions in SPR studies, paving the way for the development of more accurate and reliable SPR-based optical sensing techniques.

References

1. Q. Wang et al., Nanoscale, 2022, 14, 564-591. https://doi.org/10.1039/D1NR05400G
2. Y. Chen et al., Biosensors, 2024, 14(2), 84. https://doi.org/10.3390/bios14020084
3. W. Kong et al., Chemosensors, 2022, 10(12), 509. https://doi.org/10.3390/chemosensors10120509
4. Y. Chen et al., "Surface Plasmon Resonance Biosensors: A Review of Molecular Imaging with High Spatial Resolution," Biosensors, vol. 14, no. 2, pp. 84, Feb. 2024.
5. Q. Wang et al., "Research advances on surface plasmon resonance biosensors," Nanoscale, vol. 14, pp. 564-591, 2022.
6. W. Kong et al., "Recent Advances in Surface Plasmon Resonance Microscopy," Chemosensors, vol. 10, no. 12, pp. 509, Nov. 2022.
7. Y. Chen et al., "High Spatial Resolution SPR Imaging for Molecular Interaction Analysis," Biosensors, Feb. 2024.
8. Q. Wang et al., "SPR Biosensors with Substrate Structures: Sensitivity and Interference Resistance," Nanoscale, 2022.
9. W. Kong et al., "Technological Advances in SPR Microscopy," Chemosensors, vol. 10, no. 12, Nov. 2022.

FT7

Investigation Of Optical Properties And Wetability In Anti-Reflective Film

Yunus Emre KOÇ[1], Yashar AZIZIAN-KALANDARAGH2

[1]Gazi Üniversitesi Fotonik Bilimi ve Mühendisliği Yüksek Lisans Öğrencisi
[2]TÜBİTAK SAGE Optik Sistemler Gurubu İnce Filim Kaplama ve Litografi Birimi.
email: emre.koc@tubitak.gov.tr

Abstract: Frost may occur on the surfaces of the protective windows in various ammunition under cold weather conditions. The operating performance of imaging systems is negatively affected due to accumulated water vapors. These effects can be controlled thanks to the coating applied to these optical parts that act as windows. The wettability of coatings is directly related to the amount of icing. Within the scope of this study, the wettability of various coating materials will be examined, taking into account their optical properties, and will be improved by integrating them into anti-reflective coatings.

In this study, thin film layers produced from HfO_2 material on glass were examined in terms of permeability and wettability. Using the DC Sputter method, HfO_2 thin film layers were coated on the glass substrate from a Hafnium metal source using the DC magnetron sputter method. The materials coated at low temperatures were produced at different pressures and oxygen amounts and the most appropriate production parameters were determined. The produced thin film coatings were then dropped onto the coating surface with a Hamilton glass injector, and the connection between the contact angle of the drop and the surface was examined.

1. Experimental Studies

HfO_2 coating was applied on the glass substrate material in a single series using the Angstrom Engineering brand thin film coating device. In experimental studies, production was made using HfO_2 metal source with a diameter of 4 inches (10.16cm) and a purity of 99.95%. A wavelength of 1060 nm was chosen to suit the AR coating, and films with a refractive index of 2.11 and a bandgap of 5.4 eV with bandgap energy were tried to be obtained at this wavelength. The maximum power density in production is regulated not to exceed 20 watts/inch2. In this study, production parameters were determined as variable values pressure and oxygen. Constant values are determined as Argon flow, temperature, thickness and power. Relevant values are stated in Table 1.

Table 1 Experimental Parameters

Parametreler	Level	Value
O_2 Flow (sccm)	3	5 , 9 , 14
Pressure (mTor)	3	1 , 3 , 5
Ar Flow (sccm)	1	60
Heat (^{0}C)	1	25
Think (nm)	1	200
Power (%)	1	15
Power Per Unit (watt/cm^2)	1	4,43

After the coating, the performance of the optical properties was examined and the optical transmittance was measured and recorded. The permeability graph of 5,3,1 mTorr and 9sccm productions is given in Figure 1.

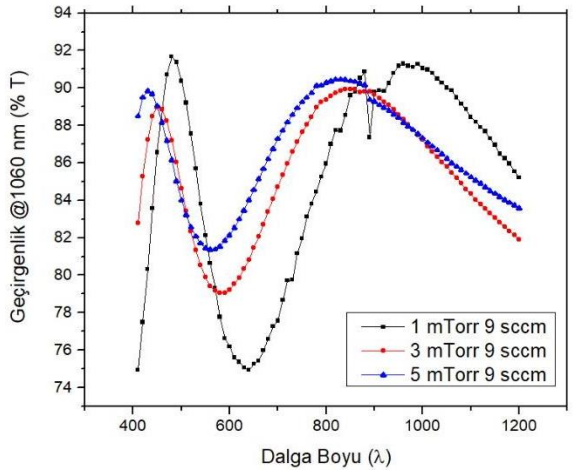

Figure 1. Permeability graph of 5.3.1 mTorr 9sccm productions

Another investigation was made on variable Oxygen rates. As a result of the examination, it was determined that there is a direct relationship between the Oxygen/Argon ratio in production. The determined wave is here (1060 nm) and the change graph depending on the changing Oxygen/Argon ratio is given in Figure 2. As seen here, the highest permeability values were determined as 9/60 ratio.

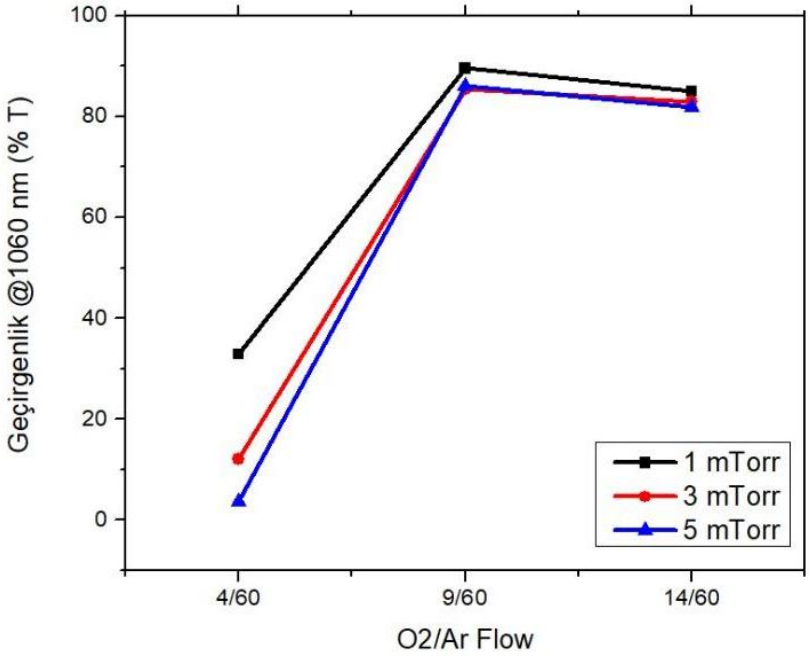

Figure 2. Permeability graph at Oxygen/Argon ratio

In addition to examining the optical properties, contact angle measurements were made to evaluate wettability. A contact angle measurement device was prepared to observe the contact angle on hydrophobic surfaces and to examine the wetting behavior of the surfaces. Hamilton microliter 81420 brand syringe was used in the experimental setup. The volume of each water drop dropped on the surface for measurement is 2500 µl. The test setup prepared for these measurements can be seen in Figure 3.

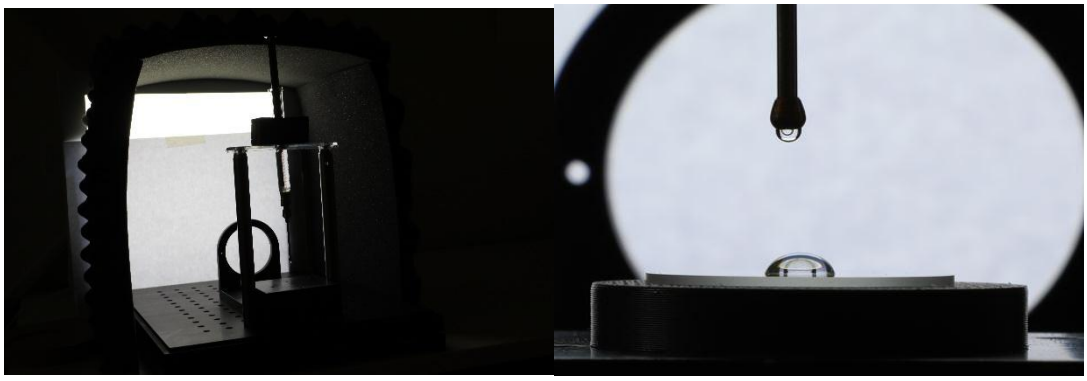

Figure 3. a) Contact angle measurement test setup b) Dropping Hamilton syringe onto HfO_2

Contact angle; The angle (φ) on the drop side between the tangent passed from the point where the drops touch the surface and the leaf surface is the contact angle, as shown in Figure 4. Image J program was used to determine contact angles.

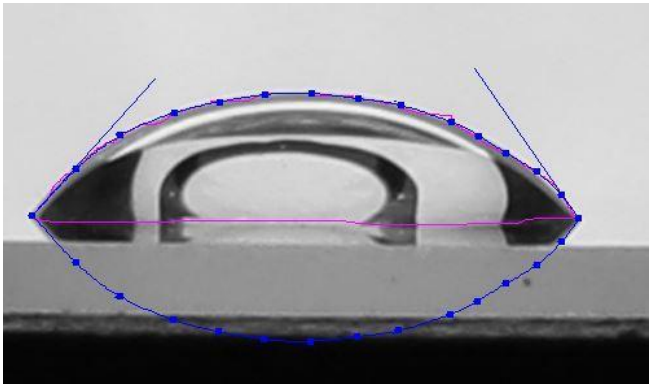

Figure 4. HfO_2 5mtor 9sccm production contact angle image j image

2. Conclusion

According to the permeability measurement results, different permeability values were encountered in different production parameters. The reason for this is that thin films with metallic properties and oxygen-saturated thin film coatings with high oxide density have different permeability values. The transmittance values at the relevant wavelength required for AR coatings are summarized in Table 2.

Table 2 Permeability values of HfO_2 productions

DOE HfO_2				
Processes Number	Processes Name	Transmittance (1060 nm)	O_2 Flow (sccm)	Pressure (mTor)
1	HfO_2-33	32,768937	4	1
2	HfO_2-35	89,539029	9	1
3	HfO_2-36	84,972372	14	1
4	HfO_2-37	12,106024	4	3
5	HfO_2-38	85,474819	9	3
6	HfO_2-39	82,780152	14	3
7	HfO_2-40	3,714858	4	5
8	HfO_2-41	85,986311	9	5
9	HfO_2-42	81,935061	14	5

According to the permeability results, thin film coatings with the highest permeability values were also examined. These films appear as coatings produced at a constant oxygen flux (9 sccm). Similarly, contact angle measurements for these coatings do not vary greatly. As a result of the experimental studies, the contact angles of the products produced at 1 mTorr pressure and 9 sccm oxygen parameters and the product produced with 9 sccm oxygen at 3 mTorr pressure were found to be close to each other.

A similar examination was made for coatings performed under constant oxygen flux (4 sccm) and at different pressure values (1,3 and 5mTorr). It has been determined that as the pressure increases, the permeability decreases, that is, the films show more metallic properties, and at the same time, the wettability of the surfaces changes. As the pressure value increases, the contact angle increases and the coating tends to take a hydroliphic structure. The results are given in Table 3 and Figure 5. As a

continuation of the studies, surface analyzes (AFM and SEM analyses) of thin film coatings will be carried out.

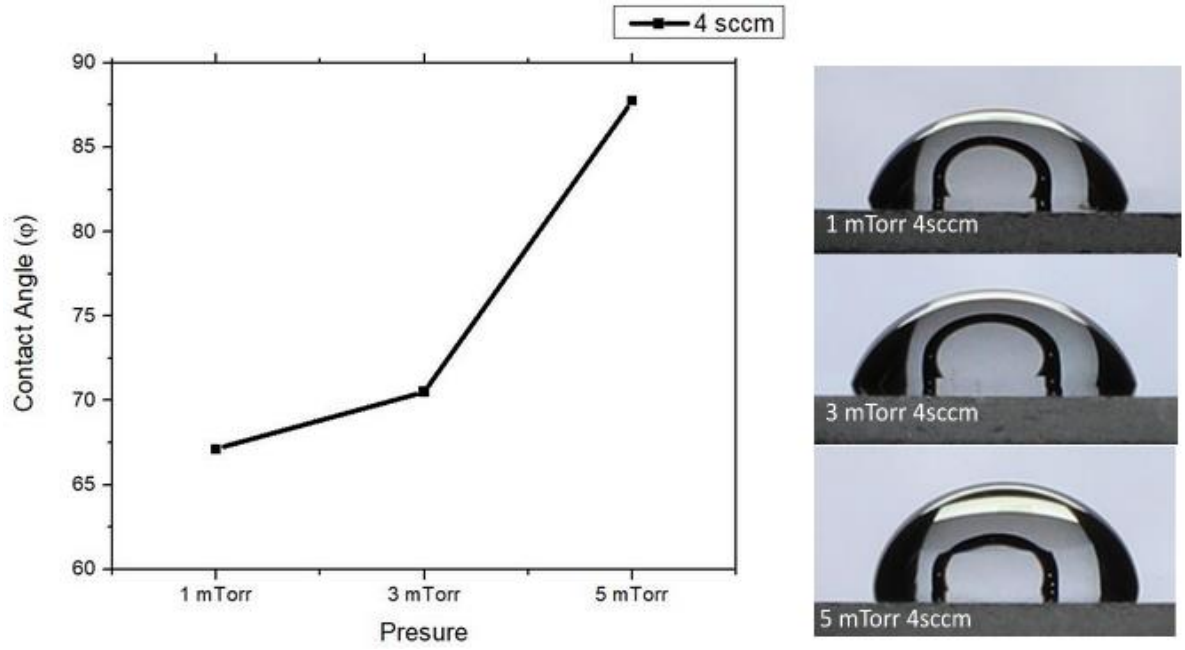

Figure 5. Contact angle graph of 4sccm 1,3,5mTorr HfO_2 productions

Table 3 Contact angles of 4sccm 1,3,5mTorr HfO_2 productions

DOE HfO_2				
Processes Name	Transmittance (1060 nm)	Contact Angle (φ)	O_2 Flow (sccm)	Basıç (mTor)
HfO_2-33	32,768937	67,118	4	1
HfO_2-37	12,106024	70,501	4	3
HfO_2-40	3,714858	87,741	4	5

References

1. E.Y. Bormashenko, Wetting of Real Surfaces, Walter de Gruyter GmbH, Berlin, 2013.
2. H. Y. Erbil, Surface Chemistry of Solid and Liquid Interfaces, Blackwell Publishing Ltd, Oxford, 2006.
3. https://www.biolinscientific.com/measurements/surface-free-energy#what-is-surface-free-energy

FT8

Comparing Illusory Movement Perception in Dyslexic and Typically Developing Children

Zahra Rasouli*[1], Saifollah Rasouli[2,3], Javad Salehi[1]

[1]*Department of Psychology, University of Zanjan, Zanjan, Iran*
[2]*Department of Physics, Institute for Advanced Studies in Basic Sciences (IASBS), Zanjan 45137-66731, Iran*
[3]*Optics Research Center, Institute for Advanced Studies in Basic Sciences (IASBS), Zanjan 45137-66731, Iran*
email: *z.rasouli57@gmail.com*

Abstract: Dyslexia, a prevalent learning disorder, poses significant challenges for affected children, impacting their educational, social, and psychological well-being. Visual perception and processing difficulties are common among children with dyslexia. Leveraging illusory motion patterns, we investigated the neurobiology of vision indirectly and non-invasively.

Reading is a cornerstone of education, enabling children to gain knowledge, explore new worlds, and engage with diverse ideas. However, reading is a complex activity that involves various cognitive processes, such as visual perception, auditory processing, motor coordination, language skills, attention, concentration, critical thinking, and analysis. Disruptions in any of these processes can lead to difficulties in reading comprehension and fluency. Dyslexia, a common neurodevelopmental disorder, specifically hinders the development of reading skills. Individuals with dyslexia often struggle with decoding spoken and written language despite having normal intelligence and proper training. This can result in inaccurate or slow reading, even though other cognitive abilities are unaffected[1]. Dyslexia affects approximately 4 to 9 percent of the global population, with boys being three times more likely to be affected than girls [2,3].

In this study, we introduce a pattern-driven approach using illusory motion designs for early dyslexia diagnosis in preschool children. Our descriptive research included dyslexic and non-dyslexic students aged six to nine years in Zanjan City during the 2020-2021 academic year. The dyslexic group (n = 19) consisted of students from four learning disorder centers, while the control group (n = 35) included students from selected schools in districts 1 and 2. In this study, we used 2 illusory motion designs as research tools. Data analysis showed that dyslexic children had significantly lower perception of illusory motion compared to their peers.

To conduct the study, we printed illusory motion stimuli on cardboard (A3 and A4 sizes) rather than using a computer screen. Students viewed these stimuli from a distance of approximately 60 cm and described what they saw in each picture.

The results for the illusory motion stimuli depicted in Figures 1 and 2 are as follows: For the stimulus shown in Figure 1, 91% of healthy children detected the illusory movement, while only 74% of dyslexic children did. For the stimulus in Figure 2, 74% of healthy children detected the movement, compared to just 32% of dyslexic children. This 32% difference in detection rates highlights the potential of using these stimuli for early dyslexia detection in preschool children.

This innovative method shows promise for predicting reading disorders during education and serves as a valuable screening tool for at-risk children before they start school.

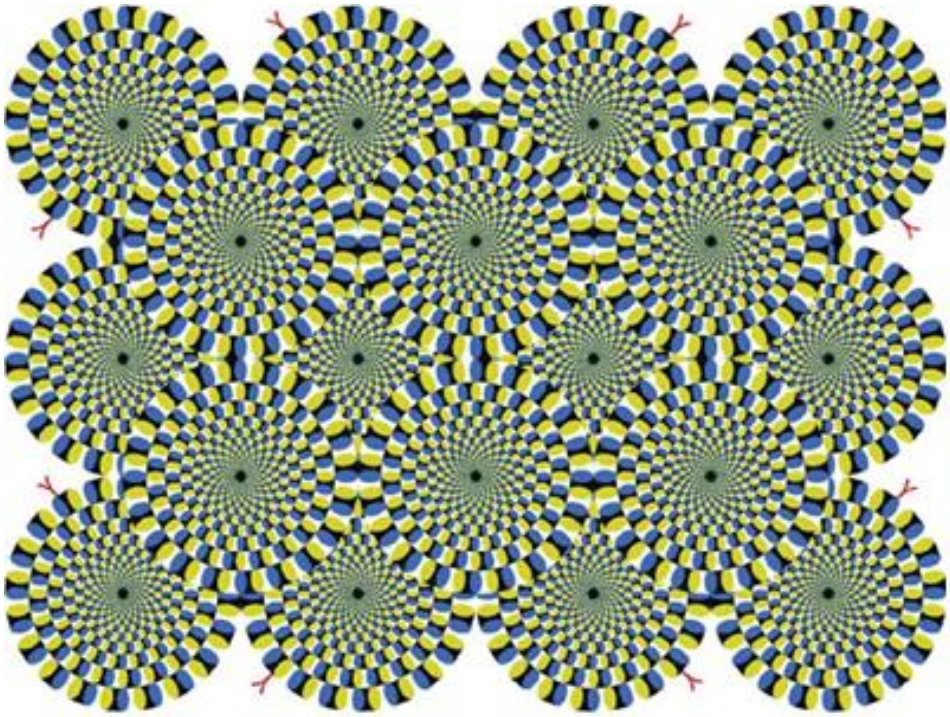

Figure 1. Kitaoka's "rotating snakes" illusion (Stimulus No. 1). Certain areas of the image create the illusion of motion, although the entire image is static (Credit: Akiyoshi Kitaoka).

The findings reveal that dyslexic children scored lower on average across all illusory stimuli compared to their non-dyslexic peers. For the illusory movement stimulus in Figure 2, 74% of healthy children detected the movement, while only 32% of dyslexic children did, indicating a significant 32% difference. Additionally, another stimulus that did not induce an illusion of movement (which is not presented here) produced interesting results: 83% of normal students accurately recognized the absence of motion, while only 58% of dyslexic students did. These results highlight differences in the perception of illusory movement and suggest potential applications for dyslexia screening in children before they enter school.

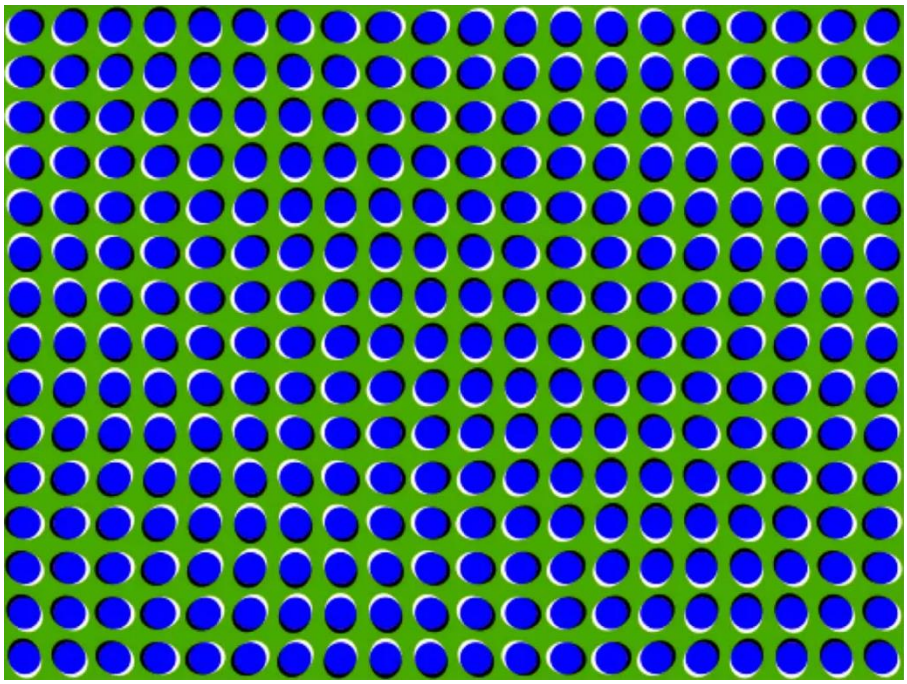

Figure 2. Stimulus No. 2. While the entire pattern remains static, specific areas of the image create the illusion of wavy motion (Credit: Paul Nasca).

References

1. American Psychiatric Association, D., Association, A. P. et al. Diagnostic and statistical manual of mental disorders: DSM-5, vol. 5 (American psychiatric association Washington, DC, 2013).
2. S. Gori and A. Facoetti, How the visual aspects can be crucial in reading acquisition: The intriguing case of crowding and developmental dyslexia, J. vision 15, 8–8 (2015).
3. I. Adubasim, Improving working memory and processing speed of students with dyslexia in Nigeria, *Online Submission 5*(2), 103-123 (2018).

AUTHOR INDEX

Author's Name	Abstract No
Ahadi Akhlaghi Ehsan	IS16, S5, S8, S19, S21, S27, P19, P20, FT2, FT3, FT4, FT5
A. Feizollahi Vahid A.	P26, P30
A. Hameed Sabreen	S2
A. Radeticchio	S1
Abby Sanders	IS8
Abdollah Borhanifar	IS10
Abdollahpour Daryoush	IS3, P24, FT6
Akbarpour Z.	S16
Akhtaryarazar D.	IS2
Akın Buket	S2
Akın Sönmez N.	S12, P27, P32, P34
Akman L.B.	S12
Alexey Andrianov	IS6
Ali Barkhordari	P10
Ali Mert GÜNDOĞDU	P29
Alihan Kumtepe	IS14
Alpan Bek	IS2, IS18, P8
Altındal Yerişkin Seçkin	S2
Aminian S.	S21
Anashkina E. A.	IS6
Arash Sabatyan	IS7, S6, S9, S24, P17, P18, P22, P25,
Ashraf M. W.	P5
Ataii M.R.	S14
Atefeh Sadeghi	P21
Avar B.	P30
Aydın S.Ş.	P1, P11, P15
Aylin YERTUTANOL	S4
Baghirov M.B.	S22
Balaban, M.	P9
Balakin A. A.	IS6
Balcı E.	P26
Balıkçı L.M.	P4
Barbara Sartori	IS19, S1
Barış Kınacı	P32
Batuhan Balkan	P8
Bayal Özlem	P16
Benedetta Marmiroli	IS9, IS19
Betül SATILMIŞ	P29
Bikbaeva G. I.	IS12
Contino T.	P5
Delgoshaei S.	P24, FT6
Dereli T.	P14
Devrim Anıl	IS5
Dilek E.	P14
Dinç, Ö.F.	S23
Durgun A.	P14
Ebrahimi H.	S9, P17, P18, P22
Ebrahimzadeh Kouyakhi A.	S19, FT4
Efkere H. İ.	S12, P1, P11, P15, P34
Elif Temel	P28
Elmas M.F.	P27
Erdem Talha	S15

Author's Name	Abstract No
Erenler B.	P27
Erkut Emin AKBAŞ	S4
Ersoy Y.	P1
Farazin J.	P19
Fatehi M.	S9, P22
Fateme Gheibi	S25, FT1
Fazlalizadeh Z.	P20
Gamze Altun	P29
Genc Sinan	S15
Gerd Leuchs	PS1
Ghazanfar Ali KHAN	IS18
Giovanni Birarda	IS19
Goodarzi A.	IS2, IS18
Güçlü Ç.Ş.	P4
Gupta H.	P5
Heinz Amenitsch	IS19, S1
Hafeez Anwar	P6
Hajipoor Z.	P20
Hajizadeh F.	S16, P19
Halime Gül Yağlıoğlu	IS1
Hamidreza Khalesifard	PS3
Hanife F.	S18
Hashemi Mozhgan	S10
Hassanzad F.	S8, FT2
Hatipoğlu İ.	S20, P14
Hosseini S.	S27, FT5
Icoz Kutay	S15
Ihor Pavlov	IS2, IS18
Jabbar pour Mahmoud	S5, FT3
Jafar Mostafavi Amjad	S25, P31, FT1
Jalali Sh.	S24
Javidi B.	S6, P25
Kaan YILMAZ	P29
KARAKAYA G.C	P13
Karakaya K.	P34
Kartaloğlu Tolga	S3, S23
Keskin M.Z.	S17
Khanjani M.	S8, FT3
Khayrullina E. M.	IS12
Kılıç K.A.	P2
Lisa Vaccari	IS19
Litvak A. G.	IS6
Luis L. Sánchez-Soto	PS2
Mostafavi Amjad J.	S11, S14, S21, S25, P24, P31, FT1, FT6
M. Zeki Güngördü	IS8
Mahdis Mirabioun	P31
Mahkame Abolfathi	S13
Mahmoudi Samad	S5, FT3
Mahmut Çağlayan	P28
Malek Mohammadi Milad	S5, S8, S16, FT2, FT3
Maleki M.	S16
Manshina A. A.	IS12
Mehmet Emre Taşgın	P8

Author's Name	Abstract No
Mollaei Mina	S5, FT3
Mollaha Maryam	P23
Morova B.	IS13
Muradov M.B.	S22
Nesrin Töre Şen	IS14
Oray Üstün	P7
Özbay Ekmel	S3, S4, S23
Özçelik S.	S12, S20, P1, P11, P12, P15, P28, P32, P34
Ozcelik U.	S7
Özdur, İ.	S23, S3, S17
Ozen Y.	P1, P11
Özge Demirtaş	P8
Özgür Selimoğlu	IS4
Öztürk M. Kemal	P16
Paolo Falcaro	IS19
Parveen Iqra	P6
Pashaei P.	S12
Patrick Kung	IS8
R. Haider	S1
Rabia Şahin	P10, P28
Rahmani M.	P19
Ramazan Alpay	P32
Ramazan Şahin	P8
Reefaz Rahman	IS8
Rezaei N.	S19, FT4
Ruhollah Moradhaseli	PS3
Saifollah Rasouli	IS15, S10
Sayın B.	P12
Salar Alizadeh	PS3
Salnikov N. I.	IS6
Selim Y.N.	P15
Şemsettin Altındal	IS17, S7, P26, P30
Seongsin Margaret Kim	IS8
Serbest B.	S12, S20, P32
Sevilay Sevinçli	IS20
Seymen O.K.	P27
Shadafrooz H.	P20
Simone Dal Zilio	IS19
Skobelev S. A.	IS6
Süha Gül KARA	P29, P32
Sumea Klokic	IS19
Tamagnone M.	P5
Taner Tarık Aytaş	P8
Tayfun AKIN	PS4
Topcu U.	S20
Toprak B.Ç.	P15
Turchet A.	IS9
Tuğçe ATAŞER	P29, P32
Ulusoy M.	P4
Urgun N.	P14
Utku Yaman Can Aslan	P28
Uyar, F.	S23
Varol B.	P11

Vasileva A. A.	IS12
Yalçın Buğra	S3
Yaqub M.A.	P5
Yashar AZİZİAN-KALANDARAGH	S4, S5, S18, S20, P3, P7, P10, P13, FT3, FT7
Yener N.N.	P27
Yentur A.	S17
Yiğit Levent Çeçen	S26
Yıldız Gülşah	S3
Yükselici, M. H.	P9
Yunus Emre KOÇ	P3, FT7
Zakikhani F.	S19, FT4
Zeynali S.	S11
Zeynep Demircioğlu	IS11
Waqqar AHMED	IS18